

**Sustainability Across Diverse Engineering Disciplines
(Geothermal Technology, District Cooling Systems, Acid Mine
Drainage, and Additive Manufacturing)**

A Thesis

Presented in Partial Fulfillment of the Requirements for the

Degree of Master of Science

with a

Major in Mechanical Engineering

in the

College of Graduate Studies

University of Idaho

by

Austin Anderson

Major Professor: Behnaz Rezaie, Ph.D.

Committee Members: Steven Beyerlein, Ph.D.; John Crepeau, Ph.D.

Department Administrator: Steven Beyerlein, Ph.D.

May 2020

Authorization to Submit Thesis

This thesis of Austin Anderson, submitted for the degree of Master of Science with a Major in Mechanical Engineering and titled "Sustainability Across Diverse Engineering Disciplines (Geothermal Technology, District Cooling Systems, Acid Mine Drainage, and Additive Manufacturing)," has been reviewed in final form. Permission, as indicated by the signatures and dates below, is now granted to submit final copies to the College of Graduate Studies for approval.

Major Professor: _____ Date: _____
Behnaz Rezaie, Ph.D.

Committee Members: _____ Date: _____
Steven Beyerlein, Ph.D.

_____ Date: _____
John Crepeau, Ph.D.

Department
Administrator: _____ Date: _____
Steven Beyerlein, Ph.D.

Abstract

Sustainability is a broad term that considers environmental aspects in any products/processes design, fabrication, application, and end of life. This thesis is an application of sustainability across multiple disciplines including power generation, district heating and cooling, mining, and additive manufacturing.

Geothermal sources as a sustainable source of energy is often an underutilized resource that has potential to offset fossil fuel sources of energy such as coal and natural gas, while still providing stable baseload power. Various methods of performance improvement, as well as integration of geothermal technology with other renewable energy sources were also discussed. The environmental impact and economic viability of the technology were mapped as well. The advantages and disadvantages of the technology and opportunities for improvement were explored based on the recent studies. Briefly, the potential role of geothermal technology in a sustainable future was discussed.

Applying exergy analysis on the district cooling in the University of Idaho, Moscow campus prioritized the exergy loss. By using TRNSYS modeling and simulation based on a modified thermal energy storage operation condition the new operation schedule for the cooling system in University of Idaho Moscow campus yielded a potential cost savings of \$140,000 annually while eliminating 428,800 kg of CO₂ emissions and improving the sustainability.

Acid mine drainage and its dangerous effects are one of the greatest challenges currently facing humanity. With sustainability approach to that issue, implementation of active and passive treatment, in conjunction with collaborative relationships between government, academia, investors, and industry were suggested to solve this crisis. Furthermore, governments must continue to enforce policy and regulations that ensure the burden of remediation rests upon those who caused the damages.

Metal additive manufacturing offers a revolutionary way to manufacture parts and components. The different type of the additive manufacturing, financial and environmental benefits, and advantages and disadvantages were studied through literature review. Through Life Cycle Analysis, a method of metal additive manufacturing (Laser Metal Deposition) and a casting manufacturing method were compared for the manufacturing of a stainless-steel pump impeller. It was concluded that additive manufacturing was a sustainable method of manufacturing components in compare with conventional method.

The four chapters combine to describe and analyze sustainability across multiple disciplines. Factors such as policy, society, economy, design limitations, performance, and efficiency have been shown to affect the sustainability of these technologies. This thesis addresses these factors and describes how improvements ranging from small to monumental within these disciplines can affect positive change in the present and future society.

Acknowledgements

The Author would like to acknowledge the College of Engineering at the University of Idaho the Richard B. Stewart Thermodynamics Scholarship as well as the Department of Defense Science Mathematics and Research for Transformation (SMART) scholarship for financial assistance. Additionally, the author thanks Dr. Behnaz Rezaie for her endless expertise, patience, and motivation that enabled this thesis to be possible. Finally, the authors would like to acknowledge their parents, Phil and Janell Anderson, for their years of financial and emotional support.

Dedication

To my Grandfather, who showed me a perfect example of what it means to be a great friend, father, husband, and person.

Table of Contents

Authorization to Submit Thesis	ii
Abstract	iii
Acknowledgements	iv
Dedication	v
Table of Contents	vi
List of Tables	xi
List of Figures	xii
List of Nomenclature.....	xiv
Chapter 1: Introduction	1
1.1. Motivation	1
1.2. Objectives and Scope	1
1.3. Outline.....	2
Chapter 2: Geothermal Technology: Trends and Potential Role in a Sustainable Future.....	4
2.1 Abstract	4
2.2 Introduction	4
2.3 Overview of Geothermal Heating Applications.....	6
2.4 Geothermal Power Plant Classes.....	8
2.4.1 Dry Steam Technological Improvements.....	12
2.4.2 Flash Steam Technological Improvements	12
2.4.3 Binary Organic Rankine Cycle Technological Improvements.....	15
2.5 Integrated Geothermal Systems	17
2.5.1 Geothermal and Solar Paired Systems	18
2.5.2 Other Geothermal-Hybrid Systems.....	22
2.6 Enhanced Geothermal Systems.....	23
2.6.1 Enhanced Geothermal Systems Projects	24
2.6.2 Enhanced Geothermal Systems Modeling	24

2.6.3	Seismic and Geological Effects of Enhanced Geothermal Systems	25
2.6.4	Working Fluid Selection for Enhanced Geothermal Systems.....	26
2.7	Environmental Impact of Geothermal Systems	27
2.8	Economics of Geothermal Systems.....	31
2.9	Discussion	34
2.9.1	Advantages:.....	34
2.9.2	Disadvantages:	34
2.10	Conclusion	35
Chapter 3: An Innovative Approach to Enhance Sustainability of a District Cooling System by Adjusting Cold Thermal Storage and Chiller Operation.....		
3.1	Abstract	38
3.2	Introduction.....	38
3.3	Methods.....	41
3.3.1	Exergy Analysis	41
3.3.2	Transient System Simulation Tool.....	42
3.4	Case Study: University of Idaho District Energy System	43
3.5	Analysis.....	44
3.5.1	Exergy Analysis	44
3.5.2	TRNSYS Modeling and Simulation.....	47
3.6	Results and Discussion.....	50
3.6.1	Exergy Destruction.....	50
3.6.2	Cold TES Performance.....	51
3.6.3	Cooling Supply.....	52
3.6.4	Savings	53
3.6.5	Further Discussion	54
3.7	Conclusions	54
Chapter 4: Sustainable Resolutions for Environmental Threat of the Acid Mine Drainage.....		
		56

4.1	Abstract	56
4.2	Introduction	56
4.3	Acid Mine Drainage Environmental Interruption	59
4.4	Acid Mine Drainage Treatment Background	59
4.4.1	Passive and Active Treatment	62
4.4.2	Emerging Technology	63
4.5	Innovative Sustainable Treatment	64
4.5.1	Option 1	64
4.5.2	Option 2	65
4.5.3	Option 3	66
4.6	Governmental Roles	66
4.6.1	Regulations	66
4.6.1.1	Some North American Regulation	66
4.6.1.2	Some European Regulations	69
4.6.1.3	Some Australian Regulations	69
4.6.2	Some Legal Cases	70
4.6.3	Collaborative Actions	72
4.7	Conclusions	72
Chapter 5: Metallic 3D printing: Study of Opportunities for Sustainable Future with a Case Study .		74
5.1	Abstract	74
5.2	Introduction	74
5.3	Metal Additive Manufacturing	77
5.3.1	Powder Bed Systems	78
5.3.2	Powder Feed Systems	78
5.3.3	Wire Feed Systems	79
5.4	Economics Aspects of Additive Manufacturing	79
5.5	Environmental Aspects of Additive Manufacturing	80

5.5.1	Consumption Reduction.....	80
5.5.2	Resource Protection	81
5.5.2.1	Recycled Powders	81
5.5.2.2	Recycled Products.....	82
5.6	Advantages and Disadvantages of Metal Additive Manufacturing.....	82
5.6.1	Advantages of metal Additive Manufacturing	82
5.6.2	Disadvantages of metal Additive Manufacturing.....	83
5.7	Additive Manufacturing Sustainability Advancement.....	83
5.8	Life Cycle Assessment of Laser Metal Deposition.....	84
5.8.1	Case Study.....	84
5.8.2	Life Cycle Inventory	86
5.8.2.1	Pre-Manufacturing	86
5.8.2.2	Manufacturing	88
5.8.2.3	Use (Service condition).....	90
5.8.2.4	Transportation	91
5.8.2.5	End of Life	92
5.8.3	Impact Analysis.....	96
5.8.4	Interpretation of Results	97
5.9	Validation.....	102
5.10	Discussion of Results	103
5.11	Conclusions	105
Chapter 6: Conclusion.....		107
6.1	Conclusions	107
6.2	Future Study.....	109
References.....		111
Appendix 1		137
Chapter 2: Supplemental Information on TRNSYS Model		137

A1.1 Introduction 137

A1.2 TRNSYS Component Description and Model Layout 137

Appendix 2 140

Chapter 3: Copyright Approval from the Journal Applied Energy 140

Appendix 3 141

Chapter 4: Copyright Approval from the Journal Science of the Total Environment 141

List of Tables

Table 2.1: Comparison of Ammonia, HCFC123, n-Pentane and PF5050 as working fluids [29].....	15
Table 2.2: Summary of geothermal power plant LCA's from cradle to grave [76].....	28
Table 3.1: Parameters used at operating points within the cooling system.....	46
Table 3.2: Equations used for calculation of component exergy destruction rates within the UI cooling cycle	47
Table 3.3: Summary of two scenarios of operation	49
Table 3.4: Operating and non-operating times of chillers in Scenario 2.....	50
Table 3.5: Exergy destruction rates for components of the cooling cycle of the UI district energy system	50
Table 3.6: Comparison of electricity, cost, and environmental impact of Scenarios 1 and 2	54
Table 5.1: Pump impeller pre-manufacturing inputs/outputs for LMD	87
Table 5.2: Pump impeller pre-manufacturing inputs/outputs for the casting process	88
Table 5.3: Pump impeller manufacturing inputs/outputs for LMD.....	90
Table 5.4: Pump impeller manufacturing inputs/outputs for casting	90
Table 5.5: Pump Impeller Transportation for LMD and casting processes	92
Table 5.6: Pump impeller EOL inputs/outputs for LMD	93
Table 5.7: Pump impeller EOL inputs/outputs for casting.....	94
Table 5.8: Pump Impeller Impact Categories.....	97
Table 5.9: Results comparison	103
Table A1: Description of additional system components in the TRNSYS model.	137

List of Figures

Figure 2.1: Installed capacity (GW) of geothermal power worldwide with estimates of installed capacity for year 2020 [3].	5
Figure 2.2: Installed capacity of worldwide direct use geothermal resources as of 2015 [14].	7
Figure 2.3: Global maximum aquifer temperature in various places worldwide [15].	8
Figure 2.4: Simplified schematic of Dry steam cycle [17].....	9
Figure 2.5: Simplified schematic of flash steam cycle [17].	10
Figure 2.6: Simplified schematic of Binary ORC [17]	11
Figure 2.7: Installed capacity in MW for each type of power plant in 2015 [3].	12
Figure 2.8: Net power and required pump input for the double flash and the single flash power plants [22].	13
Figure 2.9: Exergy use (kW) for single flash power plant. [23].	13
Figure 2.10: Exergy use (kW) for double flash power plant [23].	14
Figure 2.11: Exergy efficiency of isobutane for power generation only parallel CHP, and series CHP [30].	16
Figure 2.12: Comparison of cost for a base geothermal, optimized geothermal, solar-geothermal hybrid with constant load, and solar-geothermal hybrid with variable load [42].	20
Figure 2.13: Thermal efficiency of un-optimized versus multi-objective optimization of a geothermal-solar hybrid power plant [44].	21
Figure 2.14: Emissions of different power plant types over the course of their life cycle [84].	30
Figure 2.15: Breakdown of g-CO ₂ /kWh percentages for each part of the life cycle of a geothermal power plant [84].	30
Figure 2.16: Cost breakdown for geothermal power plants in a range of 20 MW to 60 MW [87].	31
Figure 2.17: Double flash levelized cost [94].	33
Figure 3.1: Cold TES tank located on the UI, Moscow campus, ID, USA.....	43
Figure 3.2: Schematic of the UI cooling cycle in Moscow, Idaho, US.....	45
Figure 3.3: Water flows into and out of the cold TES tank in the UI cooling district system	48
Figure 3.4: Breakdown of average exergy destruction rate by component for the month of June 2016.	51
Figure 3.5: Average temperature of tank and temperature of discharge to campus for Scenarios 1 and 2 (hour of year corresponds to first hour of each day within the simulation)	52
Figure 3.6: Moving average of cooling supplied to campus for June 2016 (hour of year corresponds to first hour of each day within the simulation)	53
Figure 4.1: AMD Treatments types [152].....	60

Figure 4.2: AMD Treatments Emergent technology.....	64
Figure 4.3: Option 1 for AMD Solution.....	65
Figure 4.4: Option 2 for AMD Solution.....	66
Figure 4.5: Number of proposed, active, and deleted NPL sites as of November 2019 [187].....	68
Figure 4.6: Governmental Roles for Controlling AMD Issue.....	72
Figure 5.1: Drawing of pump impeller used for analysis.....	85
Figure 5.2: Summary of inputs for each stage of the LMD process	95
Figure 5.3: Summary of life cycle inputs for the casting process	95
Figure 5.4: LMD and casting processes GWP comparison	98
Figure 5.5: Acidification potential of LMD and casting processes.....	99
Figure 5.6: FAETP comparison between LMD and casting processes	100
Figure 5.7: HTP for both LMD and casting processes.....	101
Figure 5.8: Ozone depletion potential for LMD and casting processes	102
Figure 5.9: Summary of LMD environmental impact reduction over the casting process	103
Figure 5.10: GWP increases resulting from decreased recycling rates.	104
Figure 5.11: Average laser power and GWP.....	105
Figure A1: Complete model view of all components.	139
Figure A2: Copyright approval for publication from Applied Energy.	140
Figure A3: Copyright approval for publication from Science of the Total Environment.	141

List of Nomenclature

ACSMP	Australian Centre for Sustainable Mining Practices
ADTI	Acid Drainage Technology Initiative
AERL	Applied Energy Research Laboratory
AeWs	Aerobic Constructed Wetlands
ALD	Anoxic Limestone Drains
AM	Additive Manufacturing
AMD	Acid Mine Drainage
AnWs	Anaerobic Constructed Wetlands
AP	Acidification Potential
APR	Area per unit Power output
BPMD	Bonita Peak Mining District
CAD	Computer Aided Design
CFC	Chlorofluorocarbon
CHP	Combined Heat and Power
CNC	Computer Numerical Control
COP	Coefficient of Performance
CWA	Clean Water Act
DAT	Decision Aids for Tunneling
DDM	Direct Digital Manufacturing
DMD	Direct Metal Deposition
EGS	Enhanced Geothermal Systems
EIA	Energy Information Administration
ENGINE	Enhanced Geothermal Innovative Network for Europe
EOFC	Enhanced Organic Flash Cycle
EOL	End of Life
EPA	Environmental Protection Agency

EROEI	Energy Returned on Energy Invested
FAETP	Freshwater Aquatic Eco-toxicity Potential
GA	Genetic Algorithm
GHP	Geothermal Heat Pump
GRS	Gas Removal System
GWP	Global Warming Potential
HDS	High-Density Sludge
HRS	Hazard Ranking System
HTP	Human Toxicity Potential
IDDP	Icelandic Deep Drilling Project
IMSS	Iron Mountain Mines Superfund Site
LBM	Laser Beam Melting
LCA	Life Cycle Analysis
LCI Life	Cycle Inventory
LCIA	Life Cycle Impact Assessment
LCOE	Levelized Cost of Electricity
LEC	Levelized Energy Cost
LLB	Limestone Leach Bed
LMD	Laser Metal Deposition
LRVP	Liquid Ring Vacuum Pump
MEND	Mine Environmental Neutral Drainage
MPC	Model Predictive Controllers
MRB	Magnesium Removal Beds
NCCP	North Campus Chiller Plant
NPDES	National Pollutant Discharge Elimination System
NPL	National Priorities List
NPV	Net Present Value

NSS	National Stream Survey
O&M	Operation and Maintenance
ODP	Stratospheric Ozone Depletion Potential
OLC	Open Limestone Channels
ORC	Organic Rankine Cycle
PBP	Payback Period
PBS	Powder Bed Systems
PFS	Powder Feed Systems
PV	Solar-photovoltaic
REY	Rare Earth Elements and Yttrium
ROI	Return on Investment
RORC	Regenerative Organic Rankine Cycle
SCCP	South Campus Chiller Plant
SEC	Specific Energy Consumption
SFF	Solid Freeform Fabrication
SLB	Steel Slag Leach Bed
SP	Self-Potential
TEG	Thermoelectric Generators
TES	Thermal Energy Storage
TES	Thermal Energy Storage
TRNSYS	Transient System Simulation Tool
TSEORC	Two-Stage Evaporation Organic Rankine Cycle
US	United States
VFW	Vertical Flow Wetlands
WFS	Wire Feed Systems
WVDEP	West Virginia Department of Environmental Protection

Chapter 1: Introduction

1.1. Motivation

If history has been any indication, it is clear that humanity is built upon continual exploration, expansion, and general improvement of the quality of life. Though, the human nature that drives innovation, humanity is met with a continually growing demand for both material and energy resources. These demands provide a strain on the environment that must be monitored carefully to ensure that present successes are not paid for at the expense of the future. This concept of meeting future demands while also providing for people and the ecosystem as a whole in the present is known as sustainability.

There is not an exact formula to achieve sustainability, rather it is a continual process of working to improve existing technology efficiencies, innovating new ideas that are resource and energy efficient, reducing demand for materials and energy, and developing long term economic benefits. Other aspects of sustainability include considering different cultures and understanding about the topic. Achieving sustainability likely requires the guiding of people's way of thinking towards a sustainable mindset. Sustainability will be reached when the consumption of resources and energy reaches an equilibrium with the rate at which it can be replenished.

With current materials and energy demands increasing, it is crucial that sustainable sources of energy and material extraction be developed. The motivation for this thesis is to provide a roadmap towards a sustainable future using different technologies, with some having been developed a long time ago while others just now being explored and have yet to reach their full potential. By applying fundamental concepts of engineering, such as energy and exergy assessment, coupled with the computational power of software, it is possible to develop some approaches to evaluate and improve upon the sustainability as described in this thesis for different type of projects in order to depict the impact of various engineering disciplines on a more sustainable future.

1.2. Objectives and Scope

The focus of the program is to investigate sustainability approaches to reduce the environmental impacts resulting from energy and resources consumption. The objective of this thesis is to show different applications of sustainable development in different engineering disciplines that serve to protect the environment while still advancing people quality of life. Within the main objective, there are many smaller objectives that are investigated within this thesis to support the overarching objective. The various objectives of the thesis are summarized as follows:

- 1) To identify and discuss various sustainable sources of energy as related to environment sustainability, (Energy Engineering).
- 2) To modify the operation of a district cooling system coupled with cold thermal energy storage with the purpose of improving the sustainability and financial saving, (Mechanical, Thermal Engineering).
- 3) To identify the severity and ramifications of Acid Mine drainage and the potential methods of remediating the damage (Mining Engineering).
- 4) To enhance the environmental aspects of metal additive manufacturing (ADM) as fast developing manufacturing method for a sustainable future (Metallurgy Engineering).

1.3. Outline

The present thesis is comprised of five chapters that all focus on improving the sustainability of differing different projects.

In Chapter 2, geothermal energy as a potential source of renewable energy is discussed from different aspects. Geothermal energy is both readily available to meet a large demand while also being environmentally more favorable than traditional energy sources such as fossil fuels. An extensive literature review is performed on the different methods of harnessing geothermal power, along with their advantages and disadvantages. Additionally, insight into current research trends that further the mission of developing a sustainable energy source are provided. Combining geothermal resources with other renewable sources, such as solar, as well as developing engineered geothermal systems present some of the greatest opportunity to enhance environmental sustainability.

By clustering heating and cooling systems into one central system, that provides the necessary heating and cooling loads to multiple locations is known as a district energy (DE) system. The concept of a DE system is not novel as they have been implemented quite liberally in the last hundred years. They have also been shown to be more efficiency compared to individual heating and cooling systems. In Chapter 3 an energy and exergy assessment of the University of Idaho cooling cycle DE system is conducted with the goal of improving sustainability. The cooling cycle DE system in the UI is composed of three vapor compression chillers, a Lithium-bromide condensing absorption chiller, as well as a thermal energy storage tank. Different operational scenarios are investigated and recommendations for an operation schedule are provided in which not only is sustainability advanced by less water and energy consumption, but also emissions. Additionally, the operation schedule proposed has drastically improved economic sustainability resulting from a large financial savings.

Chapter 4 focuses on the harsh effects of mining pits on the environment and species as well as how past mining operations, with present and future environmental impacts, can be mitigated using various technical methods and governing strategies. Additionally, there is discussion on policy and its effect on remediation of mining landscapes.

In Chapter 5 a literature review on the environmental and economic aspects of AMD is conducted followed by a life cycle analysis (LCA), which is a common tool in measuring sustainability, on ADM process by focusing on laser metal deposition (LMD). With ADM gaining traction as an alternative to traditional manufacturing methods such as milling or casting, it becomes critical that its environmental effects be quantified.

The final chapter (Chapter 6) provides conclusions and a summary of improvements on the systems described in previous chapters. Furthermore, a sustainable roadmap for the future is outlined in regards to sustainability. Additionally, future research and discussion on possible complications that stand in the way of a sustainable future are presented.

Chapter 2: Geothermal Technology: Trends and Potential Role in a Sustainable Future

Anderson, Austin, and Behnaz Rezaie. 2019

Applied Energy 248: 18–34

<https://doi.org/10.1016/J.APENERGY.2019.04.102>

2.1 Abstract

Rapid population growth as well as modern technology reliance lead to a greater demand for energy consumption. An ever growing focus on creating sustainable environment requires energy sources to be used with caution. Two effective solutions to address these concerns include utilizing renewable energy resources and increasing efficiencies of current technologies. Geothermal energy provides a renewable energy source that has potential to supply reasonable amounts of electricity, heating, and cooling. The present research elaborates upon methods of harnessing energy using various geothermal technologies. Various methods of performance improvement, as well as integration of geothermal technology with other renewable energy sources are also discussed. The environmental impact and economic viability of the technology are mapped as well. The advantages and disadvantages of the technology and opportunities for improvement are explored based on the recent studies. Briefly, the potential role of geothermal technology in a sustainable future is discussed in the study. Finally, the prospective topics of future research are presented for further investigation.

2.2 Introduction

The availability of energy is one of the most critical aspects to the development of any society. Today a significant portion of the energy comes in the form of burning organic fuels to produce useful work or electricity. The availability of these fuels are limited. For example, it is estimated that Indonesia only has 33 years of natural gas reserves and 75 years of oil [1]. These figures are sure to change over time depending on the consumption pattern. It is likely that energy demand will increase over time. From 1990 to 2050, power consumption could increase by as much as 275% of 1990 demand [2]. One approach for alleviating energy issues is by introducing renewable energy technologies to replace conventional fossil fuel technologies. Geothermal energy appears to be a potential alternative source of energy. Geothermal power is already utilized around the world. The total world geothermal power resources reached 12.7 GW in 2014, mainly from low and medium temperature sources [3]. This is approximately an increase of 17% since 2010. Figure 1 illustrates the growth of geothermal technology from 1995 to 2020. The study presented a rough linear trend of about 350 MW per year from 2010 to 2014, while also claiming 21 GW of power capacity by 2020 and 140 GW by 2050 could be installed

worldwide; in that case geothermal would encompass 8.3% of the world's power generation and serve 17% of the population, with 40 countries generating 100% of their power from geothermal sources [3]. Also, geothermal technology can eliminate over 1,000 million tons of CO₂ from the atmosphere annually. Another study depicted a more conservative figure where 3% of power generation and 5% of heating load are supplied by geothermal resources in 2050 [4].

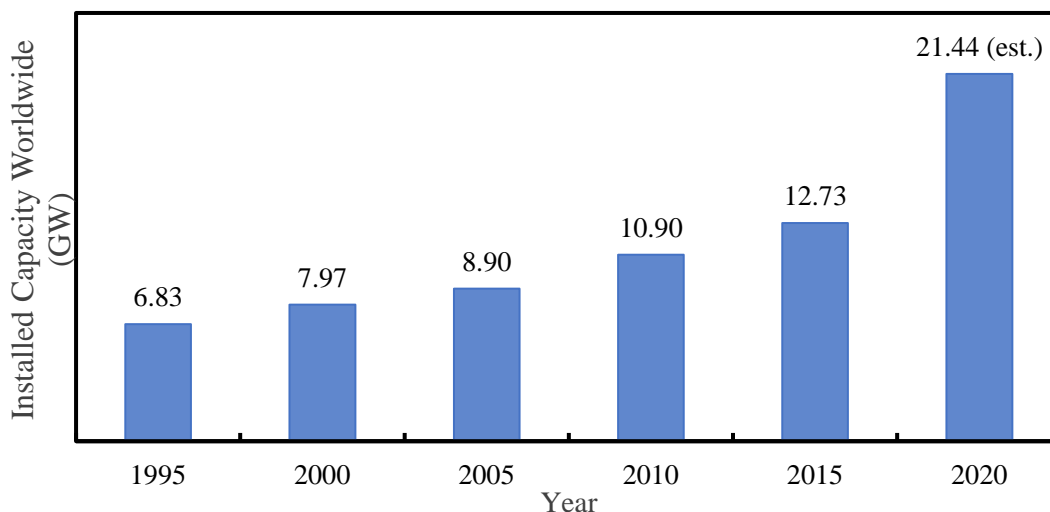


Figure 2.1: Installed capacity (GW) of geothermal power worldwide with estimates of installed capacity for year 2020 [3].

If only 1% of the total estimated available geothermal energy was utilized by humanity, it could provide 2800 years of power at a constant rate [5]. The major barrier of applying the geothermal technology lies in finding the proper location and technology for extraction. Often, potential sites are located close to tectonic plate boundaries at a depth of approximately 2 km [6]. Indonesia, being located near the Pacific Rim, has some of the greatest geothermal potential. It is estimated that around 28,617 MW are available for use while only 4% is being used currently [1]. The United States (US) has installed 3,093 MW of geothermal power as of 2010, with expectations to rise to 5,400 MW by 2015 [3]. Within the state of Idaho, U.S., there is an estimated 4,900 MW of energy available for use. A large portion of that is in the East Snake River Plain located in the southern part of Idaho [7].

Geothermal resources are often classified by their play type. The geothermal play type assists in understanding a potential resource as well as define exploration strategies to aid in evaluating a reservoir in terms of its potential use [8]. Two main types of geothermal are the convection-dominated play and the conduction-dominated play. The ratio of porosity to permeability is the key aspect to recognize the type. The geothermal play seeks to define geothermal potential on the characteristics of the material

instead of the temperature and enthalpy of the fluid while the goal is to use a geothermal play type with a more accurate identification resources in the future [8].

Specific Exergy Index (SEI) is another method of classifying a geothermal resource. Instead of classifying a geothermal reservoir based upon the temperature or enthalpy, which always differ from one source to another, SEI determines the quality of a geothermal resource based upon a non-dimensional exergy index [9]. This index provides an indication of the capabilities of a resource to produce power or heat independent of different specifications. Lower quality geothermal resources have SEI ranging from 0.0-0.04, while medium quality resources range from 0.05-0.5. SEI greater than 0.5 is classified as a high exergy resource. SEI method of quantifying geothermal reservoirs has been employed in Indonesia [9], Japan [10], and Poland [11].

Public opinion evaluation on geothermal energy in the Villarrica community in Chile indicate that people lack information on geothermal technology. Lack of information made them feel less inclined to adopt the technology [12]. The media, with its strong effect on public perception, is capable of educating people on geothermal technology. A study on the effects of the media on geothermal power acceptance in Australia showed that people are concerned about economic feasibility and the science behind geothermal power, while industry was focused upon the risks involved [13].

This study explores geothermal technology beginning with an in-depth review of the various methods of geothermal energy extraction and potential methods of improvement. An analysis of geothermal-hybrid systems is presented with an aim to improve geothermal technology by pairing it with other forms of renewable energy. A new extraction technology is introduced by presenting present and past research. The growth of geothermal technology is not only dependent on public knowledge and availability of resources, but also on the efficiency of the technology. Methods of optimization and modification of operational parameters are categorized and presented. Two major factors of decision making, cost and environmental impact, are collected from research to show the role of geothermal technology in comparison with other energy resources. Various advantages and disadvantages of geothermal technology are also presented. Finally, potential areas for future study in geothermal technology are elaborated by concluding the present investigation.

2.3 Overview of Geothermal Heating Applications

This manuscript's focus is primarily on geothermal power production. However, the direct use of geothermal resources for heating applications is abundant globally and worthy of discussion. Growth of the technology is shown to be around 7% annually, and by 2020, the world will utilize around 200 TWh annually [2]. Around 70 GW of installed direct use capacity was in place worldwide as of 2015

[14]. It was reported that 55.2% of installed capacity used geothermal heat pumps (GHPs) to transfer heat from the geofluid to the heating space . The use of GHPs instead of more traditional heating methods saves around 52.8 million tons of crude oil annually. Figure 2 illustrates the global trend of installed capacity of the GHPs during 20 years.

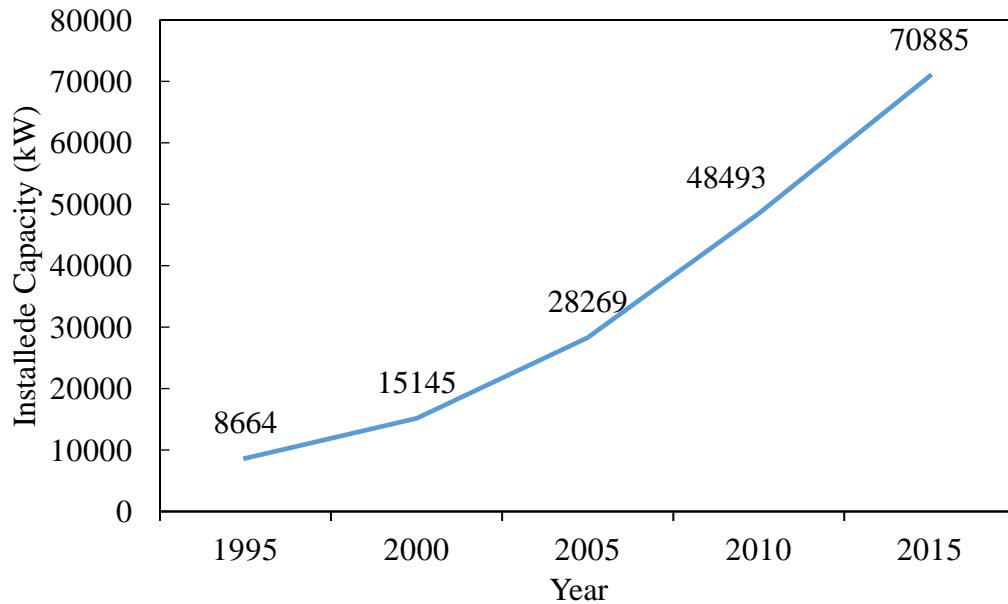


Figure 2.2: Installed capacity of worldwide direct use geothermal resources as of 2015 [14].

It has been determined that suitable aquifers underlay 16% of the Earth's land surface and between 125 to 1793 EJ/year of energy is available from aquifers for global heating use [15]. The thermal gradient is approximately $32\text{ }^{\circ}\text{C}/\text{km}$, meaning that significant energy found for direct use at a relatively shallow depth. Figure 3 depicts the maximum aquifer temperature in various locations on Earth, indicating significant geothermal resources are present throughout the world.

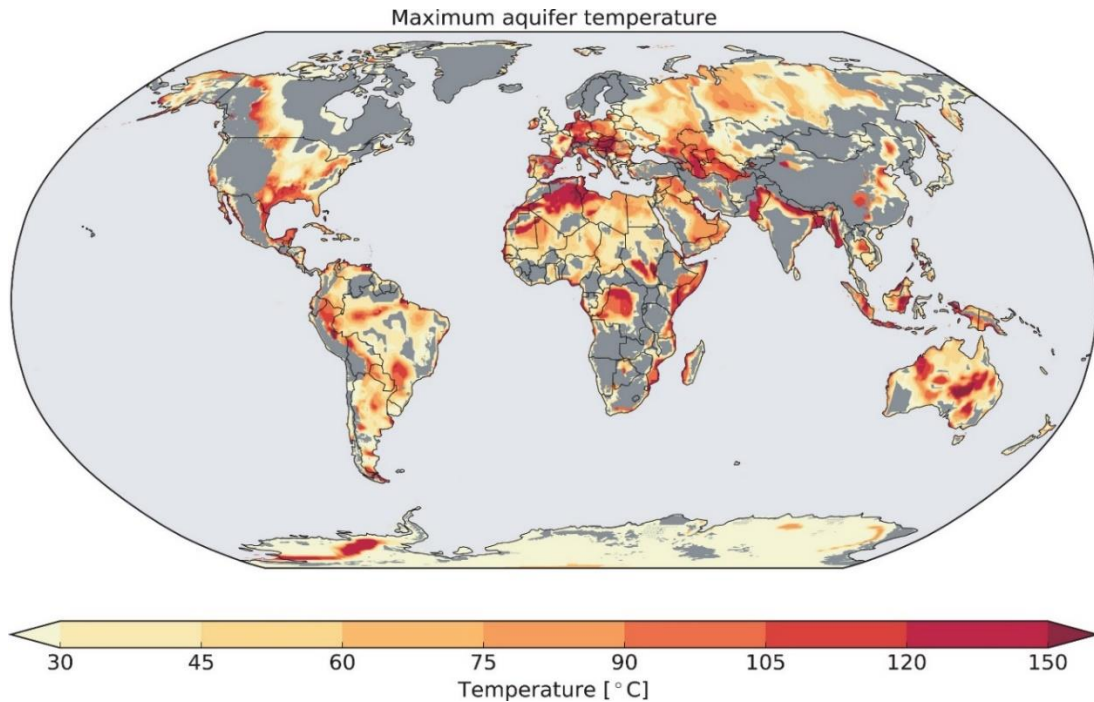


Figure 2.3: Global maximum aquifer temperature in various places worldwide [15].

Despite aquifers being a widely available resource, the use should be regulated to ensure sustainable development [16]. Since both drinking water and geothermal water come from shallow aquifers, some level of regulation should be enforced to ensure neither resource becomes contaminated [16]. Haehnlein et al. sent letters to over 60 countries inquiring about their legal standards regarding the use of shallow geothermal aquifers with the focus on the temperature limits as well as minimum distances between wells [16]. Outcomes showed a wide range of minimum distances, 5-300 m, while significant differences were found in allowable temperature drops between the extraction and re-injection wells.

2.4 Geothermal Power Plant Classes

There are multiple technologies for geothermal power extraction which depend upon the state of the resource. At higher temperatures where the geofluid exists as a superheated vapor, dry steam systems are used [17]. Dry steam plants compose around 23% of the total worldwide geothermal capacity, with 63 plants in operation generating a total of 2,863 MW as of 2014 [3]. The operation for dry steam is one of the most simple and least expensive designs for geothermal power plants. Superheated steam from the earth at high pressure is routed directly into a steam turbine, where power is extracted. Dry steam power plants typically have higher efficiencies than other types of geothermal power plants due to high temperature sources [18]. However, there are limits to using dry steam systems due to large temperature geothermal sources being harder to locate. Additionally, running hot steam from the earth increases the corrosion on turbine blades which increase operation expenses [3]. Figure 4 shows a simplified dry steam cycle for power generation.

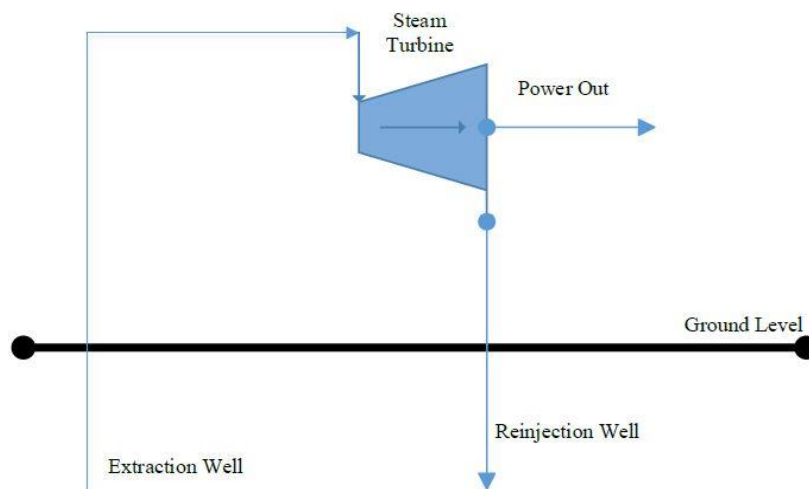


Figure 2.4: Simplified schematic of Dry steam cycle [17].

Another type of geothermal power plant is the flash steam system. As of 2014, flash steam composes the majority of the worlds geothermal power generation installed capacity at about 42% for single flash and 19% for double flash [3]. Flash steam cycles are used to harness geothermal resources that are composed of two-phase mixtures under high pressure and high temperature [17]. When these sources are brought to the surface, the geofluids are expanded within a seperator, resulting in part of the geofluid flash vaporizing. The vapor is expanded through a turbine for power generation. The majority of the total fluid remains as liquid, which is further expanded again at lower pressure to recover more energy in a double flashing cycle. Double flashing often results in higher efficiencies and power output for the same inlet conditions. Figure 5 illustrates a simplified Flash steam cycle for power generation.

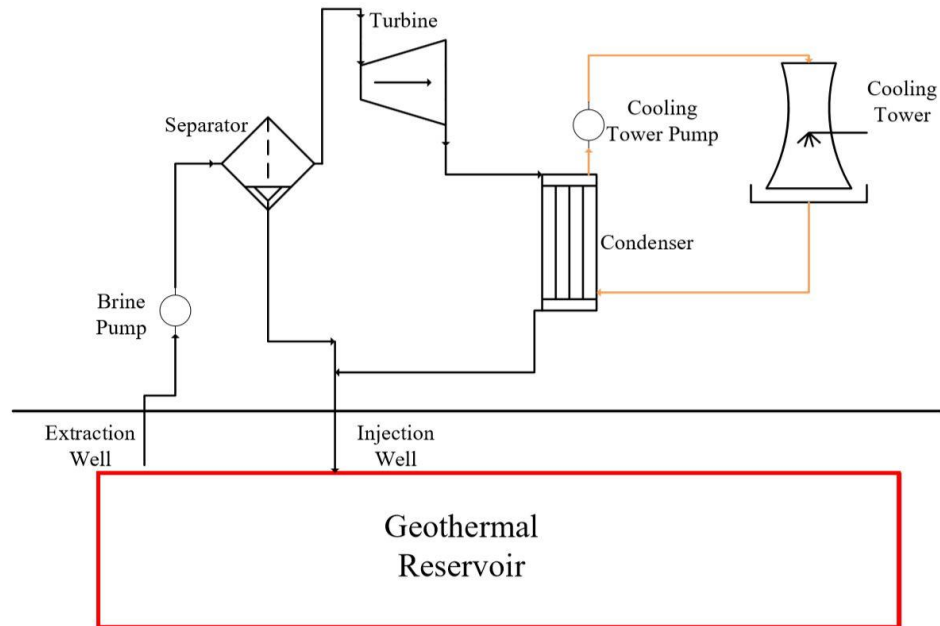


Figure 2.5: Simplified schematic of flash steam cycle [17].

A final configuration of powerplant is the binary organic rankine cycle (ORC). A binary ORC applies a heat exchanger to transfer heat from the geofluid into an organic fluid in an evaporator through a Rankine cycle, where power is extracted via a turbine [17]. The major advantage of the ORC is the ability to use low temperature geothermal resources as opposed to higher temperature ones required for dry steam and flash cycles [17]. Figure 6 depicts a simplified binary ORC for power generation. The Kalina cycle is similar to an ORC, however instead of using an organic fluid, ammonia-water mixtures are used.

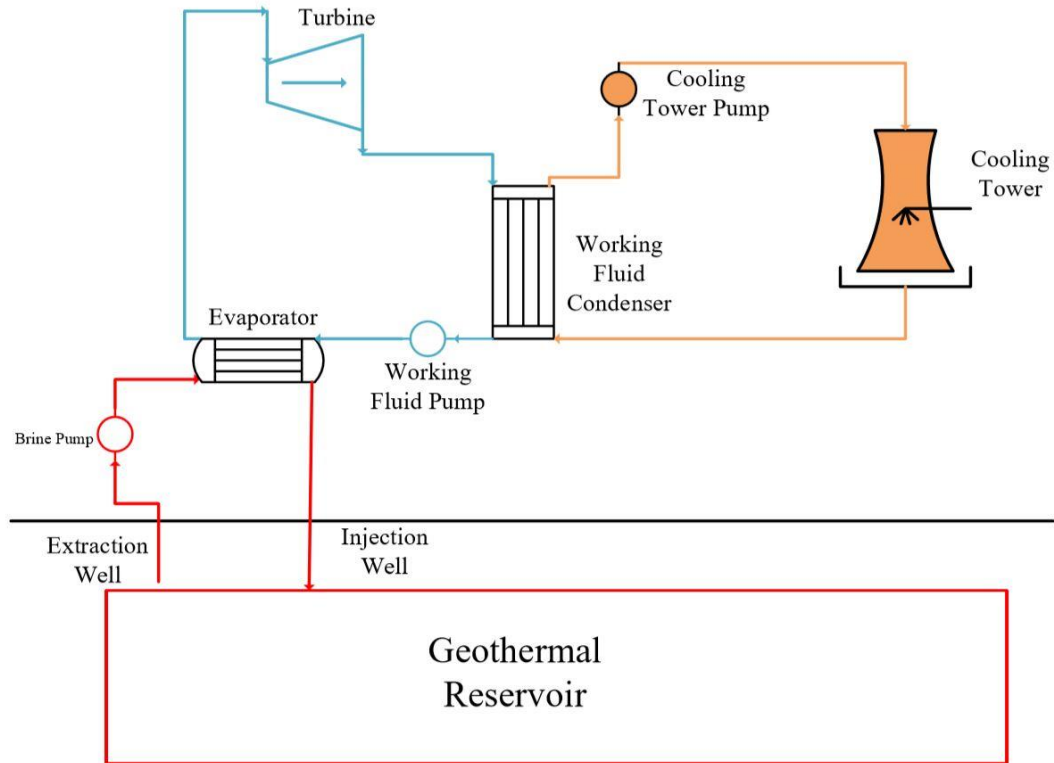


Figure 2.6: Simplified schematic of Binary ORC [17]

The use of organic fluids with low critical pressures and temperatures make it an excellent way to harvest energy from a low temperature geothermal source [19]. Other advantages include the fluid being superheated after expansion. This avoids the concern of two phase mixtures passing through a turbine and therefore extends their operational lifetime. Some estimates indicate the lifetime of ORC turbine blades are around 30 years while steam powered rankine cycle blades typically last around 15-20 years [20]. One disadvantage of ORC systems is the parasitic load resulting from pumping which is about 30% to 50% of the gross output power. Consequently the geothermal brine pump usually encompasses the greatest amount of power loss do to high flowrates and large pumping distances required [20]. Figure 7 shows capacity distribution of each geothermal technology.

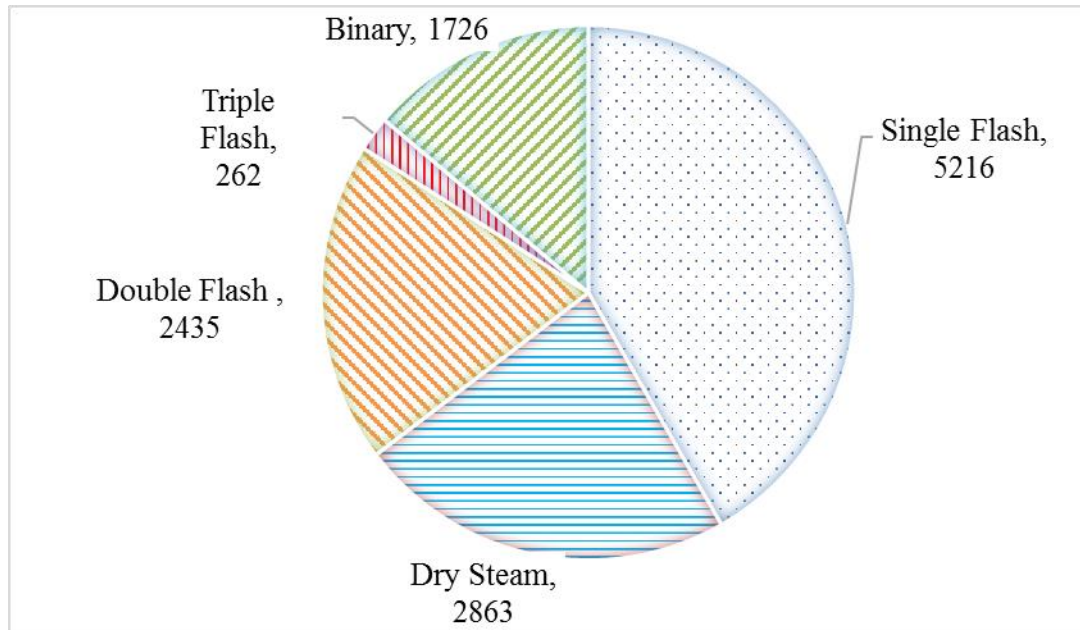


Figure 2.7: Installed capacity in MW for each type of power plant in 2015 [3].

2.4.1 *Dry Steam Technological Improvements*

By considering the simplicity of the dry steam technology, developing significant improvements is complicated. Dry steam requires a significantly high geothermal temperature source, usually greater than 200 °C. Some headway on increasing the efficiency of installed plants is underway [21]. A gas removal system (GRS) proposed in the Kamojang geothermal power plant located in Indonesia utilized excess steam to generate more power. The proposed 5 configurations were one and two stage steam ejectors, one and two stage liquid ring vacuum pumps (LRVP), and a hybrid system of an ejector plus an LRVP. The results showed the single stage LRVP increased the net power output by 7.6%.

2.4.2 *Flash Steam Technological Improvements*

Many technological innovations featuring flash steam cycles have been researched. These innovations have focused on increasing the amount of power extracted and improving efficiency. Using energy and exergy analysis for a single and double flash unit, researchers found that a double flash cycle outperformed a single flash cycle. The exergy efficiency for the double flash achieved 43.35% compared to 32.7% for the single flash [22]. The outlet temperature of the single flash water was approximately 155 °C where the double flash was around 102 °C, indicating superior utilization. Figure 8 illustrates pump power and net power output for single and double flashes.

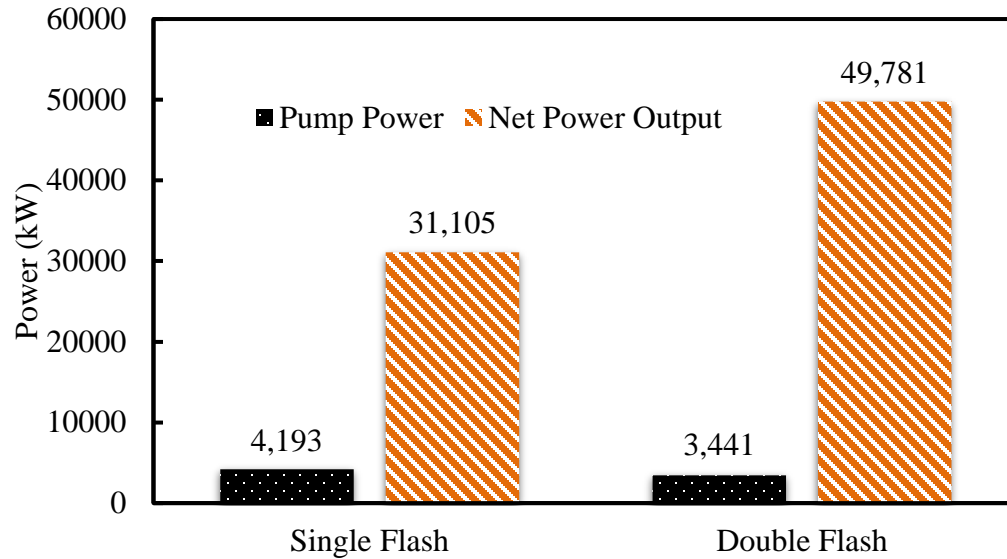


Figure 2.8: Net power and required pump input for the double flash and the single flash power plants [22].

Optimization of flash cycles can yield significant improvements in power plant performance. Researchers found that when optimizing a flash cycle for maximum power output, a separator pressure of 3 bar was optimal for single flash. Pressures of 7.63 bar and 1.06 bar were found to be optimal for the first stage and second stage separator, respectively [23]. The double flash produced 25% more power than the single flash while energy and exergy efficiencies were much higher in the double flash. Figures 9 and 10 depict the exergy use from the study.

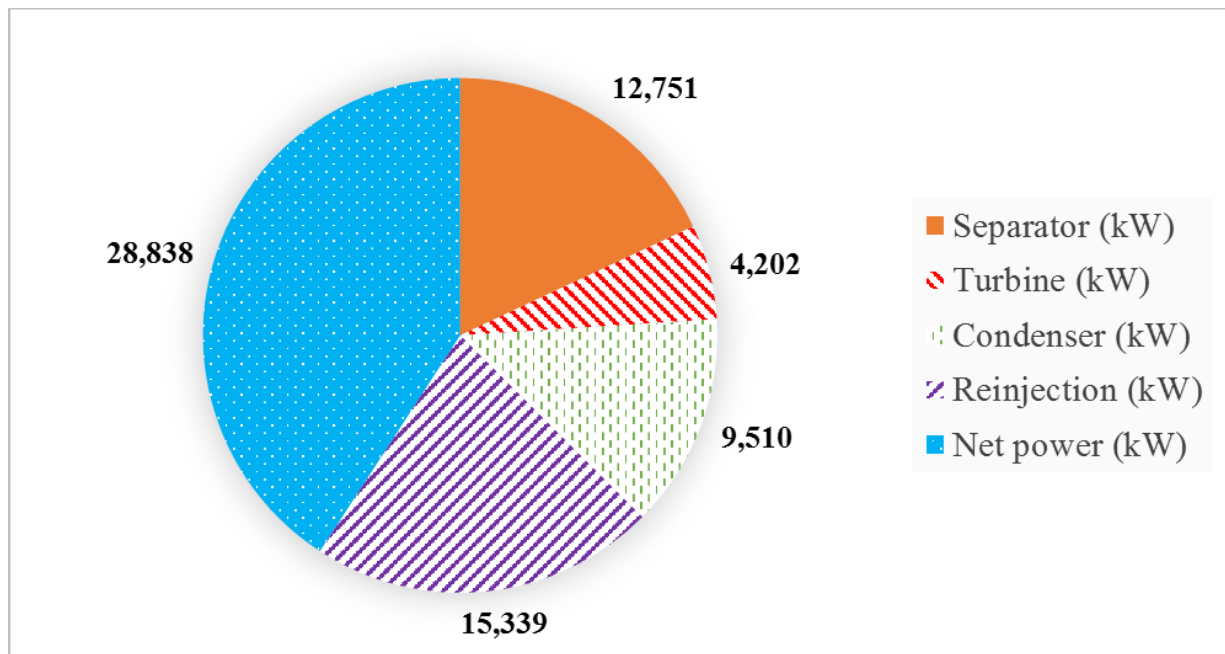


Figure 2.9: Exergy use (kW) for single flash power plant. [23].

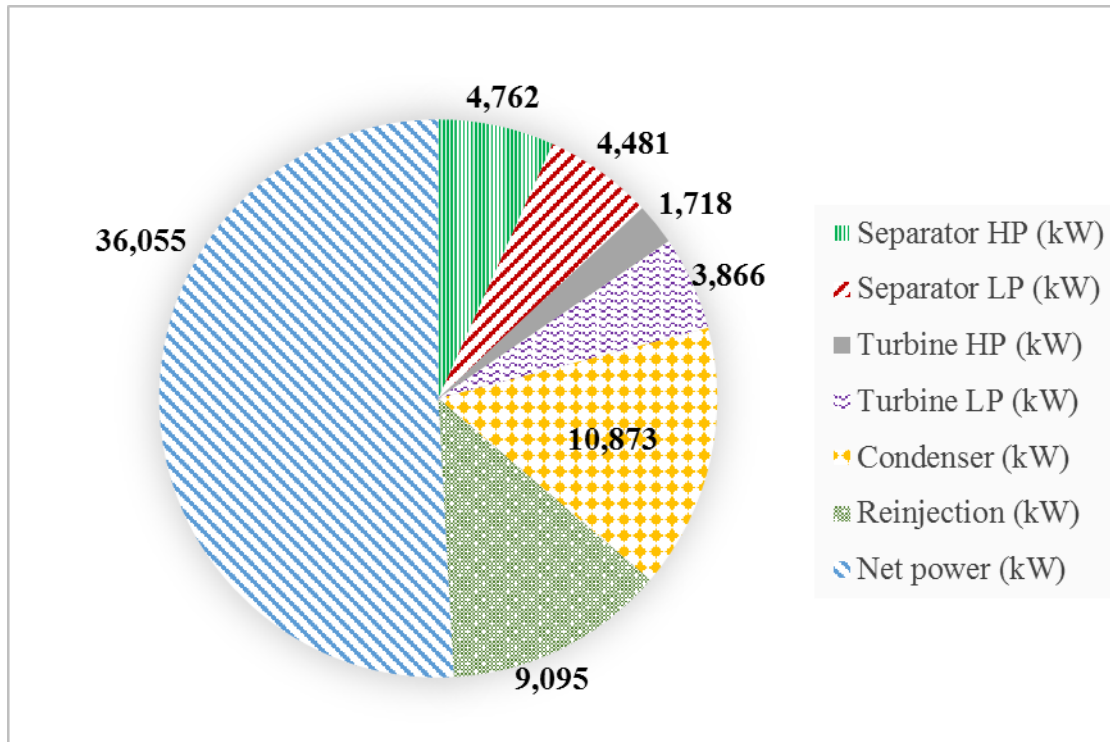


Figure 2.10: Exergy use (kW) for double flash power plant [23].

The net power output and thermodynamic efficiency of a single and double flash cycle paired with ORC and Kalina cycles were optimized by genetic algorithm (GA) [24]. The results concluded that the double flash ORC cycle had the highest exergy efficiency at 46.12%, while double flash Kalina followed with an exergy efficiency of 36.75%, and the regular double flash came in third with a 31.92% exergy efficiency. Despite the relatively high exergy efficiency of the flash Kalina cycle, an increase of turbine inlet pressure of 0.4 MPa and 1.4 MPa was required over the double flash ORC and the double flash, respectively. The double flash ORC had the simplest configuration of equipment, while pairing ORC plants with double flash plants utilized more of the available geothermal resource. An enhanced organic flash cycle (EOFC) was modeled by using an internal heat exchanger to further recover waste heat from the geofluid leaving the flash separator [25]. When the separator was replaced with a two phase expander, net power output increased by 36.7%.

Many geothermal power plants face silica scaling problems [26]. The Dieng flash steam powerplant, along with a double flash, single flash with binary, and a double flash with binary was optimized for max power output and minimal silica scaling [27]. The outcomes indicated that the binary double flash system generated the most power, while it was more susceptible to silica scaling, and degraded the geothermal system performance. Furthermore, the double flash was less expensive and mechanically less complicated than the single flash with binary.

2.4.3 Binary Organic Rankine Cycle Technological Improvements

Due to lower temperature geothermal systems being more common, current geothermal research is focused on improving the performance of binary ORC's [28]. One way of improving the cycle is selection of the optimal working fluid. The selection of working fluids affects the power plant efficiency, cost, and safety. Four different working fluids were compared in an ORC; Ammonia, HCFC123, n-Pentane and PF5050 [29]. A cost-effective design applied the ratio of heat exchanger area to net power output as the objective function. Four parameters, evaporation temperature, condensation temperature, geothermal water velocity, and cooling water velocities were considered. The results showed that ammonia minimized the objective function and maximized geothermal water utilization. However, the exergy efficiency of the ammonia was decreased during the optimization process. Table 1 compares characteristics of Ammonia, HCFC123, n-Pentane and PF5050 as working fluids.

Table 2.1: Comparison of Ammonia, HCFC123, n-Pentane and PF5050 as working fluids [29].

Working fluid	PF5050	HCFC 123	Ammonia	n-Pentane
Gross power (MWe)	10	10	10	10
Evaporation temperature (°C)	80	79.9	76.9	80.2
Evaporation pressure (MPa)	0.48	0.49	3.83	0.37
Condensation temperature (°C)	41	41.6	43	40.7
Condensation pressure (MPa)	0.14	0.16	1.7	0.12
Geothermal water outlet temperature (°C)	85.7	85	81.45	86
Geothermal water flow rate (kg-s ⁻¹)	8496	5972	3693	7236
Cooling water flow rate (kg-s ⁻¹)	6598	4864	3898	4640
Working fluid flow rate (kg-s ⁻¹)	1243	669	494	294
Net power produced (kW)	8718	8766	7766	8940
Geothermal water pumping power (kW)	395	454	767	374
Cooling water pumping power (kW)	522	567	842	518
Working fluid pumping power (kW)	365	212	624	169
Evaporator area AE(m ²)	7059	3766	1364	5660
Condenser area (m ²)	3961	2773	1377	2317
Rankine cycle efficiency η_R (%)	7.8	9.8	8.9	9.9

The research continued into optimal working fluids with four different ORC fluids, isopentane, isobutane, R245fa and R227ea, in a combined heat and power (CHP) setup at temperatures below 450 K [30]. The exergy efficiency was tested in both a parallel and series setup. CHP increases the thermal efficiency of the cycle up to 20% over power generation only [30]. It concluded that the most efficient setup for CHP consisted of a series configuration and a fluid with a high critical temperature, like isopentane. If power generation was the primary emphasis, then the preferred setup was a parallel

configuration with a low critical temperature fluid, like R227ea. Parallel setups offered a part load advantage of the ORC which allowed for more flexibility in operation [30]. Figure 11 illustrates the exergy efficiency of different circuit setups.

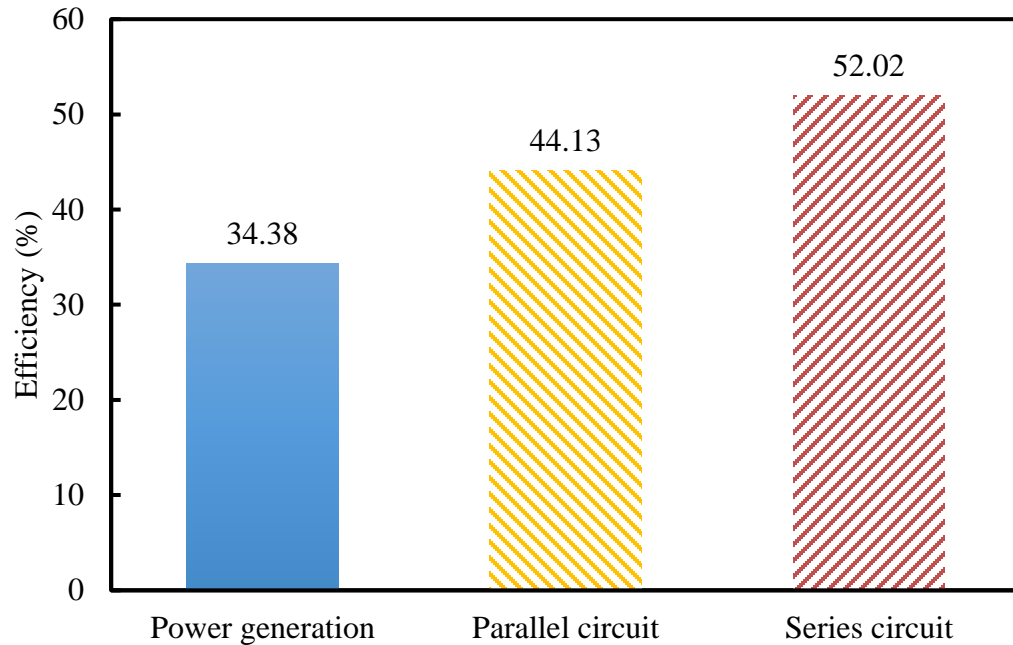


Figure 2.11: Exergy efficiency of isobutane for power generation only parallel CHP, and series CHP [30].

A wider range of working fluids investigated for thermal efficiency, exergy efficiency, recovery efficiency, heat exchanger area per unit power output (APR) and the levelized energy cost (LEC) were used to quantify the effectiveness of an ORC [31]. The recovery efficiency defined as the ratio of available energy recovered from the geothermal water and LEC as the ratio of the cost of the system to net power generated. Eighteen fluids tested, some of them operated in subcritical cycles while others operated in a transcritical cycle. The analysis indicated that R123 in a subcritical ORC system yields the highest thermal efficiency at 11.1 % and an exergy efficiency 54.1%. When R125 was used in a transcritical cycle it achieved a thermal efficiency and exergy efficiency 46.4% and 20% lower than R123. Other results indicated that fluids favoring high thermal and exergy efficiency were R123, R600, R245fa, R245ca and R600a; the liquid with the high recovery efficiency were R218, R125 and R41 while in R152a, R134a, R600 and R143a; low APR value, R152a, R600, R600a, R134a, R143a, R125 and R41 showed low LEC.

Fluid mixtures of isobutane/isopentane and R227ea/R245fa were studied as a potential working fluid in an ORC [32]. Outcomes showed that mixtures possess a non-isothermal phase change that leads to efficiency increase. Moreover, exergy efficiency increased by 4.3% and 15% over the pure fluids at source temperatures of 120 °C and below. Using mixtures allowed for further optimization of

geothermal plants by allowing safety, chemical and physical properties to be altered to suit the needs of locations.

A regenerative ORC was researched to explore the effects of extracting working fluid between turbine stages in order to preheat fluid entering the evaporator [33]. The internal heat exchanger setup transfers additional heat from the turbine exit into the fluid entering the evaporator. A regular ORC was found to cost the least while generating the most power. The internal heat exchanger setup increased the energy and exergy efficiencies from 13.51% and 49.41% in the regular ORC, to 15.33% and 54.29%.

A thermo-economic evaluation of four power plant variants of the ORC were parametrically studied and ranked accordingly using Multi Criteria Decision Making [34]. The ORC variants studied included basic ORC, dual Fluid ORC, regenerative ORC, and ORC with an internal heat exchanger and used the Sabalan power plant geothermal resource. Five ranking criteria were used; exergy efficiency, energy efficiency, net power output, production cost, and total cost rate. The most important criteria for ranking the systems was found to be the total cost. The rankings obtained from best to worst were the internal heat exchanger variant, followed by basic ORC, dual fluid ORC, and finally the regenerative ORC. Additional research has indicated that combining these variants of ORC's with liquid natural gas cold energy can provide more benefits [35].

An exergeoeconomic analysis of an ORC, dual-fluid ORC, dual-pressure ORC and Kalina cycle powerplant was performed with the goal of optimizing for highest net power output and lowest unit cost [36]. The researchers found that the dual-pressure ORC generated 15.22%, 35.09%, and 43.48% more power than the base ORC, dual-fluid ORC, and Kalina cycle, respectively. The Kalina cycle had the lowest cost of produced electrical power.

2.5 Integrated Geothermal Systems

The pairing of multiple power generation systems is known as cascading. Current systems pair geothermal power with solar, biomass, thermoelectric generators (TEG), hydrogen production, trigeneration, as well as other forms of direct use [37]. When geothermal resources are harvested there is often remaining enthalpy remaining in the geofluid that can be used in a different application. An example would be a medium temperature geothermal resource generating electricity in an ORC power plant where the outlet temperature of the geothermal brine is sufficiently high enough to be used in a heat pump heating application. Even a third or fourth level of extraction is possible by using the remaining heat for food or agricultural drying purposes, or possibly for aquaculture.

2.5.1 Geothermal and Solar Paired Systems

Hybrid solar-geothermal power systems are not complicated to configure in different operating conditions, and they are proven to be reliable by using low cost collectors to keep prices competitive with other forms of electricity [38]. There is also the opportunity of multi-generation (heating/cooling) applications while additional capital cost savings is expected from shared equipment between systems. The shortcomings of hybrid solar-geothermal power systems are lower efficiency cycles, corrosion and scaling issues, as well as multi-generation facilities requiring multiple heat sinks [38]. There are three general strategies for combining geothermal and solar [38]:

- a. Superheating the working fluid of the power cycle,
- b. Preheating geothermal brine or increasing the quality (mass fraction) of vapor in a dry steam application,
- c. Geothermal preheating of Rankine Cycle feedwater in a solar plant.

Superheating the working fluid and preheating the geothermal brine were compared while using an optimization scheme to maximize the exergy efficiency. Results showed that using solar power to superheat the steam resulted in greater power generation [39]. Both delivery methods were applied to a single and double flash power plant and results showed increases of 0.23 kWe/kWth and 0.29 kWe/kWth for single-flash and double-flash hybrid plants, respectively. Heating the geothermal brine resulted in an increase of 0.16 kWe/kWth and 0.17 kWe/kWth for the single and double flash, respectively [39]. The double flash system required less aperture area for the optimized exergy, which also results in lower costs. The levelized cost of electricity (LCOE) for the two systems was \$64/MWh and \$56/MWh, for single and double-flash hybrid systems, respectively [39].

Study of a hybrid geothermal-solar power plant in the hot climate of Australia in both steady and unsteady conditions revealed that geothermal power often suffers a decline in power output in high ambient temperatures, such as midday. The higher temperatures limits the effectiveness of the air cooled condensers to reject heat [40]. The study concluded that the optimized operation of the system for maximum power generation occurred when 48% of total energy was supplied from solar energy. Moreover, the LCOE could be lowered from 225 \$/MWh using geothermal sources only, to 165 \$/MWh with combined geothermal and solar. LCOE was dependant upon the size of the solar field area. In general, the lower the temperature of geofluid, the greater the fraction of solar energy is required to make up for the lack of available energy. However, the effect of ambient temperature as well as the availability of solar energy is likely the most critical variable, hence the effects are going to be geographic dependant [40].

A micro solar-geothermal plant was investigated by downsizing plants to a small scale to provide power for local communities without using long transmission lines [41]. The proposed system used an ORC paired with evacuated, non-concentrating solar collectors, and a 50 kW turbine. The best scenario occurred when the geothermal wells had already been previously drilled, making the project less expensive. Several major factors that caused significant problems with the system are as follows [41]:

1. The operational hours were limited by the availability of sunlight,
2. The pumps circulating the working fluid and the well fluid had a parasitic effect on power generation,
3. Considerable heat exchanger area and well depth were required, which increases cost.

The economic analysis of hybrid geothermal-solar power systems concluded that optimized geothermal was more economical than this hybrid system [42]. A binary ORC geothermal power plant coupled with a low-temperature solar trough system was compared to an un-optimized ORC as well as an optimized ORC. It was discovered that for most of the year, the constant flow of the hybrid system outperforms the geothermal, while at other times, when there was not enough sunlight and the ambient temperature was high, there was not enough difference in fluid temperature for the solar system to have higher impact [42]. The second phase of the project aimed towards varying the flow rate in the hybrid system to optimize its performance and again compare it to the geothermal scenarios. The results illustrate a 5.5% and 6.3% net power increase in the hybrid system over the geothermal only; the hybrid system showed a 2% decrease from the un-optimized geothermal; and when the geothermal system was optimized, it decreased its LCOE by 8%, making it more economical than the hybrid system despite generating less power [42]. The cost of different scenarios of hybrid geothermal-solar power systems and optimized geothermal systems are depicted in Figure 12.

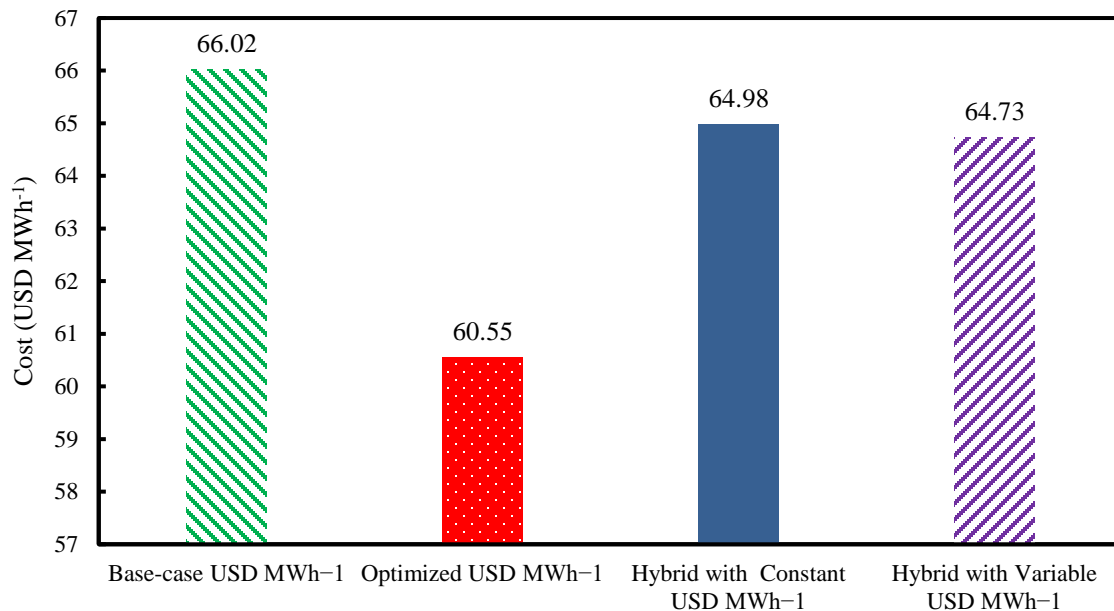


Figure 2.12: Comparison of cost for a base geothermal, optimized geothermal, solar-geothermal hybrid with constant load, and solar-geothermal hybrid with variable load [42].

A study on integration of a solar-powered steam-Rankine topping cycle to an existing geothermal plant in southwest Turkey indicated that greatest source of exergy destruction occurred in the solar collectors [43]. The hybridization allowed for more power to be generated at midday, when temperatures were hottest and electricity prices were the highest, while power plant output was at its lowest. Consequently, the solar surplus decreased the LCOE and increased the exergy efficiency of the cycles [43]. The choice of working fluid within the solar collector was investigated by considering a binary ORC with four different working fluids, R134a, R423A, R1234ze and R1234yf, paired with a solar collector using copper oxide nanoparticles in the working fluid [44]. An objective function for optimizing several variables including cost, thermal and exergy efficiencies, and heat exchanger area was developed. Figure 13 shows thermal efficiency before and after optimization for various working fluids. Four major conclusions were drawn from the study [44]:

- First, the use of water/CuO as the heat transfer fluid in the solar collector increased the daily thermal and exergy efficiencies, decreases product cost rate, and increases the total heat exchanger area required when compared to pure water.
- Second, the maximum thermal efficiency of 39.94% and minimum total cost rate of 5,819\$/yr. was found when using R1234ze, the maximum exergy efficiency of 3.148% was calculated for R134a, the minimum total heat exchanger area was 120.3 m² for R1234ze.

- To maximize single objective functions, the daily thermal and exergy efficiencies of R134a were raised by 62.14% and 4.98% over the initial total optimization. By optimizing the thermal and exergy efficiencies, the heat exchanger area was raised to 353.6 m² and 352 m² for thermal and exergy efficiencies respectively.
- When heat exchanger size was optimized, R423a was found to have the least area and least cost at 63.28 m² and 3424 \$/yr., which was a 47% and 46% improvement over the baseline. After multi-objective optimization, R134a had the best thermal and exergy efficiencies of 52.058% and 3.19% while R423A had the minimum heat exchanger area of 116.984 m² and R1234yf had the lowest cost at 5267 \$/yr.

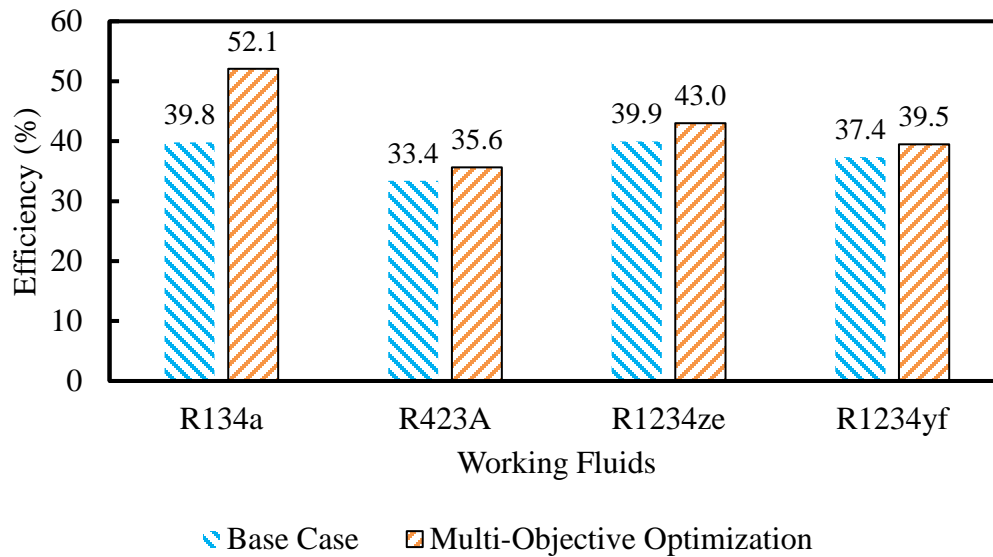


Figure 2.13: Thermal efficiency of un-optimized versus multi-objective optimization of a geothermal-solar hybrid power plant [44].

A hybrid multi-generation solar-geothermal system with five outputs of electrical power, cooling, space heating, hot water and industrial process heat was studied for energy and exergy efficiencies and then compared with a single generation system [45]. The single generation yielded an energy efficiency of 16.4% while the multi-generation yielded 78% efficiency. Moreover, the exergy efficiencies were calculated 26.2% and 36.6% for single and multi-generation respectively with 75% of the exergy destruction occurring in the solar collectors.

In Nevada, Enel Green Power implemented a triple generation setup including a geothermal, PV, and solar trough system. Stillwater was the first plant to integrate all three technologies into one power plant [46].

The integration of thermal energy storage (TES) with solar-geothermal plants provides favorable economic conditions. Geothermal-solar system enhanced with TES was investigated to study the impact of TES [47]. The system used an air cooled ORC with a solar trough heating system to provide higher temperatures for the geofluid. The use of the TES allowed for excess energy to be captured during inefficient running times. The use of the solar trough and TES increased power generation by 6.3% and lowered the LCOE [47].

2.5.2 *Other Geothermal-Hybrid Systems*

Despite the majority of research for geothermal-hybrid systems being focused on pairing geothermal and solar technologies, there is a considerable amount of research into systems that use geothermal technology paired with biomass, hydrogen production, thermo-electric generators (TEG's), and cogeneration with additional fresh-water production.

A proposed geothermal-biomass system for the Rotokawa 1 powerplant in New Zealand with a 29 MW flash-binary showed the addition of a biomass superheater inserted between the separator and the steam turbine increased the net power output around 32% [48]. Combined geothermal and biomass systems that provided both heat and power to Cornell's campus were studied in Ithica New York [49]. It was concluded that the CO₂ emissions were reduced to 43% of the 2012 campus emissions when implementing the geothermal pairing [49].

Recently, a novel combined cooling, heating and power system that integrated biomass, natural gas, and geothermal energy was proposed in an effort to maximize energy efficiency, maximize use of renewable energy, and improve reliability of energy delivery [50]. The team found that introducing natural gas into the system increased system reliability while also improving efficiency. A methodology for evaluating the potential benefits of geothermal energy and biomass resources using multiple energy pathways for meeting energy demand in urban areas was examined in Lausanne, Switzerland [51]. In the model, multiple options for pairing geothermal energy and biomass resources are implemented. The options included combustion in boilers and cogeneration engines, pyrolysis, gasification, and synthetic natural gas (SNG) production for woody biomass. The team concluded that pairing geothermal resources with biomass allowed for reduced cost and reduced environmental impact when compared to stand-alone systems. The best scenario was found when excess geothermal heat is used to increase the efficiency of biomass conversion processes.

Hydrogen production using geothermal resources as an energy source is showing increased research attention. A new way of producing hydrogen through electrolysis powered by geothermal resources was investigated by conducting an exergoeconomic analysis [52]. The team concluded that the cost of

producing the hydrogen was proportional to the cost of generating the electricity, while the temperature of the water source and the exergy cost of electricity generation increased [52]. The system reported energy and exergy efficiencies of 6.7% and 23.8%, respectively. Based on that study, the cost of generated Electricity was 0.0234 \$/kWh while the hydrogen price was 2.37 \$/kg H₂. Hydrogen production and liquefaction using geothermal energy was developed by seven models that utilized a binary ORC to generate the required power as well as a Linde–Hampson cycle for hydrogen liquefaction [53]. Results of the study stated that the prices of hydrogen production range from 0.979 to 2.615 \$/kg, depending upon the model. Higher temperature geothermal water source produced the least expensive hydrogen. In comparison, the average price of hydrogen in California for purchase is \$13.99 per kg, suggesting that these prices of produced hydrogen may be competitive in the market. [54] A multi-objective optimization of an ORC power plant using TEGs and hydrogen production was performed with the goal of comparing the optimized system to a basic ORC system from an energy, exergy, and exergoeconomic viewpoint [55]. It was concluded that optimizing an ORC cycle with a TEG for additional power production increased exergy efficiency by 21.9% while optimizing the cycle and using the electricity from the TEG for hydrogen production increased the exergy efficiency by 12.7% over the base ORC. Additionally, the specific product cost of the two optimized systems were lower than the base case. Research into the integration of TEGs and Kalina cycles for electricity generation only illustrated that the energy efficiency, exergy efficiency, and net power output increased by 7.3% when using TEGs. The most economically feasible option was found when cost of the TEG was less than 6.4 \$/W [56]. Increasing the turbine inlet pressure was shown to improve system energy and exergy efficiencies but results in increased cost.

Recently, replacing the condenser in an ORC with a TEG as well as installing a TEG to recover waste heat from geothermal brine was investigated [57]. Exergy efficiency, total product cost, and payback period were calculated. Exergy efficiency was increased by 4.67% over the base ORC system. The payback period for the TEG system was 15 days lower than the base ORC and power output was increased by 9%.

2.6 Enhanced Geothermal Systems

Enhanced Geothermal Systems (EGS) requires drilling to a depth where the temperatures of the mantle are sufficiently hot to transfer heat from the porous rock into a working fluid [5]. The working fluid is then pumped to the surface and power generated from any of the available power plant types. Hot dry rock is very commonplace on earth, with average thermal gradients being 25 to 30 °C/km of depth [5]. Some initial discussion proposes using dense fluids to increase the circulation pathways and reduce the permeability of the rock, allowing for easier flow from the injection well to the extraction well [5].

2.6.1 *Enhanced Geothermal Systems Projects*

The Fenton Hill hot dry rock site in New Mexico was one of the first EGS sites in the world and was drilled in 1980 by a team of German, Japanese, and US scientists [58]. Exploration revealed temperatures around 330°C at the bottom of a well. In the western United States, thermal gradients as high as 40°C/km are present, which makes it an attractive location for EGS [5]. As of 2018 there are 18 worldwide EGS operations and research teams working towards finding better ways to implement EGS [59]. The Enhanced Geothermal Innovative Network for Europe (ENGINE), is a group of 35 teams working towards reducing exploration costs by 20% and decreasing drilling costs by 20–30% [59]. The US has similarly provided a large amount of funding towards research as well as subsidies of 47-70% to perform exploration into EGS. The short term goals are to have five plants in operation capable of five years of operation by 2020 and reduce the price to 0.06 \$/kWh, and long term goal of 100 GW of installed capacity by 2050 [59].

Feasibility studies of EGS are being conducted in Europe to explore possibilities of EGS. Over 474 GW of power was estimated to be available using EGS in Germany [60]. The temperatures and rate of heat flow were calculated at depths ranging from 3500-9500 meters. Using the temperatures at the surface, 1000 meters and 2000 meters below the surface as indicators of further depths, the results indicated that a potential of over 6500 GW of power available at temperatures above 150 C and between 3 and 10 km below the surface [61]. Recently, a drilling operation from the Icelandic Deep Drilling Project (IDDP) drilled a borehole into magma at a depth of 2100 m where temperatures of steam reached as high as 450°C, indicating that there is potential for EGS sites [62].

2.6.2 *Enhanced Geothermal Systems Modeling*

Modeling is another crucial part of identifying the potential of an EGS site as different geological properties effect the success of EGS. The impact of reservoir stimulation in Western Malm Karst (Bavaria) was investigated by stimulating of a reservoir. Stimulation involves injection of high pressure fluids at a high flowrate into the underlying rock formation [63]. The stimulation created fissures and cracks in the rock bed that allowed heat transfer to take place between the hot rock and the working fluid. Commercially available hydraulic fracturing software was used to evaluate the tensile fractures from various stimulation and reservoir parameters. It was found that the stress state, permeability, porosity, and Young's Modulus of a rock formation had to be known before performing a stimulation [63]. High fluid leak-off zones required identification prior to stimulation to prevent fracture growth out of formation, and an increase in flowrate was found to increase fracture width and height, while increased volume was found to increase the fracture half-length. Lower flow rates led to

a more confined fracture zone, suggesting intermediate flow rates from 50 to 100 L/s was optimal [63]. Finally, it was concluded that higher permeability rock could reduce the number of stimulations in order to achieve the desired heat transfer [63].

Other models developed applied a 3-D numerical solver to optimize the output of the Soultz-sous-Forêts EGS project in France with regards to LCOE [64]. The modeling was based on previous geological models to create a thermo-hydraulic model focused on previous hydraulic faults and fractures. The outcomes showed that multi-well systems, such as Soultz-sous-Forêts, could be optimized faster than a doublet well due to the many different injection and extraction scenarios. Additionally, multi-well systems allowed for a greater heat exchange area through more fracture loops [64]. An in-depth simulation for a potential EGS site in the Dikili region using FLAC3D^{plus} and TOUGH2MP indicated that this region would be able to provide 83.7 MW over the course of 20 years [65]. The area was once an active volcanic zone, but since has cooled down considerably. The available power was found to increase linearly with increased injection rate. At higher rates the benefits tended to diminish, indicating an optimal injection rate existed [65].

In a collective study, modeling techniques of EGS reservoirs were categorized through a fuzzy inversion model and a direct inversion model [66]. The fuzzy inversion model output was able to create a temperature profile of the entire geothermal field as well as completely calculate all parameters of a potential geothermal reservoir, suggesting it may be superior to direct inversion models [66].

2.6.3 Seismic and Geological Effects of Enhanced Geothermal Systems

Often, seismic effects occur during stimulation which result in small earthquakes that present obvious safety concerns. Troiano et al. investigated the underlying reasons and sources of the seismicity by studying the effects of hydraulic stimulation within a reservoir [67]. Self-Potential (SP) monitoring is a well established method of examining fluid flow beneath the surface of a reservoir. Using real injection data from an earlier experiment, the SP was found to be a post-seismic effect. Additionally, the front of the SP anomaly follows the overpressure front of injection. The time delay between the two fronts decreases at increasing distance from the injection well [67]. The results showed that SP measurements provided the required information to understand the fluid expansion path during injection.

Geochemical and petrophysical effects of water injection into fractures was researched by Fritz et al. and several conclusions were drawn from the study [68];

1. When using analyzing the short term reaction kinetics, carbonates were more active in secondary phases of the system while long term reaction kinetics indicate silicates are more important for dissolution and precipitation processes,
2. Mass balance equations based on petrographic and mineralogical studies indicate the illitization processes due to hydrothermal alteration of plagioclases was predominant during earlier geological time periods. This explained high porosity in the illitized granites,
3. Silicates are very reactive in fluid-rock interaction zones, leading to secondary phases such as illites, smectites, and chlorites forming.

A software called Decision Aids for Tunneling (DAT) was developed to predict the costs of drilling an EGS field [69]. Uncertainties such as lithology, fractures, or water over-and under-pressure, all effect the drilling operation difficulty and time required. The DAT system modeled the cost of drilling by taking these uncertainties into account and allowed for a parametric study to find which uncertainties had the greatest effect on cost [69].

2.6.4 Working Fluid Selection for Enhanced Geothermal Systems

Water and CO₂ as the working fluids were compared for EGS systems by testing fluid losses, heat extraction rate, and CO₂ sequestration using different reservoir permeability parameters, geothermal gradients and surrounding formation permeabilities [70]. The results depicted that CO₂ has higher heat extraction compared to water when the surrounding rock permeability is high. When the parameters between both water and CO₂ were kept constant, the rate of CO₂ sequestration was twice the amount of water loss, the CO₂ loss ratio was 26% of the water loss ratio, the steady state heat extraction was about 7 times higher for the CO₂ compared to water, and the cumulative net electricity output of the CO₂ was found to be 25 times higher than water [70].

Another study showed CO₂ is superior to water as a working fluid. CO₂ has greater buoyancy forces due to its larger compressibility and expansion properties, which easily separate the colder and hotter CO₂ in the well [71]. Water is also a solvent for many minerals, which effects permeability of the rock structure. CO₂ has a lower heat capacity than water, however this is made up for the ease of extraction and much lower viscosity of CO₂ than water which allow it to move through a pipe much easier [71]. At typical operation conditions of 200°C and several bars, CO₂ has fluid-like density but gas-like viscosity, and fluid losses for CO₂ EGS are around 1 Ton/s per 1000 MW, which makes a 1000 MW EGS system able to store all of the CO₂ emitted by 3000 MW worth of coal fired plants [71]. The added effect of CO₂ sequestration has potential to provide an economic and environmentally safe way

to reduce atmospheric carbon [72]. CO₂ sequestering is gathering large amounts of research attention [73]. In particular, CO₂ sequestration efficiency predictions using neural networks shows the feasibility of sequestering CO₂ for EGS [74].

2.7 Environmental Impact of Geothermal Systems

The environmental impact of high and low enthalpy geothermal systems using an in depth life cycle analysis (LCA) was investigated [75]. Their results concluded that working fluid losses in ORC power plants accounted for 73% and 28% of ozone layer depletion (ODP) and global warming potential (GWP) respectively. They also concluded the use of eco-friendly fluids and optimization of material resources would further increase the benefits of ORC's. In a review of several LCA's for binary, single flash, double flash, and dry steam plants, it was shown that local geological characteristics, system boundaries, life span, and the impact assessment method and allocation procedure were all shown to effect the outcome of an environmental LCA [76]. Table 1 illustrates the summary of LCA of different geothermal power plants around the globe.

Since most studies focus on local geological, technological, economic and environmental aspects, it is difficult to analyze geothermal technology as a whole due to the individual complexities involved in each power plant configuration. LCA of geothermal plants is further complicated by the availability of reliable data [77]. Most data is reported anonomously, which results in large uncertainty. Additionally, some places do not regulate emissions of CO₂ which furthers the problem of unreliable data.

The environmental impact of four geothermal power plants located in Italy concluded that greenhouse gasses emitted from the plants rivaled natural gas plants. The likelihood of acidification was 2.2 times higher in the geothermal power plants than coal power plants and 28 times higher than natural gas power plants [78]. Open loop systems, such as dry steam or flash steam cycles, release gasses normally trapped underground. Binary cycles, which are closed loop systems, offer a potentially better option in regards to releasing gasses [78].

Table 2.2: Summary of geothermal power plant LCA's from cradle to grave [76]

Technology	Impact assessment method/approach a	LCA software	Goal and scope	Country
Dry steam and Flash power plants	GHG emissions aggregated based on GWP values	GREET	Comparative evaluation of geothermal power plants	U.S.
Dry steam and Single flash	CML, 2002	Simapro 7.3	Environmental assessment of electricity production from geothermal power plants	Italy
Double flash	LCE	NA	Comparative evaluation of nine power generation technologies	Japan
Double flash	CML2, 2000fCED	Simapro 7	Environmental assessment of geothermal power production	Iceland
Double flash	GHG aggregated based on the GWP from IPCC 2007	GREET v 2.7	Comparative evaluation of geothermal and other electricity generation technologies	U.S.
Double flash	NA	NA	Environmental assessment of electricity production from geothermal power plants	France
Double flash	CML 2001	GaBi v6	Comparative evaluation of geothermal and other electricity generation technologies	Turkey
Binary cycle	GHG aggregated based on the GWP potential from IPCC 2007	GREET v 2.7	Comparative evaluation of geothermal and other electricity generation technologies	U.S.
Binary cycle	CO ₂ emissions aggregated	Simapro 7	Comparative evaluation of four renewable energy technologies	New Zealand
Binary cycle	CML 2001	Simapro 7	Environmental assessment of geothermal power production	Spain

a. SI unit system used in all studies.

Based on a study on dry steam plant in Italy, energy returned on energy invested (EROEI) was 4, which compared quite well with fossil fuel power plants that typically operate in a range from 3.7 to 10.6, additionally, the power plant emitted around 248 g CO₂/KWh, which less than natural gas (380 g CO₂ kWh⁻¹) [79]. CO₂ emissions were higher than other renewable energy sources such as solar and hydropower. Despite a favorable GWP, gasses such as hydrogen sulfide, mercury, arsenic and other chemicals are released into the atmosphere during operation.

LCA of an ORC plant indicated that the majority of environmental impact is caused by the construction of the well systems. Proper exploration techniques reduce impact by yielding a superior well system with minimal drilling and maintenance [80]. ORC's face an increased auxilliary power requirement for the mnay pumps, which limit the efficiency of the plant and increase environmental impact.

In Monte Amiata, Italy, a flash steam power plant utilized a re-injection system for non-condensable gases [81]. The emissions of the power plant were reduced considerably while the power output of the system was decreased by 10%-20%, suggesting that environmental improvements can be made at the expense of power plant output.

The environmental effects of using geothermal power in transportation to generate electricity for electric vehicles was studied [82]. Since all geothermal plants differ, a stochastic approach was used to determine the variation in plant operations and outcomes. It was concluded that geothermal electricity provided far greater environmental benefits than fossil fuels when looking at providing electricity for transportation.

Shallow geothermal wells were evaluated with the goal of providing a framework for sustainable use. Static regulations, such as specific temperature threshholds, were not advisable when applied to geothermal systems [83]. Every geothermal system is unique with respect to their technical, economical, ecological, and social aspects and ultimately it was recommended to consider flexible limits based upon long-term undisturbed local groundwater temperatures.

Nine different power generation systems with respect to their CO₂/kWh emissions in Japan were compared [84]. Figure 14 shows the comparision between power plants. The life cycle emissions of goothermal power plants were broken down further into specific processes and parts of the plants life cycle [84]. The results are shown in Figure 15.

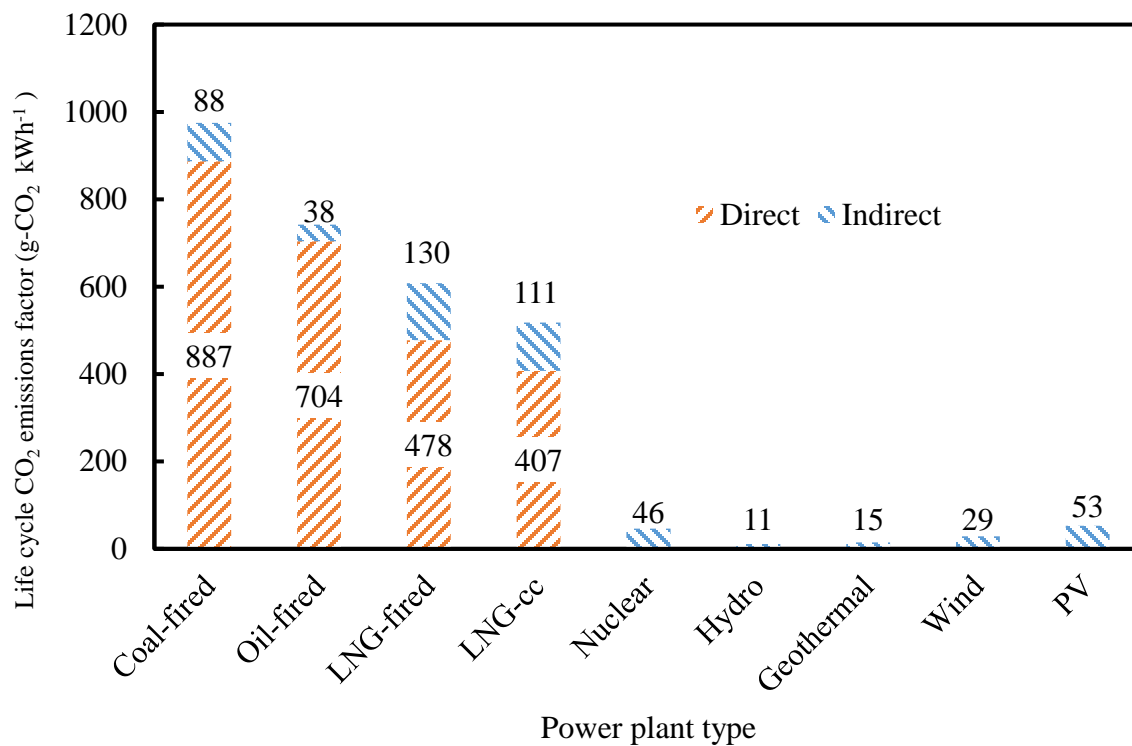


Figure 2.14: Emissions of different power plant types over the course of their life cycle [84].

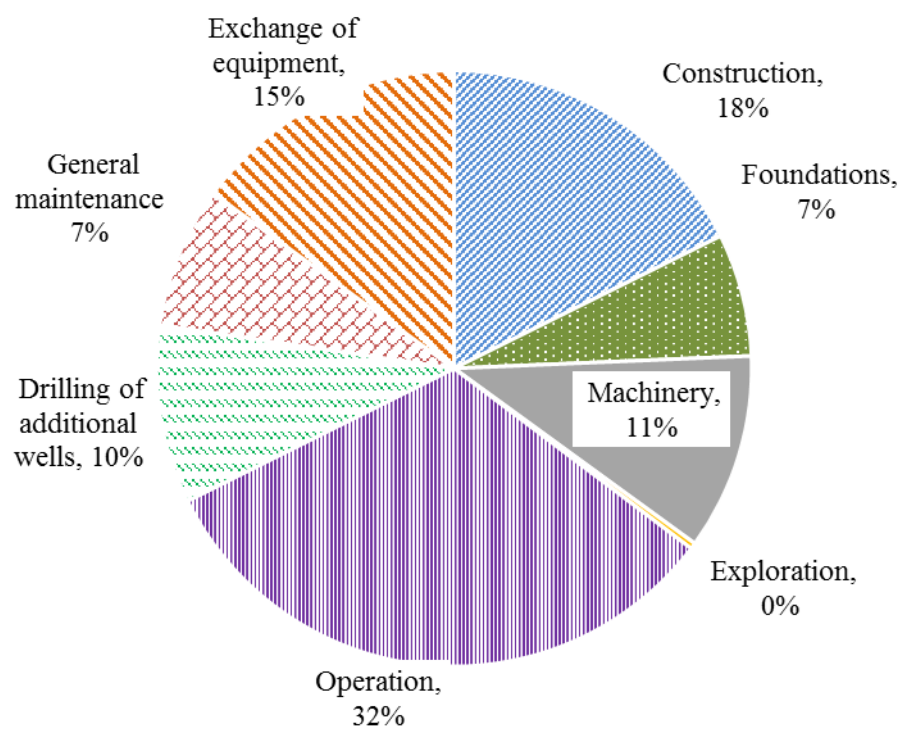


Figure 2.15: Breakdown of g-CO₂/kWh percentages for each part of the life cycle of a geothermal power plant [84].

An LCA of an EGS in the Upper Rhine Valley recently indicated that the majority of GHG emissions occur during the construction phase, meaning that longer operational lifetimes for the power plant will result in lower CO₂ emissions per unit energy production [85]. The researchers also concluded that using EGS for industrial heating instead of power may result in less GHG emissions.

2.8 Economics of Geothermal Systems

This section attempts to provide a general outline of economic elements that characterize geothermal technology as well as some generalities found among literature. Geothermal power plants are characterized by having high initial costs and longer payback times than other renewable technology. Anywhere from 5-7 years is often the amount of time it takes from exploration to commercial operation [86]. Even more burdensome is the quality and size of a resource is not known until drilling is complete, making geothermal technology more economically risky to attempt.

The cost of a powerplant is typically split into surface costs and subsurface costs. An analysis of investment costs for a geothermal power plant in an unknown geothermal field was performed in Iceland [87]. The surface costs consisted of surface exploration, designing and constructing the infrastructure, and the operation of the site while subsurface costs consist of the drilling. The outcomes indicated that the cost of an unknown field is greater than the cost of a known field. Cost breakdown for geothermal power plants from 20 MW to 60 MW of installed capacity are presented in Figure 15.

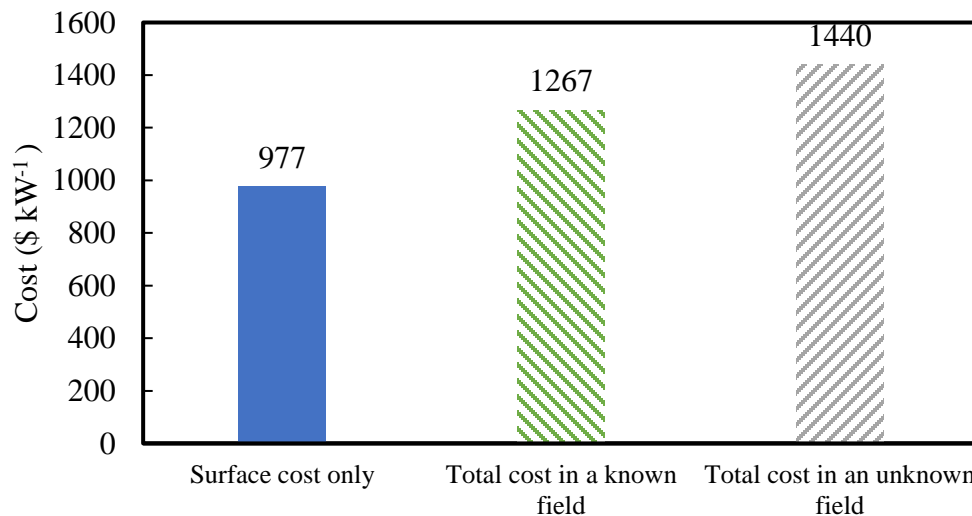


Figure 2.16: Cost breakdown for geothermal power plants in a range of 20 MW to 60 MW [87].

The economics of geothermal power generation, direct use, and combinations of both showed that using lower temperature geothermal sources for heating and cooling was more economical than power

generation [88]. If the same source was used for power generation and for heating/cooling, the heating/cooling would be able to generate about three times the revenue of power generation only.

Comparisons between drilling for geothermal and drilling for oil or gas indicated that while oil and gas were typically found in sedimentary rock, geothermal sources were often found in much different lithologies. Such lithologies included hard, abrasive, and fractured rock which increased the cost of drilling compared to oil and gas [89]. The geothermal wells have higher lithological heterogeneity which require a greater amount of stabilizing casing strings. The greater number of casing strings results in increased drilling times and costs for shallower wells. Hence wells of less than 3000 meters in depth were found to be less expensive for oil and gas, while deeper wells greater than 5000 meters in depth tend to favor EGS wells.

Drilling costs in the Soultz-sous-Forets EGS site in France was modeled by Euronaut. Euronaut aids in the decision process of determining drill sites and allows for better understanding of potential costs [90]. It was shown the drilling costs exponentially increase as the required well depth increases [90]. Since there is considerable room for optimization within geothermal power plants, economical optimizations are able to be performed. When optimizing the economic performance of a binary ORC geothermal power plant for multiple economic scenarios, the highest net present value (NPV) was reached when the cost of electricity was high [91]. Higher costs of electricity made it feasible to install a higher performance, and more expensive ORC. The analysis of internal economic factors showed that a higher availability factor led to the greatest NPV due to more power being available for sale at any given time [91]. The payback period (PBP), return on investment (ROI) and LCOE on 3 variants of a binary ORC including a regular ORC, regenerative ORC (RORC), and a Two-Stage Evaporation Organic Rankine Cycle (TSEORC) showed the degree of superheat was the most influential parameter in optimization [92].

Comparison of geothermal power adoption to wind and solar study suggested the lack of suitable locations to build a geothermal plant was the main reason it trails wind and solar. Most places with geothermal were located along plate boundaries and volcanic areas. It is also suggested that alternative forms of energy, such as fusion, fission, or solar are receiving more research funding compared to geothermal [93].

Study of the economics of geothermal power in the western US concluded that the higher gas prices were a catalyst for increased effort for geothermal power [94]. Electricity prices were found to be controlled primarily by the price of natural gas, due to the power generation portfolio in the western US being composed of large amount of natural gas power plants. It was suggested a special Geothermal

Portfolio Standard provide financial incentive to build geothermal baseload power plants [94]. Using Monte Carlo simulations, the costs associated with a double flash power plant were quantified. Figure 16 illustrates double flash levelized cost calculated.

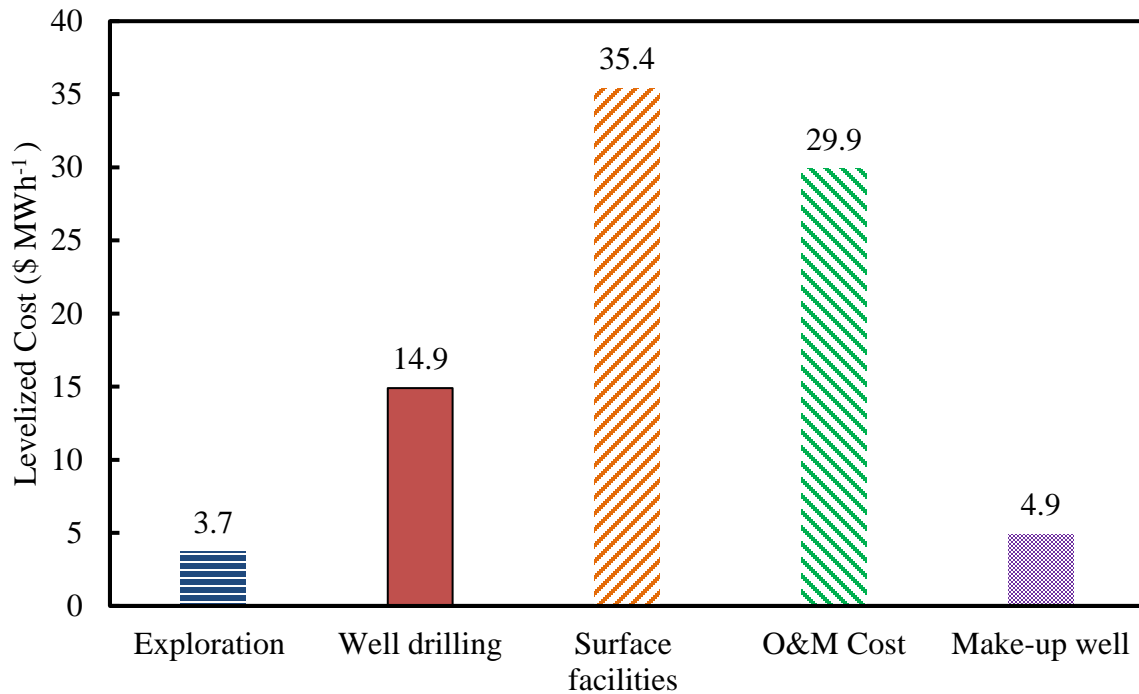


Figure 2.17: Double flash levelized cost [94].

Low temperature EGS for home heating in New York and Pennsylvania was researched with the goal of developing a supply curve for the region. The regional supply curve could then be used to predict the use of geothermal district heating in other northern areas. It was suggested that with current technology as well as the low price of natural gas, it was not better for the consumer to make the switch to geothermal district heating [95]. Although future improvements, coupled with an increase in gas prices, would surely make geothermal much more appealing.

A comprehensive methodology for the sustainable design of geothermal power plants is presented by Franco et al. [96]. The goal was to minimize the cost and maximize the efficiency of a geothermal power plant with a long operational lifetime as a source of sustainable energy. Using sustainable practices, it was possible to leverage the effectiveness of geothermal plants by making them economically feasible as well as meeting the world's considerable energy demand [96].

A recent study in China evaluated various investment strategies for geothermal heating by taking into account uncertainty in policy, technology, and geology [97]. The team constructed a thermo-hydrological model to develop a relationship between geological conditions and cost of investment.

Heating and carbon price, as well as investment and operation cost are taken into account in order to establish an investment strategy for geothermal heating projects. The team concluded three main ideas; first, they had established an assessment framework to evaluate the economic conditions of geothermal heating projects, second, the best way to improve economic scenarios for locations featuring low geothermal gradients is to improve the technology through technological innovation rather than rely on subsidies, third, geothermal investors are encouraged to adopt new and flexible financing models such as public-private partnership models and crowdfunding. Adopting new and flexible investment options will alleviate the pressure of the initial cost faced by investors during the construction phase.

2.9 Discussion

Having such an efficient power source with low environmental impact is very promising for a sustainable future. However, some drawbacks make geothermal power less attractive in comparison with solar and wind technology. That potential advantages and drawbacks are summarized below:

2.9.1 Advantages:

- **Lower land requirement:** Geothermal power plants require approximately 404 m²/GWh of land space, much lower than 1335 m²/GWh by wind [62].
- **Water scarcity:** The future will heavily be influenced by the availability of freshwater [98]. Geothermal power reported to use around 20 L/MWh of freshwater while other sources such as coal require over 1000 L/MWh [62].
- **CO₂ Sequestration:** Using CO₂ as the working fluid in an EGS has superior performance compared to water as well as an environmental benefit of sequestering CO₂ from the air [71].
- **Reliability:** Since geothermal power generation utilizes heat within the ground, its operation is not influenced by surface weather conditions. This allows for weather independent operation and gives geothermal power a comparative advantage over both wind and solar [1]. Geothermal power is also able to provide reliable base load power [93], [1].
- **Local job opportunity:** Effect of geothermal energy plant on job creation was compared to wind and PV job creation in Japan, and results showed that geothermal created an employment of 0.89 person-years/ GWh during its lifecycle, and 66% of this was associated with long term employment like operation and maintenance while wind and solar technologies had lower employment and more temporary jobs [99].

2.9.2 Disadvantages:

- **Lower efficiency:** The historical performance of geothermal power plants compared with other energy sources results reveals that over the course of the last century, the efficiencies of geothermal plants has risen only slightly while sources such as fossil fuels have risen by a significant amount. Early coal plants had efficiencies around 15–20%. In the 1950s,

efficiencies increased to around 35–40%, while combined cycle gas turbine–steam turbine plants today achieve efficiencies of 55–60% [100].

- **Higher initial investment:** Geothermal power with wind and solar were financially compared and it showed high initial capital costs, long payback time, difficulty to access the resource, and difficulty of modularization inhibit the growth of geothermal over wind and solar power generation technologies. [101].
- **Silica Scaling:** Geothermal power plants are often faced with the issue of silica scaling. Maintaining the proper head pressure to condense particulates out of the fluid is an approach to reduce foul up [102]. The effect of silica scaling in a geothermal power plant located in Turkey was measured and results revealed a continual drop of performance of the power plant over time. a 270 kW decrease was recorded in 2009 and by 2012, the decline was 760 kW [103].
- **Risk of geological changes:** EGS systems, which are based on pumping a working fluid into the fractured rock and extracting heat, can create seismic disturbances, called seismicity. Seismicity can lead to dangerous geological alterations and unsafe environments [104]. The seismic events are studied by applying both physics based models and statistical methods to predict seismicity. Physics based seismicity models help bridge the gap between induced seismicity and geothermal operations, while statistical seismicity models give insight into uncertainty quantification of the results [104]. Prior to injection, background seismicity should be monitored to establish a baseline for the site. When injecting fluid, it is important to perform stress mapping in order to understand the stress field. Using both of these allows for better understanding of seismic events [105].
- **Risk of a hydrothermal eruption:** A potential geological problem occurs when the pressure in geothermal aquifers near the surface reach a critical level and eject the surface material above it [4]. Craters ranging from 5-500 m in diameter and up to 500 m deep have been observed in Ahuachapan geothermal field, El Salvador and Wairakei, New Zealand. The possibility of a hydrothermal eruption must be considered when designing a geothermal system [4].

2.10 Conclusion

This paper has presented methods of harnessing energy through various geothermal technologies, as well as their potential integration with other technologies. Current advancement in technology, as well as an economic analysis, environmental impact, and summary of benefits and drawbacks have been presented. As time progresses, demand for energy is sure to increase, hence it is crucial that all viable sources of energy technology be considered. Geothermal technology has potential to supply baseload power, heating, and cooling for a wide range of consumers. Numerous studies are performed to show, modify, optimize, explore, and expand the capabilities of the geothermal technologies for more efficient and sustainable performance. There is likely a maximum amount of hydrothermal reservoirs available for power extraction. EGS are artificially created geothermal reservoirs that offer an alternative source of extraction. Temperature gradients within the Earth indicate that drilling to a sufficient depth yield temperatures hot enough for power generation. EGS may be an excellent way to sequester CO₂ and use it as a working fluid. Preliminary research indicates that CO₂ may be superior to

water due to being easier to pump through pipes and having greater buoyancy forces, which leads to greater heat transfer within the EGS reservoir. Despite the potential of EGS, some caution must be exercised because of risk associated with stimulating and fracturing rock that is only partially understood. However, extensive modeling has been performed from the perspective of power generation.

Geothermal power plants experience a large range of costs due to the high variability of the geothermal resource. Surface costs are dependant upon the location and type of power plant constructed. Another major obstacle facing geothermal power is the availability of suitable sites for power extraction as geothermal power requires drilling to a sufficient depth where geothermal fluid is present at a significantly high enough temperature and pressure. An alternative to finding more geothermal sources is to upgrade existing geothermal power plants. The following methods suggest the advancement methods of the current geothermal technology:

- Optimizing the working fluid and operational parameters of all types of geothermal power plants, which lead to significant increases in efficiency with little to minimum cost;
- Alternative power plant configurations, such as binary flash systems, internal heat exchangers, regenerative ORC, and additional flashing cycles to improve performance at a reasonable cost;
- Integration of geothermal technology with solar heat or biomass heat to boost the efficiency of the hybrid system;
- Pairing hybrid systems with thermal energy storage to enhance the efficiency of the hybrid system;
- The use of cascading allow for more utilization of a geothermal resource;

The environmental impact of geothermal power is often touted as environmentally friendly. Since the environmental effect of power plants is evaluated by different national standards, geothermal power has wide range of environmental effects depending upon the resource. Presence of accurate and reliable data for all power plants globally will unify the methodologies and will lead to comparable results. From the available data, it appears geothermal power emits significantly less GHG than coal or natural gas power plants. Using safe working fluids minimizes environmental impact of binary ORC's loss of working fluid. Also, considerable amounts GHG's are released from the consumed diesel during construction of geothermal power plants.

- Future study on the following topics would be beneficial for expanding and enhancing the geothermal energy technology: Expansion of public perception on the technology by providing proper education for different group of individuals;

- Reduction of drilling cost for EGS;
- Reduction of surface cost in general;
- Methods of increasing energy and exergy efficiencies;
- Normalizing the available data to provide clarity to find environmental impact of each power plant affects globally;
- Minimizing the environmental impacts during construction phase;
- Methods of gas removal systems to limit the NCG to the atmosphere;
- Modeling of EGS impact on the rock structure, soil and the surrounding environment;

Geothermal technology has the ability to provide a larger fraction of energy globally. There is potential for existing power plants to increase their performance as well as various exciting technologies that can provide several ways to extract energy in a safe and responsible manor from the Earth. With energy load increasing, there is a push for alternative energy sources to meet the demand. Geothermal energy studies have to expand for a sustainable energy supply and even growth of smart cities in the present and future.

Chapter 3: An Innovative Approach to Enhance Sustainability of a District Cooling System by Adjusting Cold Thermal Storage and Chiller Operation

Austin Anderson, Behnaz Rezaie, and Marc A. Rosen

Forthcoming in Renewable and Sustainable Energy Reviews

3.1 Abstract

Enhancing sustainability and performance, as well as saving costs, are important goals for the industry. Based on the impact and the size of the heating and cooling sector, district heating and cooling systems are good case studies to propose plans that provide the benefits of the three goals. There are many options for the upgrading and alteration of the equipment which demand a large initial investment. Usually, the initial cost is a barrier to implementing the plan. In this study, sustainability, performance and cost savings are improved without any equipment change. Exergy assessment along with TRNSYS modeling and simulation are the tools applied in this study. The focus is on the operation time of the equipment. By adjusting the operation time of the equipment with the highest exergy destruction, district cooling system is capable to achieve all three goals without any equipment change. Electricity consumption is reduced to 38%, which is beneficial in terms of sustainability, as it eliminates 428,800 kg CO₂ emissions in electricity generation and provides an annual cost saving of \$140,000.

3.2 Introduction

Meeting humanities energy demand in a sustainable manner is an ongoing challenge. Energy consumption has a strong relationship with economic development [106]. As developing countries continue their economic growth, worldwide energy demand is expected to grow [107]. In 2018, energy demands in the United States were met as follows: 13% coal, 31% natural gas, 36% petroleum, 8% nuclear, and 12% renewable energies such as hydropower, solar, geothermal, and biomass [108]. Fossil fuel sources are being used rapidly and they are finite, motivating growth in renewable energy sources. However, before renewable energy technologies can replace existing fossil fuel technologies, significant advances must be realized [109]. In the meantime, it is important to improve the efficiency of existing fossil fueled energy plants.

One way to increase the efficiency of resource usage is through centralized district heating and cooling. Lake et al. provide a review of district energy systems [110]. By centralizing energy production, higher efficiency equipment can be used to satisfy a larger overall demand. It has been shown that district

energy systems often have reduced greenhouse gas emissions compared to traditional systems [111]. This factor will likely become more important in the future, when emissions standards and carbon taxes may become more common. For example, the state of Washington recently proposed a carbon tax, which planned to tax carbon at a rate of \$15 per metric ton in the first year with an increase of \$2 per ton plus inflation for each year after [112]. Rezaie et al. performed an enviro-economic assessment of district energy systems and found them to be economically beneficial when coupled with tax breaks [113].

One obstacle to greater use of renewable energies is inadequate energy storage. Grid level battery storage is being studied, however it is not yet economic or practical [114]. One alternative to traditional batteries is the use of thermal energy storage (TES). Alva et al. provide an extensive overview of the many different applications and operating characteristics of TES systems [115]. One of the most common TES methods uses water due to its availability and high thermal capacity. Rismanchi et al. provided a review of design strategies for both latent and sensible cold TES [116] They concluded that cold TES systems have high energy efficiencies, in the range of 90% to 98%, and low exergy efficiencies, often below 20%. TES can be designed for durations ranging from daily cycles through to seasonal cycles [117]. When used to supply energy for a daily demand, thermal energy can be generated during times of low pricing and high efficiency, such as nighttime, and then used during the day when electricity costs are higher and equipment operates less efficiently.

Absorption cooling systems have some advantages over vapor compression systems. The primary advantage of absorption cooling systems is operate using low grade heat such as waste heat from industrial processes as well as heat from solar processes. Absorption cooling systems also have lower maintenance requirements, which result in considerable operational lifetimes [118]. Some absorption systems use lithium bromide solutions; these have little to no environmental effects as they do not use harmful substances, unlike some refrigerants [119]. Some potential drawbacks of absorption cooling is its relatively low coefficient of performance (COP). COPs for single-effect absorption cooling cycles typically range from 0.5 to 0.9 whereas the COP for vapor compression cycles is often greater than two [120]. Another disadvantage of absorption cooling is the crystallization of the fluid above certain temperatures. Crystallization often occurs in absorption cooling cycles where salt is used, and can cause obstruction of pipes and degradation of plant performance. Razmi et al. found that crystallization starts at generator temperatures above 35°C [121].

Exergy is defined as the maximum amount of work that can be extracted from a system undergoing a process in a specified environment [122]. Exergy, unlike energy, is quantified relative to the surrounding ambient conditions and is not conserved [123]. Szargut et al. suggest that, in analyses of

systems, exergy losses should be considered to better understand the impact on the environment [124]. Dincer and Rosen have reported extensively on exergy and its use in quantifying thermodynamic systems as well as its potential role in policy making [125]–[127]. They suggest that exergy analysis is superior to energy analysis as it provides a deeper level of understanding of system performance. Bejan outlined the fundamentals of exergy analysis and entropy minimization [128]. Exergy destruction is directly related to the entropy generation within a system and the ambient temperature. Optimization of a thermodynamic system by minimizing the exergy losses and costs results in obtaining the most useful work for the least cost.

In a lithium bromide water absorption system the useful output energy of the system for cooling applications is heat that is extracted from the evaporator, while the input energy is supplied to the generator in the form of hot water or steam. Lithium bromide/water absorption refrigeration systems have been modeled and assessed using both energy and exergy analyses by Şencan et al. [129], Kilic et al. [130], and Talbi et al. [131]. They all concluded that COP increases with higher generator and evaporator temperatures, while higher condenser and absorber temperatures caused the COP to decrease. Talbi et al. showed that majority of exergy destruction in a lithium-bromide absorption cycle producing 10°C chilled water via a waste heat source at 500°C occurs in the absorber (59.1%), followed by the generator (27.0%), the evaporator (7.6%), the solution heat exchanger (2.9%) and the condenser (2.8%) [131].

Avanessian et al. performed an exergy analysis of a single effect absorption cooling system, accounting for the exergy destruction resulting from chemical reactions [132]. They found that the effect of chemical exergy was negligible. Gogoi et al. performed an exergy analysis of a single effect absorption chiller and an optimization using the concentration of the LiCl solution as the objective function [133]. They concluded that LiCl solutions offer greater performance than LiBr solutions. Kaushik et al. performed an exergy analysis of single effect and series flow double effect LiBr absorption refrigeration systems to establish an optimum generator temperature for maximizing exergy efficiency [134].

The application of exergy analysis to cold TES systems has been examined in detail by Rosen et al. [135], [136], [137]. They outline several measures for increasing TES exergy efficiency. These include reducing mixing losses by improving thermal stratification, reducing heat loss through improved insulation, using more efficient pumps, and using smaller heat exchanger temperature differences to increase effectiveness. Stratified TES systems rely on avoiding mixing of fluids as exergy is destroyed from the mixing of fluids at different temperatures [138]. Density gradients can help prevent mixing [139]. The gradient is preserved by introducing and extracting cold water in the bottom of the tank and

warm water at the top. Carefully designed diffuser systems attempt to reduce turbulence within a tank during charging and discharging [139]. Within a TES tank, the modes of energy degradation typically arise from several factors. These factors mainly include heat losses to the ambient environment, heat conduction from hot layers to colder layers, vertical conduction in the tank wall, and mixing during charge and discharge processes [139]. The exergy efficiency of a cold TES tends to increase as the temperature difference between the top and bottom of the tank increases [140]. Discharge processes often have greater lost capacity than charging processes due to the mixing occurring during discharging. [141]. This can be somewhat mitigated by reducing the inlet flow rate during discharging.

In this study, the objective is to perform an exergy analysis to improve the sustainability of biomass district cooling by identifying components of greatest exergy loss. Then, based on the exergy analysis outcomes, the electricity consumption is reduced significantly without changing any equipment. While cold TES is beneficial for improving the performance of cooling operations in district cooling systems, the present research has conducted to show the impact of cold TES performance in optimal operational range on district cooling. It is explained how by manipulating the charging and discharging time of the cold TES, the electricity consumption of the district cooling can be significantly reduced. This energy saving results environment impact reductions as well as economic savings of more than \$100,000 per summer. The authors believe this is an innovative approach for improving environmental stewardship and sustainability while providing substantial cost reductions for managing district cooling facilities.

3.3 Methods

In this study an exergy analysis is used to find the exergy destruction within the cooling system for identifying areas of greatest inefficiency. The highest exergy loss is usually the highest priority for improvement efforts. Also, TRNSYS is used heavily in this study for modeling and simulation of the district cooling system during the summer under different scenarios.

3.3.1 Exergy Analysis

Applying exergy analysis to a thermal system allows for a deeper comprehension of its performance in comparison to energy analysis. The reason for this increased understanding is that different energy forms like heat and work are categorized identically when using energy analysis [128]. With exergy analysis, work has a higher exergy associated with it than an equivalent quantity of thermal energy [128]. The use of exergy analysis is also more valuable when examining costs as well as environmental effects [128]. The exergy rate balance on a system or component includes an exergy destruction rate. The higher the exergy destruction rate the less efficient is the process [142]. The exergy rate balance can be written as:

$$\left(\sum \dot{X}_{Q_{in}} - \sum \dot{X}_{Q_{out}}\right) + \left(\sum \dot{X}_{W_{in}} - \sum \dot{X}_{W_{out}}\right) + \left(\sum \dot{m}x_{f_{in}} - \sum \dot{m}x_{f_{out}}\right) - \dot{X}_{des} = \frac{dX_{des}}{dt} \quad (1)$$

Here, $\dot{X}_{Q_{in}}$ and $\dot{X}_{Q_{out}}$ are the exergy rates of heat transfer across the system boundary, $\dot{X}_{W_{in}}$ and $\dot{X}_{W_{out}}$ are the exergy rates of work, \dot{m} is the mass flow rate of the fluid, $x_{f_{in}}$ and $x_{f_{out}}$ are the inlet and outlet specific exergies of the fluid, \dot{X}_{des} is the exergy destruction rate, and $\frac{dX_{des}}{dt}$ is the rate of exergy storage within the system. The exergy rate associated with heat transfer can be written as follows [142]:

$$\dot{X}_Q = \dot{Q} * \left(1 - \frac{T_o}{T_b}\right) \quad (2)$$

where T_b is the temperature of the system boundary where heat is being transferred and T_o is the ambient temperature.

The exergy rate associated with work rate are the same by definition [142]. Exergy is the available energy of a process to create work in reference to an environment at ambient temperature (T_o):

$$\dot{X}_W = \dot{W} \quad (3)$$

The work input rate for the present model is in the form of electrical work input to the system.

The specific exergy of the fluid is a function of its specific enthalpy and specific entropy at that state and its properties at the ambient conditions. Ambient conditions are denoted with subscript zero.

$$x_f = (h - h_0) - T_0 * (s - s_0) \quad (4)$$

3.3.2 Transient System Simulation Tool

Knowing the nature of transient heat transfer of a system during a defined time period and interval is useful for efforts to modify the system for more efficient performance. The Transient System Simulation Tool (TRNSYS) is a software that provides such a capability [143]. It has a library of components as well as an ability to model system performance over time. TRNSYS is useful for simulating the energy rate of the modeled system as a whole and of its components. TRNSYS is beneficial for modeling and simulation of heating and cooling systems [143].

TRNSYS is operated by dragging and dropping different “types” from the component library. Each type is designated by a number and contains a brief description of the component and its intended use. There are often different intended uses for each type.

3.4 Case Study: University of Idaho District Energy System

The UI main campus in Moscow, Idaho, US has a unique district heating and cooling system, which was established before 1900. Advancements in technology for steam generation allowed steam production to be generated from not only coal but also biomass [144]. The UI district heating and cooling system is capable of producing 120 million kg of steam per year by utilizing wood chips from local forestry operations. The biomass boiler generates 95% of the steam with a thermal efficiency of 76% and an exergy efficiency of 24% [144]. The steam is used for the heating of 61 buildings on the campus during the cold months. In hot months the steam is divided among the campus heating demand, laboratory use, and the condensing steam absorption chiller. The absorption chiller utilizes 27% of this steam to produce chilled water for cooling purposes in hot months. The electric chillers operate mostly during the cool night and early morning hours to assist the absorption chillers in charging the cold storage tank. A cold TES with a total cooling capacity of 70,340 kWh and with a peak discharge/recharge rate of 8230 kW at a flow rate of 0.25 m³/s was added to the cooling system in 2010. Figure 1 shows the cold TES located in the UI, Moscow campus.



Figure 3.1: Cold TES tank located on the UI, Moscow campus, ID, USA

The cold TES increases the cooling capacity during peak periods by storing chilled water for meeting the campus cooling demand. The tank is charged during the nighttime by three electric vapor compression cycle chillers along with an absorption chiller.

3.5 Analysis

An exergy assessment of the heating cycle of the UI district energy system was completed previously and the exergy destructions of the different components were identified [145]. The results provided guidance regarding the most beneficial improvements in the heating plant. In the present study, the exergy destructions of the components of the cooling system are calculated and prioritized for finding the highest exergy loss. Then the focus of the study shifts toward reducing the greatest exergy loss. In this way the performance of the district cooling plant can be improved. For identifying ways to reduce the highest exergy destruction, there are two methods:

- Equipment Alteration
- Operation Alteration

Since the authors decided not to consider equipment alteration as the first choice, the focus shifted to operation alteration of the cooling cycle. With this strategy, TRNSYS is used to model and simulate the cooling cycle of the UI district energy plant during the summer time based on the actual operation data of the cooling district energy plant. The actual operation in this study is called Scenario 1. The modified operation time is called Scenario 2, which is developed based on the outcomes of exergy analysis described in the subsequent section.

3.5.1 Exergy Analysis

For identifying the area of greatest exergy loss, an analysis was implemented to establish baseline exergy destruction rates using constant values within the model. Equations (1) through (4) were used within TRNSYS using an ambient temperature of 22°C (295 K) and a campus return temperature of 22°C (295 K). The temperature used represents the average ambient temperature during the month of June 2016. The UI cooling system is shown in detail in Figure 2 and the thermodynamic properties for each point are presented in Table 1.

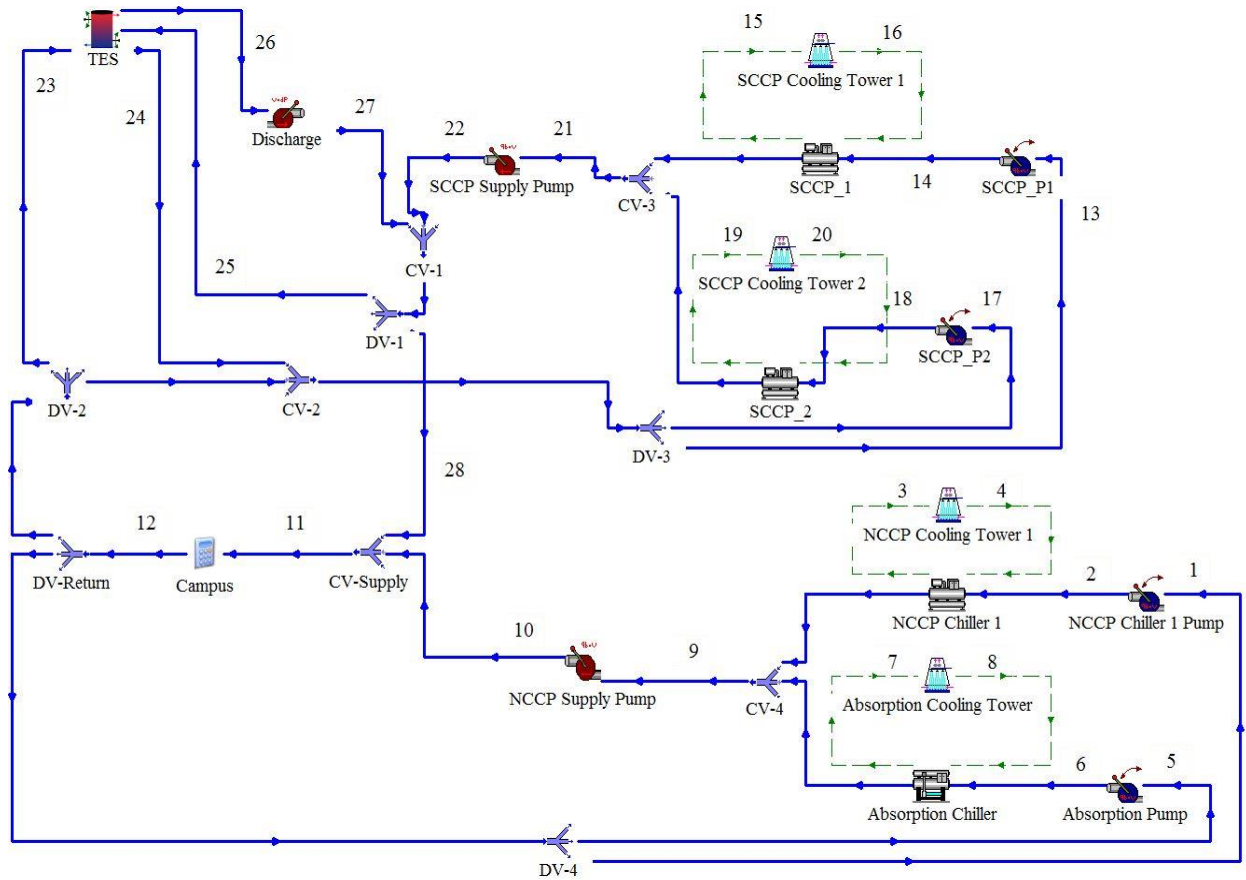


Figure 3.2: Schematic of the UI cooling cycle in Moscow, Idaho, US

Using the values in Table 1 with the relevant equations from Table 2 results in the exergy destruction rates for the baseline. The numerical value of exergy destruction rates of the components are tabulated in ascending order in Table 5.

Table 3.1: Parameters used at operating points within the cooling system

Point	T (K)	P (kPa)	h (kJ/kg)	s (kJ/kg-K)	x_f (kJ/kg)
0	290	101	70.82	0.2512	-
1	285	101	49.88	0.1784	0.01827
2	285	185	49.96	0.1784	0.2668
3	296	101	116.8	0.407	0.851
4	292	101	79.19	0.28	0.02873
5	285	101	49.88	0.1784	0.1827
6	285	185	49.96	0.1784	0.2668
7	300	101	112.7	0.3931	0.7049
8	295	101	91.75	0.3228	0.1783
9	280	101	28.9	0.1041	0.7404
10	280	345	29.14	0.1041	0.9845
11	280	345	29.14	0.1041	0.9845
12	285	101	49.88	0.1784	0.01827
13	285	101	49.88	0.1784	0.01827
14	285	185	49.96	0.1784	0.2668
15	295	101	91.75	0.3228	0.1783
16	292	101	79.19	0.28	0.02873
17	285	101	49.88	0.1784	0.01827
18	285	185	49.96	0.1784	0.2668
19	295	101	91.75	0.3228	0.1783
20	292	101	79.19	0.28	0.02873
21	280	101	28.9	0.1041	0.7404
22	280	345	29.14	0.1041	0.9845
23	285	101	49.88	0.1784	0.01827
24	285	101	49.88	0.1784	0.01827
25	280	101	28.9	0.1041	0.7404
26	280	101	28.9	0.1041	0.7404
27	280	345	29.14	0.1041	0.9845
28	280	345	29.14	0.1041	0.9845

Table 3.2: Equations used for calculation of component exergy destruction rates within the UI cooling cycle

Component	Equation
Absorption chiller	$\dot{X}_{desChiller} = \dot{m}_6 * (x_{f_6} - x_{f_9}) + \dot{m}_7 * (x_{f_7} - x_{f_8}) + \dot{Q}_{abs} * \left(1 - \frac{T_0}{T_{steam}}\right)$
NCCP Chiller 1	$\dot{X}_{desNCCPchiller1} = \dot{W}_{NCCPchiller1} + \dot{m}_2 * (x_{f_2} - x_{f_9}) + \dot{m}_3 * (x_{f_3} - x_{f_4})$
SCCP Chiller 1	$\dot{X}_{desSCCPchiller1} = \dot{W}_{SCCPchiller1} + \dot{m}_{14} * (x_{f_{14}} - x_{f_{21}}) + \dot{m}_{15} * (x_{f_{15}} - x_{f_{16}})$
SCCP Chiller 2	$\dot{X}_{desNCCPchiller2} = \dot{W}_{NCCPchiller2} + \dot{m}_{18} * (x_{f_{18}} - x_{f_{21}}) + \dot{m}_{19} * (x_{f_{19}} - x_{f_{20}})$
NCCP Chiller 1 Pump	$\dot{X}_{desNCCPchiller1Pump} = \dot{W}_{NCCPchiller1Pump} + \dot{m}_1 * (x_{f_1} - x_{f_2})$
Absorption Chiller Pump	$\dot{X}_{desAbsorptionPump} = \dot{W}_{AbsorptionPump} + \dot{m}_5 * (x_{f_5} - x_{f_6})$
SCCP Chiller 1 Pump	$\dot{X}_{desSCCP1Pump} = \dot{W}_{SCCPchiller1Pump} + \dot{m}_{13} * (x_{f_{13}} - x_{f_{14}})$
SCCP Chiller 2 Pump	$\dot{X}_{desSCCP2Pump} = \dot{W}_{SCCPchiller2Pump} + \dot{m}_{17} * (x_{f_{17}} - x_{f_{18}})$
SCCP Supply Pump	$\dot{X}_{desSCCPsupplyPump} = \dot{W}_{SCCPsupplyPump} + \dot{m}_{21} * (x_{f_{21}} - x_{f_{22}})$
NCCP Supply Pump	$\dot{X}_{desNCCPSupplyPump} = \dot{W}_{NCCPSupplyPump} + \dot{m}_9 * (x_{f_9} - x_{f_{10}})$
TES Discharge Pump	$\dot{X}_{desTESDischargePump} = \dot{W}_{TESDischargePump} + \dot{m}_{26} * (x_{f_{26}} - x_{f_{27}})$
Campus	$\dot{X}_{desCampus} = \dot{m}_{11} * (x_{f_{11}} - x_{f_{12}})$

3.5.2 TRNSYS Modeling and Simulation

Based on the results of the exergy analysis (Table 5), the focus shifts to the chillers and cooling towers, which have the highest exergy destruction rates. The strategy, as set out earlier, is to modify the operation schedule to reduce the exergy destruction rate in the cooling system. Avoiding use of chillers, reduces energy and exergy losses. But consumer demands still need to be met.

Scenario 1

The regular operation of the cooling cycle in the UI district energy system (Scenario 1) is modeled and simulated in TRNSYS. The cooling cycle is split into a north campus chiller plant (NCCP) and a south campus chiller plant (SCCP). The NCCP contains one 600 ton capacity absorption chiller and a 1200 ton capacity electric vapor compression chiller. Both chillers feed chilled water directly to the campus.

The SCCP contains two electrical 500 ton chillers. These chillers operate to supply campus demands as well as charge the cold TES tank, which is located within the SCCP.

The types of components used in the analysis and their operating conditions and parameters considered for building the TRNSYS model is presented in the Appendix A.

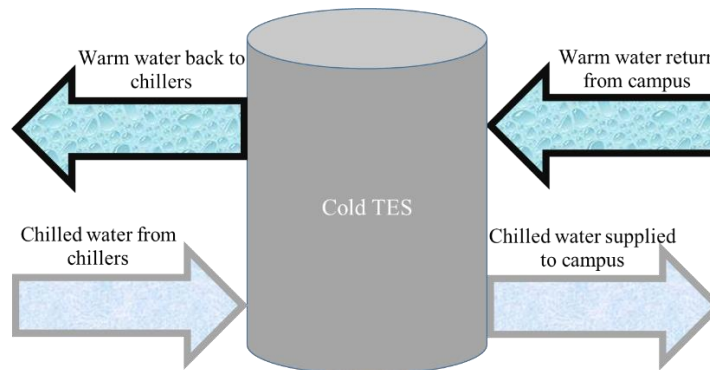


Figure 3.3: Water flows into and out of the cold TES tank in the UI cooling district system

In the TRNSYS model, heat is transferred from campus to the chilled water in the form of the campus cooling load. There is also some heat transfer from the ambient environment into the chilled water storage tank. For the campus cooling load, the boundary temperature is taken to be the average of the chilled water supply and return temperatures to campus. Thermal exergy is also supplied to the absorption chiller in the form of steam input from the campus biomass boiler. All four chillers (absorption and electrical) operate continuously every day. They chill the campus return water to the set point of 7°C. The campus return water temperature is input from data files recorded by UI facilities operators. Each chiller is supplied with water from its respective supply pump. Thus, the chillers modulate their flows in order to meet the required cooling load. The campus is assumed to fully utilize the cooling load supplied by the chillers. The cold TES tank is charged for total of 12 hours, from 22:00 to 10:00 the next day. Discharging occurs for 12 hours, from 10:00 until 22:00. The inlet/outlet water from the cold TES is presented in Figure 3. The rate of discharge is set at 23 kg/s, which represents the average discharge rate used by UI facilities. The ambient temperature for Moscow, Idaho is supplied to the model via external data files and utilized for calculation of exergy destruction rates of all components [146]. The simulation is carried out for the month of June 2016.

To develop the modified scenario (Scenario 2), there is the major condition of customer satisfaction, which necessitates that the cooling demands of the buildings should be fulfilled. In regular operation of the UI cooling system (Scenario 1), all chillers (coupled with cooling towers) operate during the day to cover the cooling demand of the buildings. They also operate during the night to charge the cold TES. To ensure customer satisfaction during the day, the chillers stay on. The only option for charging

the cold TES is nighttime operation of the chillers. In a recent study, the performance of the cold TES in the UI district cooling was assessed and results suggested the best operation time for effective charging and discharging of the TES [140]. The tools in that study were also exergy analysis and TRNSYS. The exergy efficiency of the charging stage of the cold TES is a maximum between 40 to 45% of the capacity of the TES; therefore charging further than that level is not efficient [140]. Similarly, discharging to lower than 23% of TES capacity is not efficient from the viewpoint of exergy [140]. Based on the results of that research, it is understood that there are several hours during the night when electrical chillers are running at full capacity while the TES tank is fully charged, and the exergy efficiency is low. Thus, energy would be wasted by supplying chilled water to the fully charged TES tank. When this occurs, the electrical chillers and cooling towers can be shut down. With the same approach, the discharging of the cold TES can be planned to discharge during the hottest period of the day and reduce chiller demand. Therefore, in Scenario 2 charging of the cold TES occurs from 1:00 to 8:00 for 7 hours of charge time. Discharging occurs from 12:00 to 18:00 for a total of 6 hours of discharging time. The operation of the chillers is defined based on the charging and discharging operation of the TES in this scenario. An exergy assessment for Scenario 2 is conducted to determine the exergy destruction rate of each component in the cooling cycle of the UI district cooling system. Scenario 2 also is modeled and simulated using TRNSYS.

Scenario 2

Scenario 2 examines the effects of enforcing a strict operating schedule for the chillers and the TES tank. Under this operation schedule, the absorption chiller runs continuously every day. This is due to the availability of inexpensive biomass material. The other chillers progressively turn on during the day as the ambient temperature and the required cooling load increases. Table 3 depicts the run times of each chiller for both scenarios.

Table 3.3: Summary of two scenarios of operation

	Absorption Chiller	NCCP Chiller 1	SCCP Chiller 1	SCCP Chiller 2
Scenario 1	Always on	Always on	Always on	Always on
Scenario 2	Always on	15:00-17:00	1:00-20:00	10:00-19:00

The operating and non-operating time for each chiller (and the cooling towers) are listed in Table 4.

Table 3.4: Operating and non-operating times of chillers in Scenario 2

	Operation time (hr/day)	Non- operating time (hr/day)
Absorption Chiller	24	0
NCCP	2	22
SCCP Chiller 1	17	5
SCCP Chiller 2	9	15

3.6 Results and Discussion

The purpose of the study was improving the sustainability of the cooling cycle of the UI district energy system. In the first step the exergy assessment was performed for all major components of the cooling cycle to determine and prioritize the exergy destruction rates. Then TRNSYS was used for modeling and simulation of the cooling cycle. The results of all analysis are presented in the following subsections.

3.6.1 Exergy Destruction

The results of the exergy assessment in the form of the exergy destruction rates for the major components of the cooling cycle are presented in Table 5. Chillers (including the cooling towers) have the highest exergy destruction rates. It can be concluded that, for modifying the cooling cycle from the perspective of exergy utilization, the focus should be on reducing the exergy destruction rates of the chillers.

Table 3.5: Exergy destruction rates for components of the cooling cycle of the UI district energy system

Component	Average Exergy Destruction Rate (kW)
Absorption Chiller	319.11
NCCP Chiller 1	249.15
Campus Buildings	103.23
SCCP 1	77.59
SCCP 2	77.59
NCCP Supply Pump	37.25
SCCP Supply Pump	17.74
NCCP Pump	5.36
Absorption Pump	3.21
SCCP Chiller Supply Pump 1	2.04
SCCP Chiller Supply Pump 2	2.04
TES Discharge Pump	0.99

Scenario 2 is defined with reduced chiller (and cooling tower) time operation. The exergy destruction rates for Scenario 2 are also calculated. Figure 4 breaks down the average exergy destruction rate for each component of the cooling cycle of the UI district energy system for Scenarios 1 and 2. Every component, with the exception of the absorption chiller, which has no operation change in Scenario 2, experiences a decrease in its exergy destruction rate. The absorption chiller is responsible for 35.6% and 62.5% of total exergy destruction for Scenarios 1 and 2 respectively. From Scenario 1 to Scenario 2, the NCCP Chiller 1 decreases its average exergy destruction rate from 249.2 kW to 20.7 kW. This is directly due to the large decrease in daily runtime for the chiller. The total average exergy destruction rate decreases by 42.9% in shifting from Scenario 1 to Scenario 2.

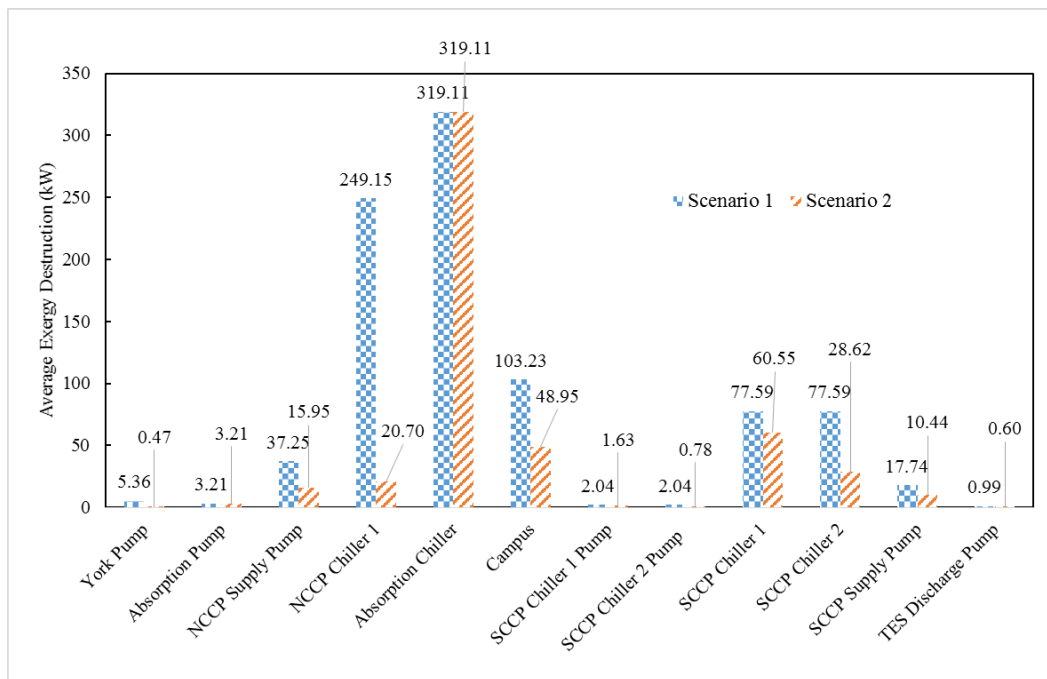


Figure 3.4: Breakdown of average exergy destruction rate by component for the month of June 2016.

3.6.2 Cold TES Performance

When supplying chilled water to the campus, it is important that the temperature of the bottom of the tank does not rise beyond 7°C. Figure 5 illustrates the average and discharge temperatures for the two Scenarios. The average tank temperature is seen to be several degrees lower for Scenario 2. These results were expected, because Scenario 2 was built based on optimum operation of the cold TES. Additionally, the temperature of the chilled water supplied to the campus remains at 7°C for the entirety of the month.

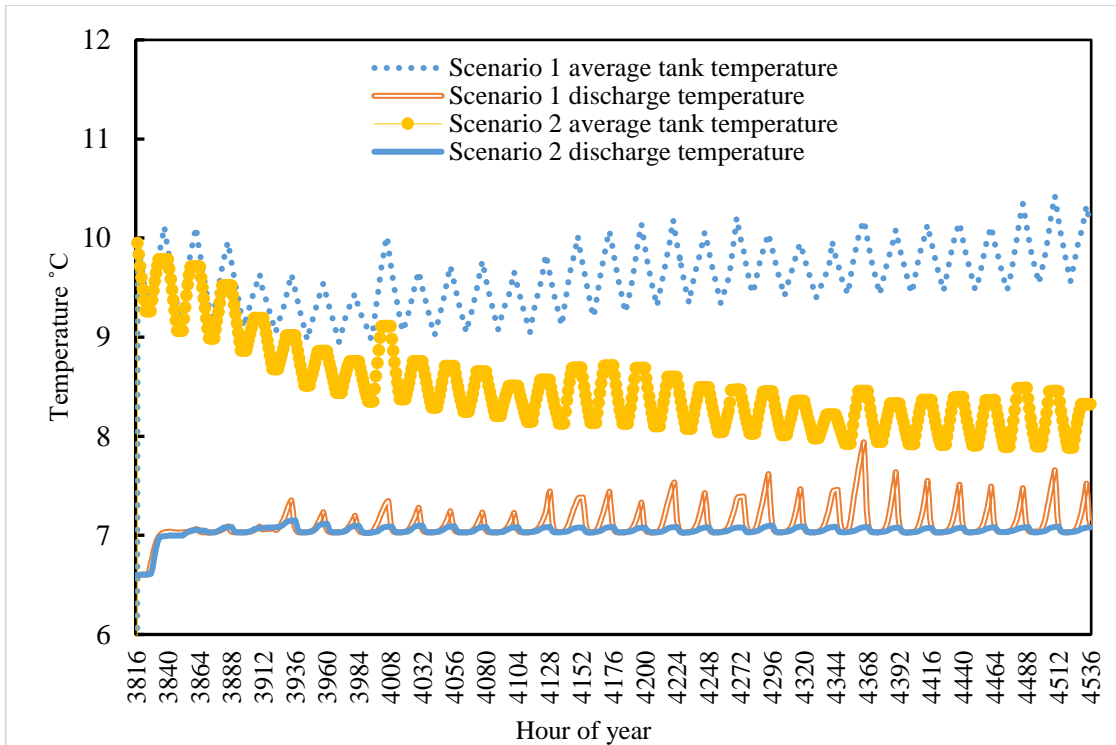


Figure 3.5: Average temperature of tank and temperature of discharge to campus for Scenarios 1 and 2 (hour of year corresponds to first hour of each day within the simulation)

It can be observed that, for Scenario 1, the supply temperatures of water tend to fluctuate over the course of the day. This is a function of the cold water in the tank being depleted during the day and recharged at night.

3.6.3 Cooling Supply

The total cooling supplied is calculated for Scenarios 1 and 2. Figure 6 presents a moving average of the cooling supply over the course of the month. Scenario 1, with its chillers operating all the time, produces about twice the total cooling supply of Scenario 2. Basically, in Scenario 2, the inefficient cooling load for charging the cold TES is removed. Also, discharging the cold TES is performed more effectively which eliminates the excess cooling load.

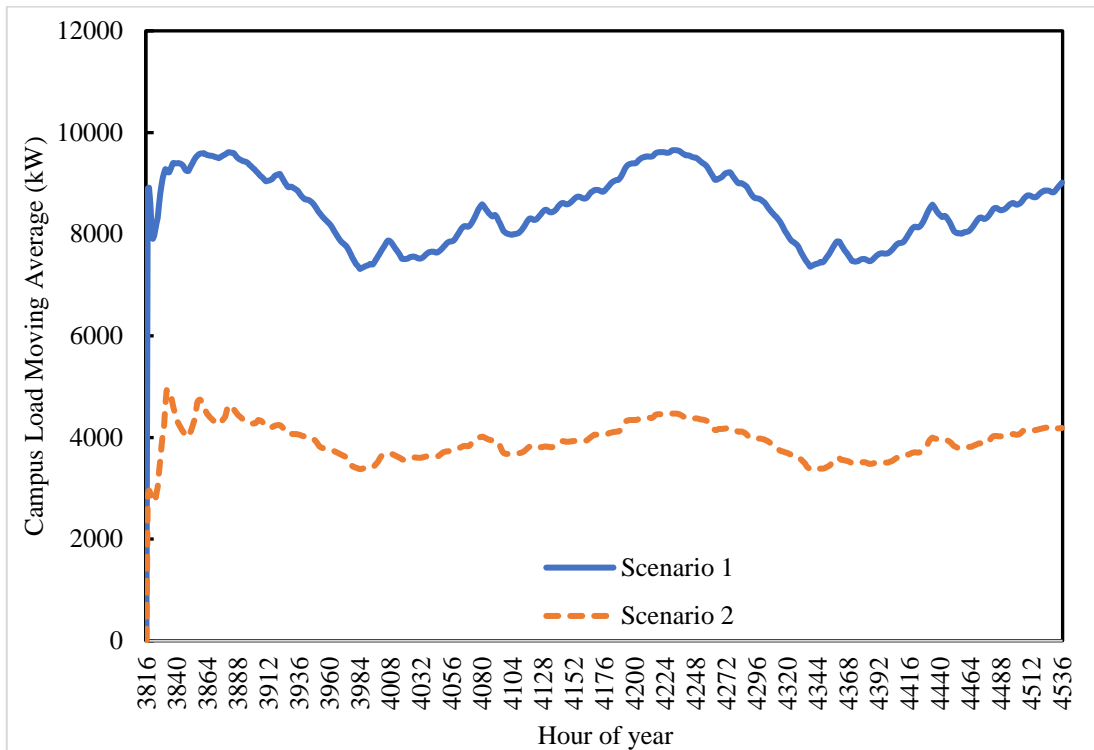


Figure 3.6: Moving average of cooling supplied to campus for June 2016 (hour of year corresponds to first hour of each day within the simulation)

3.6.4 Savings

A comparison of Scenarios 1 and 2 reveals the following savings:

- Electricity
- Cost
- CO₂ emissions

The differences between the operation schedule in Scenarios 1 and 2 are depicted in Table 6, which shows a 592,200 kWh saving in electricity consumption of the UI cooling district cooling system with Scenario 2.

Monthly costs for each scenario are calculated by summing the electrical energy required and then multiplying by the cost of electricity for the UI, which is 0.059 \$/kWh (Idaho is one of the least expensive electricity rate in the US). There is a significant cost difference between the scenarios. Scenario 2 has an electricity cost that is \$35,000 lower compared to Scenario 1 (Table 6).

Table 3.6: Comparison of electricity, cost, and environmental impact of Scenarios 1 and 2

	Electricity (kWh)	Cost (\$)	CO₂ (kg)
Scenario 1	945,700	55,800	171,200
Scenario 2	353,500	20,860	64,000
Saving in June	592,200	35,000	107,200
Saving for four cooling months	2,368,800	140,000	428,800

The improvement in sustainability due to the operational alteration is measured here in terms of the CO₂ emissions reduction brought about by the reduction of electricity consumption. The U.S. Energy Information Administration (EIA) estimates that 0.181 kg-CO₂ kWh⁻¹ are emitted from a natural gas power plant [147]. By using the EIA rate, the CO₂ emission rate for each scenario is determined and listed in Table 6. A difference in emissions of 107,200 kg of CO₂ is found between Scenario 1 and Scenario 2 for the month of June. Depending on the source of energy for electricity generation, this value varies with location. For the four months of the cooling season in the UI district cooling system, an annual saving of 2,368 MWh of electricity and a corresponding cost savings of \$140,000 is attained. The operation change of chillers (and the cooling tower) in the UI district cooling system reduces environmental impact by reducing CO₂ emissions for the cooling season by 428,800 kg, which is significant (Table 6).

3.6.5 Further Discussion

Since the UI is an institutional building, most of the buildings are without occupants during the weekend. There are some laboratories which require cooling all days, and there are some offices that occasionally may be used during the weekend. If an administrative system is defined to identify the building cooling requirement during the weekend, it can be used to minimize the operation of the cooling system in the UI district cooling facility. By reducing the excess load during the weekend, many of the chillers can be shut down. This mitigating of excess operation of the electrical chillers results in further savings and sustainability enhancements.

3.7 Conclusions

With the idea of improving sustainability and performance, and reducing energy consumption, this study focused on determining the exergy destruction rates of components of district cooling systems.

A case study is considered, comprising the district energy system of UI, located in Moscow, Idaho, US. The results of the exergy assessment demonstrate that chillers integrated with cooling towers are the highest source of exergy destruction. A transient model of the cooling system operation of the UI district cooling facility was modeled and simulated as Scenario 1, while Scenario 2 was developed based on the modified operational time of the electrical chillers, where the modified operation considered the cold TES in the UI cooling system. The purpose of this approach was to propose a model to facility management for reducing the exergy destruction of the UI district cooling cycle without any alteration to the equipment and related expenses.

The largest source of exergy destruction, and thus inefficiency, of the system occurs in the absorption chiller. One reason for this is the need for large quantities of heat for operation. From an exergy standpoint, heat has less value than an equivalent value of work. The absorption chiller is used due to the availability of inexpensive biomass fuel from the local logging industry, which makes it an attractive option. However, it would be beneficial to use a more exergy efficient device to provide the cooling. The remaining electric chillers are required to reject heat through a cooling tower. This is likely the main source of exergy destruction. If there is a way to utilize the rejected heat elsewhere within campus, then the efficiency can be improved.

The cold TES tank on campus allows for chilled water to be stored during night when the heat load is much lower in the cooling system. Having the TES tank allows for the chilled water load to be met during the hottest parts of the day and prevents an excess cooling load on the chillers. By adjusting the times of charging and discharging of the cold TES, it is possible to keep the discharge temperature more constant and to avoid discharging water that is too warm to the campus. The chillers operation is arranged based on the effective charging and discharging the cold TES to prevent an excess cooling load along with the corresponding ineffective charging and discharging of the cold TES.

Removing the excess cooling load in a month results in 592,200 kWh of electrical energy savings which financially, using the inexpensive electricity of Idaho, results in a cost savings of \$56,000 when constantly running all chillers in the system. These electricity savings result in enhanced protection of the environment. The operation change results in significant sustainability improvement by reducing emissions by 107,200 kg CO₂ per month.

The energy savings from Scenarios 1 and 2 indicate that closer attention should be given to reduce the excess cooling load by removing ineffective operation of equipment (like the cold TES) in the cooling cycle of a district cooling system. Future research could focus on finding ways to remove excess cooling demand of individual buildings in a district cooling system.

Chapter 4: Sustainable Resolutions for Environmental Threat of the Acid Mine Drainage

Behnaz Rezaie and Austin Anderson

Science of the Total Environment

<https://doi.org/10.1016/j.scitotenv.2020.137211>

4.1 Abstract

Acid Mine Drainage (AMD) caused by abandoned mines are an enormous source of negative impact on the environment and the species that inhabit it. The low levels of pH and high concentration of metals and metalloids (copper, gadolinium, lithium, etc.) in mining pits with standing water lead to changing the balance of surrounding organisms and ecosystems. The scale of the issue and the quantity of AMD sites throughout the globe are factors that make AMD a critical environmental threat. Many AMD treatments have been implemented to reduce the negative impact of AMD, with many solutions being very costly and only suited for particular project situations. Policymakers have strong leverage in correcting AMD problems by developing regulations and laws. This study proposes three more sustainable solutions for reducing and eventually eliminating the impact of AMD with less capital investment while also resolving the landfill problem as well. Also, some governmental strategies are suggested for forming collaborative relationships between industry professionals from different perspectives with the goal to resolve the AMD issue through innovative ideas. Implementation of previous strategies and suggested ones, as well as the further involvement of more communities, can enhance the sustainability of life exposed to AMD.

4.2 Introduction

The origin of the acid lakes or AMD are flooded abandoned mines. AMD begins to occur after the closing of mines. In active mines, continual pumping prevents flooding during operations. By stopping the operations and consequently discontinuing pumping, water, at temperatures ranging from 6-28 °C and sometimes even higher [148], flows into the retired mine. During this process, sulfites oxidize with oxygen which generates sulfuric acid with low levels of pH and high concentration of metals such as iron, aluminum, manganese, etc. The effect of low pH acid manifests when the drainage water from mines becomes neutralized by the precipitation of iron oxide and hydroxides [149]. It then forms a new precipitate, called ochre, that deposits on the bottom of river or stream beds and prohibits bottom feeding organisms from obtaining food [149]. These organisms form the bottom of the food chain and their decline strongly effects all the species above, resulting in fish declines [149]. The most critical

reaction is the oxidation of pyrite into dissolved iron, sulphate, and hydrogen. *Thiobacillus ferrooxidans* has been shown to increase the rate at which pyrite is oxidized by a factor of 100 to as much as a million [149]. By considering the size of mines, vast amounts of sulfuric acid infiltrate flooded abandoned mines. This infiltration of sulfuric acid is a serious hazard not only for the water, soil, and air, but also for the humans and other species in the area. The croplands in vicinity of AMD are severely contaminated to safely grow food [150]. The similarity of appearance between sulfuric acid and water makes it easy for both animal and humans to accidentally consume the acid water, further increasing the risk of the acid lakes for surrounding lives. Approximately 2,260 flooded mines have been identified in Canada [151]. Around 19,300 km of streams and rivers, and 72,000 hectares of lakes and reservoirs worldwide have been extremely damaged by mine effluents containing high levels of acidity [152].

AMD effects are classified into metal-toxicity, sedimentation processes, acidity, and salinization issues [153]. AMD are divided into two components known as 'vestigial' and 'juvenile' [154]. The vestigial component is created when a mine floods for the first time following its closing. The vestigial component is composed of ferrous and pyrite oxidation products being dissolved into the flooded solution over the course of around 40 years [154]. The mine's hydraulic retention time is the primary mode effecting the length of time required for dissipation [154]. Juvenile components, in comparison, are more long term and are the result of on-going pyrite oxidation in the water table fluctuation zone within the mine. Reactions will continue as long as pyrite is present and able to oxidize [154].

AMD is a result of accelerated sulfites oxidizing with water and oxygen during the process of mining, while sometimes metalloids such as arsenic are included as well [152]. Arsenic levels have been found in ranges of detection limits from 340,000 µg/L, and even up to 850,000 µg/L in the Iron Mountain mine in California. Normal levels for water bodies typically have concentrations of less than 10 µg/L [155]. The permeability of mine waste rock is shown to have a dramatic increase of the rate of oxidation of pyrite (FeS_2). Higher permeability waste rock is indicative of higher rates of AMD [156]. In the late 1980's, the National Stream Survey (NSS) provided an estimation for numbers and distribution of acidic streams in the Mid-Atlantic and Southeastern United States (US). 500 streams were sampled to generate probability samples for the areas 64,300 streams [157]. AMD and its effects on the local area concluded that around 10% of streams in the Northern Appalachians sub-region had high levels of acidity during the spring, which is when runoff would bring the highest amount of acidic water in contact with lakes and streams. In total, an estimated 4590 km (± 1670) of streams were acidic, while 5780 km (± 2090) were moderately acidic due to AMD impacts [157].

About 20,000 to 50,000 mines worldwide release acidic drainage. This results in 6,400 km of rivers and 8,000 to 16,000 km of streams affected by the metal mining [158]. As of 1982, it is estimated that

the worldwide production of mine wastes was around 4.5 Gt. The costs of potentially remediating these effects was estimated to number in the tens of billions of dollars [158].

AMD discharge from Britannia Creek mine and its effect on mussels in the Howe Sound resulted in mussel populations having much higher concentrations of Cu and Zn in their system. This led to higher rates of mortality and other adverse health conditions [159]. The mussel populations closest to the creek, which was the source of AMD into the sound, were concluded to have the lowest chance of survival [159].

The long-term changes in rivers reported to be heavily affected by AMD was investigated by Raymond and Oh [160]. The 1910's encompassed the peak of mining, the majority of which was in the Eastern U.S. [160]. The presence of carbonates in watershed soils have a buffering impact on AMD and the capacity of the soils in Pennsylvania led to highly acidic mine wastewater and streams and the degassing of a large amount of CO₂ from these carbonates [160].

The AMD effects on structural and functional formation of epilithic biofilms and nutrient during development were studied to understand the effects on algae [161]. Algal biomass was found to be strongly damaged in places with high levels of AMD. Low algal biomass is the ability of the streams ecosystem to retain necessary nutrients and energy to support itself [161]. Over 7200 km² of area in Appalachia region in eastern U.S was affected by AMD in this way [161].

Pit lakes often have relative depths of 10-40%, compared to around 2% for natural lakes. Relative depth is the ratio of the depth to the width of a lake, with higher ratios indicating deep lakes with small surface. High relative depth means these pit lakes become stratified, and chemical composition varies greatly with depth, which results in total dissolved solids and electrolytic conductivity increasing with depth [162]. The standard heat of reaction for pyrite is -349.2 kcal/mol, while in waste piles, oxidation causes convective cells that bring in air from the bottom of the pile and create steam vents at the top, which usually encompasses covering up mine waste as most of the acid was generated from runoff going through the waste rock [162]. There were 86 major open-pit mining operations in the U.S extracting precious metals and/or base metals other than iron or aluminum by the year 2000 [162].

The objectives of this study are to map a holistic picture of AMD by approaching it from multiple aspects while also proposing some solutions. This is accomplished by 1) showing the significant damage and negative impact associated with AMD on the environment; 2) detailing some of the remediation strategies for AMD and their related barriers; 3) discussion of regulation of AMD throughout multiple locations around the globe; 4) presenting legal court battles featuring AMD. The author's aims are to propose new AMD treatments that demand less financial capital while also solving

several environment issues at once. It is also suggested that governments take on a constructive and innovative role in dealing with AMD so that resources be maintained and used in a sustainable manner.

4.3 Acid Mine Drainage Environmental Interruption

Presence of AMD with heavy concentration of metals and related metallic chemicals either interrupts the balance of the surrounding organisms and ecosystem in marine and soil sides or wipes out the surrounding life depending upon following parameters:

- type of the metals and metallic chemical concentrations in AMD,
- level of the metals and metallic concentrations, and
- type of the species' strength and reaction toward the metals and metallic chemicals.

There may be other parameters, which are not in the scope of this study. Low pH as well as increased metal concentrations affected aquatic biota by disturbing the complexity of the food web and resulted in removing sensitive species [163]. Finding a 700-acre area covered with the white feathers of dead geese is an example of the devastating effects of AMD while Tree Swallows with avian liver tissues is an example of a manipulated ecosystem.

- **Canadian Geese flock death:** About 4000 snow geese on their migration path from Canada to the south settled down into the toxic artificial lake high in the Rocky Mountains (Montana, USA) in November 2016. The toxic lake, which is called Berkeley Pit, used to be a mountain where copper and other metals were discovered in the 1860s. The lake was built of the wastewater that fills a 700-acre former open pit mine [164].
- **Tree Swallows livers' damage:** Abnormal concentrations of 31 metals, metalloids (arsenic, barium, cadmium, mercury, thorium, titanium, uranium, etc.) in insects and insectivorous avian liver tissues were documented from Snake and Deer Creeks (Colorado, USA) around three AMD sites in 2003, 2004, and 2005. This excess concentration of elements was a result of the AMD generated by the abandoned mines in those regions [165].

4.4 Acid Mine Drainage Treatment Background

Various methods of mitigating the detrimental effects of AMD are possible. Conventional AMD treatments involve neutralization of the acid by adding alkaline materials such as limestone, lime, sodium hydroxide, sodium carbonate, and magnesia. These conventional treatments require considerable investment as well as additional costs for reagents, operation and maintenance (O&M), and disposal of resulting sludge [166]. Passive systems use naturally occurring geochemical and biological processes to remediate AMD with minimal operation effort. Passive systems usually require

a large amount of area to operate and also take longer amounts of time to take effect in comparison with conventional methods [166]. There are three types of passive systems, described as follows [166]:

1. Aerobic wetlands that allow for oxidation to occur and cause metals to precipitate as hydroxides and oxyhydroxides,
2. Compost wetlands that foster anaerobic bacteria growth, which results in sulphate reduction and subsequent precipitation of metal sulphides and generation of alkalinity.
3. Anoxic limestone drains generate alkalinity and they are used to pretreat acidic mine waters.

Aside from the above passive systems, recent emerging technologies are being developed by implementing membrane technology. The AMD treatment are also defined using chemical and biological methods with subgroups of active and passive, [152] which is depicted in Figure 1.

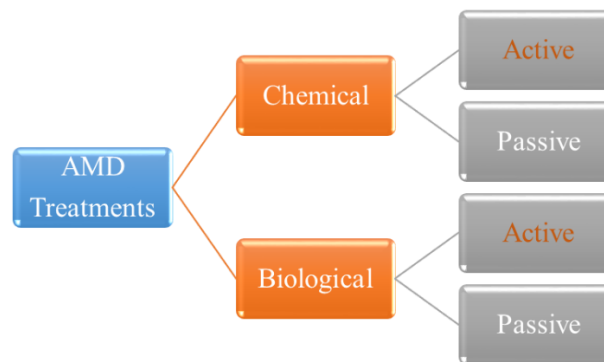


Figure 4.1: AMD Treatments types [152]

Over 200 wetlands are being used to treat AMD from coal mines in the Appalachia region of the eastern U.S by passive systems [166]. The intensive treatment of the vestigial discharge and passive treatment of the juvenile waste for AMD are superior to active options due to the capital investments being smaller as well as operation and maintenance costs being smaller as well [154].

The current process of treating AMD are as follows [156]:

- Using lime to neutralizes the acid and cause metals to precipitate. This forms a high-density sludge (HDS).
- The GYPCIX process uses a cation-anion exchange resin to treat the AMD. After the resins become saturated, they are regenerated using acid and alkali. Typically, sulfuric acid and lime are used due to being inexpensive. However, the use of nitric and/or phosphoric acid can regenerate the cations while ammonia and potassium carbonate can be used for regeneration of the anion. This is more expensive but has the added benefit of producing fertilizer in the process. Which ends up making the process almost cost neutral [156].

From 2003 to 2012, over 2×10^{11} liters of water were pumped from the Berkeley Pit mine in Montana to a copper recovery plant. In this recovery plant, Cu^{2+} was precipitated on scrap iron that released Fe^{2+} back into the pit, where the mixing from the pumping allowed the lake to change from a meromictic to holomictic state [167]. In this state, oxidation of dissolved Fe^{2+} induced and caused subsequent precipitation of more than 2×10^8 kg of secondary ferric compounds such as schwertmannite and jarosite which then settled to the bottom of the lake. Other substances, such as As, P, and sulfate also settled to the bottom [167]. With these compounds precipitating out of the lake solution, a roughly 25–30% reduction in the lake's calculated and measured total acidity was discovered.

Reductions in concentration for H^+ , acidity, Fe, Al, Mn, and SO_4^{2-} of 68%, 67%, 81%, 48%, 34%, and 8%, respectively, were observed within 50% of the total amount of installed wetlands [168]. Although, in 11% of tested wetlands, the effects worsened. This leads to some uncertainty in predicting an accurate performance of a fabricated wetland to mitigate the harmful effects of AMD [168].

Even when mitigation efforts were performed, rivers and streams in the Appalachian region, North America, were found to have higher levels of harmful chemicals [169]. Even after 15 years, biomass recovery is little to nonexistent in mine-affected areas [169].

Akcil presents three levels of strategy to lower AMD negative effects. The first level is prevention of the acid generating process, the second uses acid drainage migration prevention to limit its affected area, and the third is direct treatment of the effluent [156].

Soil contaminated with As has typically been dealt with using traditional measures such as soil removal, soil washing, and physical stabilization, all of which require a considerable amount of expense and further add additional disruptions to the environment [155]. Hydroxides containing iron, aluminum, manganese, clay, and natural matter known to be arsenic absorbents while the geological conditions of the site, such as pH, redox potential, and co-occurring ions affect the sorption of arsenic [155]. Microbial activity has been shown to catalyze the transformation of arsenic species and hyperaccumulate arsenic that remove the As from the contaminated soils [155]. Chemical processes performed on soil, groundwater, and aquifers enable arsenic sorption onto solid phases and prohibits it from entering groundwater [155].

Bacterial sulphate reduction is shown to aid in the removal of metals and sulphate from AMD by using different types of biologically and chemically treated biomass; approximately 2.5 kg of biomass would allow for the removal of 1 kg of sulphate [170].

The availability of rare earth elements and yttrium (REY) in AMD is orders of magnitude greater than other streams or lakes. REY's have been used in the renewable energy sector to create permanent magnets for wind turbines, batteries, and LED's [171]. The effects of AMD multistage sequential treatment on the behavior of REY resulted in obtaining some REY from the treatment process [171].

4.4.1 *Passive and Active Treatment*

There are two types of passive systems for AMD treatment; biological and geochemical. The biological passive treatment technologies use bacteria and organic matter to stimulate microbial sulfate reduction and absorbing contaminants, while the geochemical systems use alkalinity generating materials to promote acid neutralization and oxidation of metals [172]. Biological systems include aerobic and anaerobic constructed wetlands (AeWs and AnWs), vertical flow wetlands (VFWs), bioreactors (SRB), and Mn removal beds (MRBs) [172]. Geochemical systems include anoxic limestone drains (ALDs), open limestone channels (OLCs), limestone leach beds (LLBs), steel slag leach beds (SLBs), diversion wells, limestone sand, and low pH Fe oxidation channels [172]. Typically, the flow, acidity, alkalinity, metal, and dissolved oxygen concentrations are critical parameters when designing the proper passive system. [172].

Design of passive systems are discussed by [172]. Aerobic wetlands are sometimes a simple basin with vegetation such as Typha (cattails) typically planted in a loose substrate to promote slow flow and attachment sites for metals. Wetland vegetation also encourages more uniform flow for more effective treatment. They typically are used as a final form of treatment. In pH levels >6 , $10\text{--}20\text{ g m}^{-2}\text{ day}^{-1}$ of iron was removed and $0.5\text{--}1.0\text{ g m}^{-2}\text{ day}^{-1}$ for Mn [172].

The concept of integrated metal recovery schemes (e.g., Cd, Zn, Al) with the goal of zero waste production in mining activities is being explored as a method of active neutralization of AMD [173]. The idea has potential to be part of sustainable mining practices globally. An effective management process is required for protecting the aquatic life because of AMD interaction with rainfall and organic acids [173]. Anaerobic wetlands are more suitable for net-acidic water. Around $16.6\text{ g m}^{-2}\text{ day}^{-1}$ of acid was removed. These systems can often become filled with metal oxyhydroxides, thus a maintenance schedule is required to keep them performing at the best condition [172]. Anoxic Limestone drains are able to reduce the acidity of water and are generally cost efficient [172]. Since 1972 active mines are required to treat AMD prior to discharge. However, mines older than this are untreated, and no responsible party exists [172].

4.4.2 *Emerging Technology*

Membrane technology is simple and flexible in its operation while it is compatible with other AMD treatment methods and offers ability to generate drinkable water [174]. The electro dialysis process is one method of using membrane technology and is capable up removing up to 97% of metal. Electro dialysis uses a semipermeable ion-exchange membrane to filter out the ions from AMD [174]. Membrane zeolite sorption system is another emerging technology that is thermal based [175]. The process is driven by harnessing vapor pressure differences to produce freshwater. Up to 90% of water has been recovered using this process and almost 100% of Fe and Al ions could be removed using their process at temperatures of 500 °C [175].

Both reverse osmosis (RO) and nano-filtration (NF) processes are capable of treating AMD while they provide clean water [176]. However, NF is more effective at treating gold AMD than RO due to higher permeate flux and solutes retention efficiency [176]. Maximum water recovery rates of 60% were observed with an operational cost of 0.26 US\$/m³ [176]. Another pilot scale study comparing RO and NF systems in copper mining showed that both systems were capable of removing over 90% of ions, sulphates, and metals such as copper, aluminum, iron and manganese [177]. The NF system, however, achieved five times the permeate flux of the RO system [177]. At optimum treatment performance, it was estimated that over 20,000 liters per day of AMD could be treated with magnesite and RO membrane filtration [178].

Rare earth elements are often contained within AMD flows and due to their demand in industry, it is worthwhile to find ways of extracting them while also limiting harmful effects of acidic effluent [179]. A forward RO process using different orientations of the membrane, solution pH, and temperature variation was used to simulate the flux performance and rejection of lanthanum, cerium, and dysprosium [179]. The results showed the pH significantly affected the ability of the membrane to reject the metals. Nanotechnology is fast, effective, and highly efficient while at the same time being costly, not feasible for large scales, and may cause eco-toxicity [180]. Figure 2 shows the major emerging technology treatment for AMD.

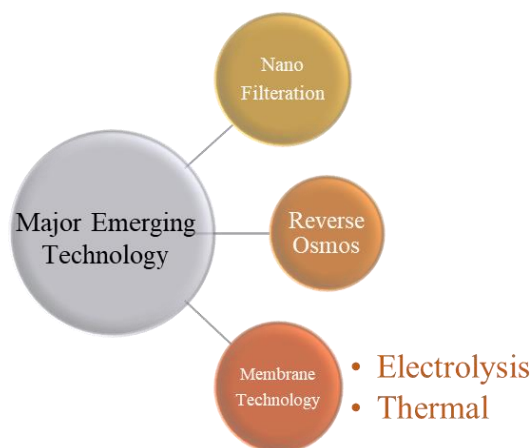


Figure 4.2: AMD Treatments Emergent technology

4.5 Innovative Sustainable Treatment

One of the major barriers for AMD treatments is the cost by considering the size of AMD and amount of chemicals requiring neutralization. Treatment that is both less costly and potentially solve other environmental issues would be ideal solutions. The other major global issue is Landfills. In the U.K. and Wales alone, there are over 20,000 landfill sites, with shortages of space already occurring [181]. In the 1990's, it was projected that one third of all landfills would close from lack of space in the early 90's while 80% would be completely filled over the next 20 years [182]. When coupled with the fact that 2/3 of Americans did not want the landfill to be sited in their community, this created an enormous landfill problem [182]. Concrete is one of the major sources of landfill waste in the US. It is estimated that the percentage of solid waste accumulated in the US may be in the range of 15% to 28% of total solid waste [183].

By having this in mind, three sustainable methods of neutralizing AMD are suggested in this study. In these methods, not only is AMD neutralized but also other environmental concerns are resolved. These environmentally sustainable treatment options are theoretical and demand financial support to implement. Since the solutions are not based on case studies and already defined circumstances, no detailed data is presented in the following solution options.

4.5.1 Option 1

Tons of building debris are occupying landfills. They cause instability of the environment by preventing the land from receiving sunlight, eliminating the natural plants of that area to grow, and disturbing the life of species that are dependent on land by disturbing the regions ecosystem. The financial value of the landfills is another disadvantage of using lands for dumping building debris. Majority of building debris consists of concrete. Discarding building debris in AMD sites relieves the occupied landfills and removes environmental issues caused by them in the area. Figure 3 shows a

simplified schematic of Option 1. Furthermore, the chemical reaction between concrete (CaOH) and sulfuric acid (SO₂) results in Calcium sulphate (CaSO₄) and water (H₂O).

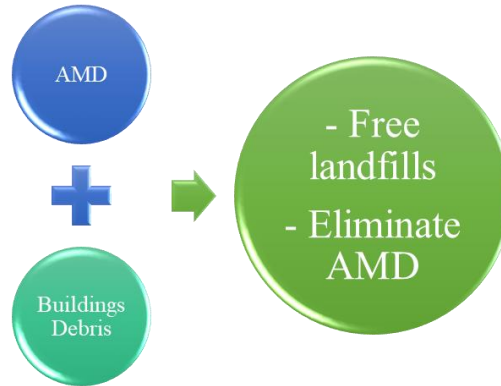


Figure 4.3: Option 1 for AMD Solution

It can be seen that water is the outcome of this chemical reaction. Turning acid to water reduces the acidity (pH) of the water system and thus reduces the harmful effects of AMD. At some point all of the acid can be chemically reduced to water depending on the volume of the acid and amount of concrete. Since water scarcity is one of the most life threatening issues on the earth, producing water using this treatment provides great benefits in alleviating this problem.

Advantages of the Option 1 are:

- Free up the landfills;
- Elimination of the environmental disruption of the landfills and their surrounding ecosystem;
- Purging AMD eventually;
- Generation of water;
- Exclusion of environmental hazard by AMD.

4.5.2 Option 2

Tons of waste sulfuric rocks are usually around the mines. Presence of these rocks not only pollute the soil but also pollute the air (by dust) and water (underground water). Filling up the AMD with these surrounding sulfuric rocks are another option for recovery of the AMD. When the pit is full there would not be any interface between air and water in the lake. Then the issue of AMD and its danger for the environment will be resolved, then. Figure 4 shows a simplified schematic of Option 2.

Advantages of the Option 2 are:

- Cleaning up the surrounding land from sulfuric rock;

- Freeing up the landfills;
- Preventing water and air pollution by sulfuric rocks;
- Possibility of using rocks in the pit as thermal energy storage.

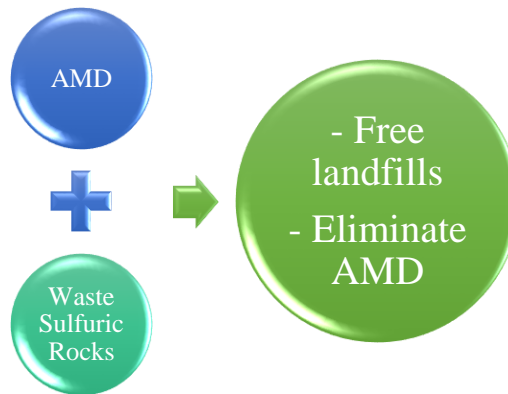


Figure 4.4: Option 2 for AMD Solution

4.5.3 Option 3

The open pit (as result of mining) can be filled by building debris as well as surrounding rocks both together. Essentially, Option 3 is integration of Options 1 and 2 for undertaking the AMD problem. There are some parameters that require further consideration for Option 3, such as if the size of the lake has the capacity to receive rocks and concrete debris, amount of the concrete debris found locally and its impact on the acidity of AMD, and amount of the surrounding rocks available.

Advantages of the Option 3 are the collective benefits of Options 1 and 2.

4.6 Governmental Roles

Since the 70's AMD has presented a considerable issue facing the mining industry and no entity has yet had the ability or resources to deal with it on a significant scale. The local, state, and federal governments as the legislator are able to encourage creative ideas and facilitate the implementing the ideas to reduce or eliminate the danger of AMD. Several laws have been employed around the world governing mining operations. These are in response to the obvious danger presented by the production of AMD as well as the massive number of global closed and abandoned mines.

4.6.1 Regulations

4.6.1.1 Some North American Regulation

Currently, there are several U.S. laws that concern themselves with mining operations. Most prominent is the Clean Water Act. The Clean Water Act (CWA) regulates discharges of pollutants into the waters

of the United States in any source [184]. Mining operations typically require two CWA permits, the first of which concerns navigation of water systems while the second is focused on channel run off water and storm water into point source discharges. Permits are required to ensure discharges do not upset the required water quality standards of the receiving waters or exceed the effluent limitation guidelines. Both the environmental protection agency (EPA) and the U.S. Army Corps of Engineers are the controlling authorities.

The 30 USC Ch. 25: Surface Mining Control and Reclamation concerns itself with the effects of mining operation within the United States. It was written with the goal of protecting both the people and the environment from the negative aspects of mining operations. The Department of the Interior, the Office of Surface Mining Reclamation and Enforcement enforces it. Among its many purposes, it is also tasked to “promote the reclamation of mined areas left without adequate reclamation prior to August 3, 1977, and which continue, in their un-reclaimed condition, to substantially degrade the quality of the environment, prevent or damage the beneficial use of land or water resources, or endanger the health or safety of the public” [185]. The code provides funding for both research and remediation of harmful mining operations, including AMD. Outside the US, there exists many variations of governmental policy regarding AMD. South Africa, for example, has several pieces of legislature that govern the treatment and remediation of mine effluent. One of the biggest difficulties concerning AMD is discerning what entity is responsible for remediating the damages. Many of the companies that performed the mining are no longer around, and existing legal framework did not exist on determining responsibility. Thus, South Africa has adopted laws that “stipulates that those who are responsible for producing, allowing or causing pollution should be held liable for the costs of clean-up and the legal enforcement” [186]. Additionally, water resources are owned by the government and are not able to be privately owned, thus leading to the government having the obligation to protect the resources.

As part of its duties, the EPA must to create a "National Priorities List" (NPL) of the nation's most polluted sites. They quantify the pollution levels by using the Hazard Ranking System (HRS). Scores on the HRS range from 0 to 100; a given site that scores at or above 28.50 is eligible for inclusion on the NPL. Figure 5 depicts the quantity of sites placed on the NPL as of November 2019.

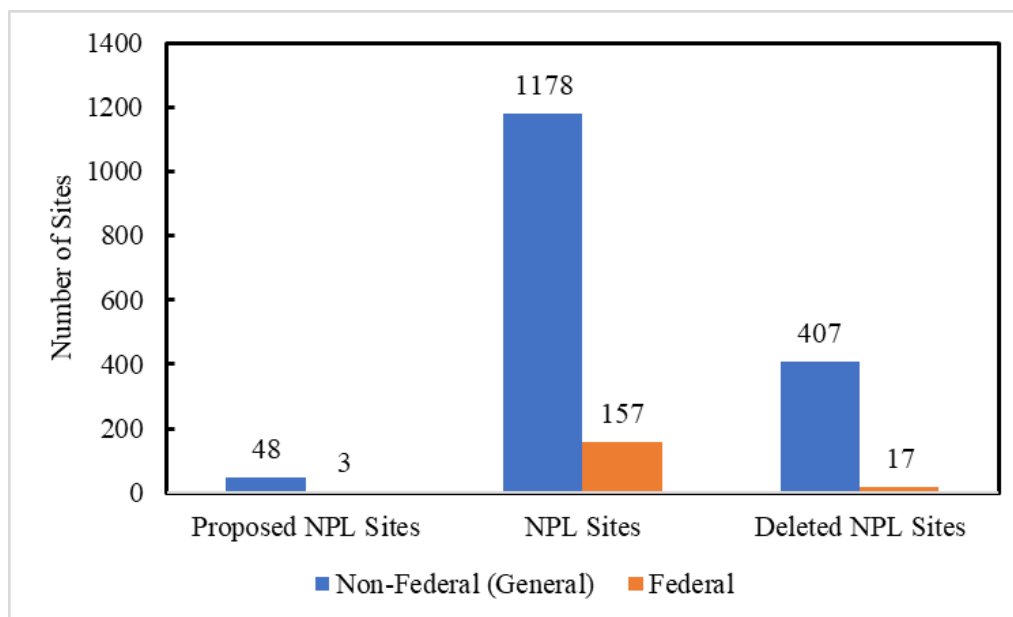


Figure 4.5: Number of proposed, active, and deleted NPL sites as of November 2019 [187]

Proposed NPL sites refer to new sites that have been identified as posing a significant and imminent threat to the surrounding environment. Over 1300 sites around the US have been identified and are currently undergoing remediation efforts. Upon a successful completion of remediation, which is determined according to the EPA's guidelines in addition to input from the state in which the site is located, the site can be deleted from the NPL. Upon deletion, there is typically a 5-year review and monitoring period to ensure more work is not needed.

Canada has also faced significant environmental issues as a result of AMD, which has led to them to include a mining reclamation section in their Minerals and Metals federal policy [188]. This section outlines the significance and potential environmental threat resulting from mining operations. Additionally, it spells out that while many abandoned and orphaned mines exist within Canada, the government will do its best to remediate and treat these older mines while also trying to find an amicable solution as to who is financially responsible [188]. The Canadian Environmental Protection Act of 1999 outlines specific guidelines on the treatment and protection of pollutants and other critical environmentally damaging substances [189]. AMD is not specifically mentioned but there are strict rules that regulate the quality of water and other ground resources must be protected. More specifically, Canada's Metal and Diamond Mining Effluent Regulations outline the specifics of the required testing, monitoring, permitting, emergency action plans, discharge points, and proper reporting procedures for all mining operations in Canada [190]. The owner or operator of the mine is responsible for following the prescribed regulations. Canada formed the Mine Environmental Neutral Drainage (MEND) organization in response to the AMD problem in 1989. This organization

is a conglomeration of governmental personal, mining stakeholders, and academic personnel that has the goal of furthering the sustainability of mining operations in Canada. The focus of their work is to develop mitigation technologies, manage closures, early prediction, and develop passive strategies [191]. Thus far, MEND has made great strides in reducing the problems associated with AMD by publishing over 200 research papers and case studies, with future plans to contribute more to developing sustainable mining practices in Canada.

4.6.1.2 Some European Regulations

In Europe, there is specific legislation that is relevant to mine waste. Specifically, Directive 2006/21/EC of the European Parliament and of the Council of 15 March 2006 on the management of waste from extractive industries and amending Directive 2004/35/EC, directs that owners of closed or abandoned mines “shall ensure that an inventory of closed waste facilities, including abandoned waste facilities, located on their territory which cause serious negative environmental impacts or have the potential of becoming in the medium or short term a serious threat to human health or the environment is drawn up and periodically updated” [192]. Thus, in Europe it is required that dangerous mining situations be reported to the public. Furthermore, this law outlines the required procedure for proper mine closures.

Likewise, the Partnership for Acid Drainage Remediation in Europe (PADRE) exists to promote best practices in the stewardship of water resources, research abatement techniques for AMD, advance training of best practices in the field of AMD, and collaborate with other similar institutions globally [193]. Coalitions such as these that focus on connecting industry, policy, and research fosters a collaborative environment where people work together to create a sustainable future.

Governmental role in prohibiting AMD is further established by participation in consortiums and coalitions. One such coalition is the Acid Drainage Technology Initiative (ADTI). ADTI is a coalition of several governmental agencies, industry, and academia that are focused on addressing issues within the mining industry related to AMD within the U.S [194]. ADTI had an initial focus of prediction and avoidance of AMD. Their recent work has been spent on developing a five-year roadmap towards a more sustainable future. To achieve this, ADTI outlined a series of priorities that will be looked into being solved with future action.

4.6.1.3 Some Australian Regulations

In addition to ADTI, there exists many other coalitions and consortiums aimed towards prevention and rehabilitation of AMD around the globe. The Australian Centre for Sustainable Mining Practices

(ACSMP) was established in 2009 as a means of researching sustainable mining practices. They have facilitated research and policy making regarding mines within Australia [195]. They collaborate with both industry and government to work towards a sustainable future.

4.6.2 *Some Legal Cases*

The issues regarding mining in general and AMD in particular as laws have occasionally been presented in courts. There have been legal battles over the enforcement and interpretation of the law since 1960s. The CWA is typically the driving force behind the legal battles. Below is a brief summary of some relevant legal cases regarding AMD in the U.S.

- The CWA requires a permit in order to discharge pollutants into water systems. In the 1960s, the East Bay Municipal Utility District acquired a portion of the Penn Mine property located in California. They constructed a facility to clean the water leaking from the leftover mine tailings and waste rock from the previous mine owners [196]. Despite their efforts, some acidic water would periodically spill over their constructed reservoir and enter the Mokelumne River. The Committee to save the Mokelumne River formed and filed a lawsuit and sought a judgment declaring that defendants violated the CWA by not having a correct permit. They also sought judgement that required the district to devise a remediation plan. The court ruled in the Committee's favor, and upon appeal, affirmed their decision [196].
- In 1986 the EPA took action in the removal of hazardous waste that was leaked by the Iron Mountain Mines Superfund Site (IMSS) [197]. In the removal and remediation of massive amounts of AMD, the EPA incurred significant response costs. The EPA filed a suit against the perpetrators, seeking to get back their response costs. After years of settlement negotiations, the EPA was awarded a settlement of \$57,139,669.53 in costs [197].
- Oftentimes, mine companies have insurance in order to protect themselves from some of the potential damages they cause. Bellaire operated a bituminous coal mine known as Conemaugh Mine No. 1 in west central Pennsylvania from 1968 to 1981 [198]. After closure, they formed and implemented a plan to seal the mine to prevent AMD. It was anticipated that potential for AMD formation would persist for years, and so it was suggested to keep the treatment plant open. Despite the warning, Bellaire sealed their mine and removed the treatment plant. Three years later, "red water" began flowing out of the mine into local properties. Property damage claims were filed and paid for by Bellaire's primary liability carrier. In order to prevent additional damages, Bellaire constructed a new treatment plant requiring an investment of around \$15 million. Bellaire submitted a claim to their insurers for the \$15 million but were

denied. Bellaire then took their insurers to court for the damages. The court ruled in favor of the insurers [198]. Their reasoning was that since the CWA makes it abundantly clear that Bellaire was responsible for preventing AMD from escaping the mine, hoping that Bellaire's initial sealing would function indefinitely did not mean that they had prevented future occurrences of AMD from the mine [198].

- While the CWA requires all mines to file for National Pollutant Discharge Elimination System (NPDES) permits, states can petition to run their own NPDES programs. West Virginia successfully petitioned to administer their own program [199]. The way West Virginia runs their programs is that if mine operators default on their duties, the West Virginia Department of Environmental Protection (WVDEP) forces the performance bonds into forfeiture. State regulations require WVDEP to treat AMD at these sites in accordance with the EPA's effluent limitations for coal mining point sources. During 2007 in north central West Virginia, the West Virginia Highlands Conservancy and West Virginia Rivers Coalition determined there was 18 sites actively discharging AMD while the WVDEP has only issued one permit for bond forfeiture. After taking the WVDEP to court, the WVDEP was ordered to apply for permits within 180 days and obtain final permits within 360 days [199].
- In 2015 a leaching of AMD into the Animas River watershed spurred the EPA into evaluating the Bonita Peak Mining District (BPMD) using the HRS [200]. The EPA scored a total of 19 separate sources while noting, but not recording 29 other sources that might contribute to contamination. Each scored source was eligible for placement on the NPL. Because of this, the EPA added the entirety of the BPMD, which included both scored and unscored sources, to the NPL. Sunnyside Gold Corporation was one of the unscored sources that was added to the NPL. They contested the inclusion of their mine on the grounds that their mine was its own "site" and therefore the EPA had to score all of the separate sites before adding the entirety of the BPMD to the NPL. The courts denied the petition for review as the BPMD is considered one site that included the Sunnyside mine. Thus, even though Sunnyside claims that it has rehabilitated its mine, it still may be required to participate in future remediation efforts within the entire BPMD [200].

The above listed cases are presented to establish an understanding of how the law regarding AMD is implemented within the U.S. In general, the CWA is quite explicit in its requirements that those who cause the damage are liable for remediation.

4.6.3 Collaborative Actions

It can be concluded from the above subsections that preparation of regulation and reasonable policy is time intensive and costly for lawmakers. To use the public and private resources in a constructive way government in different levels can be encouraged to brainstorm innovative methods of AMD control. The role of government is to encourage private sectors, academia, and researchers to get involved to clean or/and eliminate the environmental concerns of mining industry including AMD. These are some suggestions:

- different incentives for the miners who are environmentally responsible,
- grant opportunities for collaboration of academia and industries to find a way out,
- funding opportunities for all researchers for innovative resolutions.

Implementation of the above policies can allow for more efficient treatment and prevention of AMD. If the government and the mining companies can come to reasonable agreements on policy and take a team-like approach to finding solutions to the AMD problem, court costs as well as other unnecessary costs can be removed from the process. Moreover, making people involved in these projects leads to greater public awareness, which is another achievement for the local government. Figure 6 depicts governmental roles in resolving AMD problem.

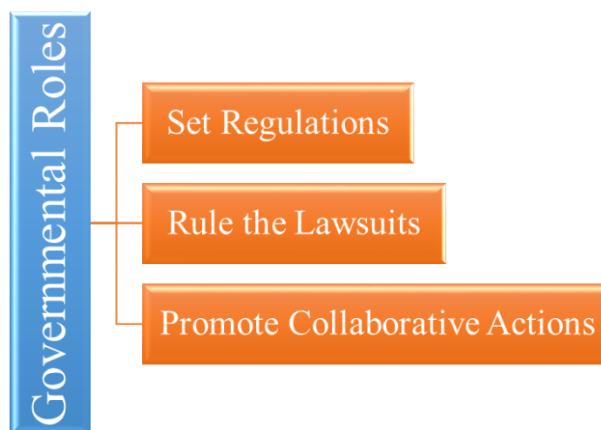


Figure 4.6: Governmental Roles for Controlling AMD Issue

4.7 Conclusions

The environmental problems caused by abandoned mines including AMD, have interrupted ecosystems and organisms. The death of 4000 Canadian geese in Barkley Lake in the Rocky Mountains (Montana, USA) during their migration in fall 2016 is one of the many disasters contributed by AMD as a result of the low pH and high concentration of chemicals in the water systems. Different methods

of AMD treatments have been proposed and some have been implemented on different AMD sites. Emergent technology based on recent advancements, such as nano-filtration and membrane technology have been offering constructive solutions for AMD treatments with the advantage of providing drinkable water. One of the major issues for traditional and emergent remedies is the cost of materials and process for treatments. It can be concluded the most practical treatment is application of alkaline lime for neutralizing the AMD. There are variety of policies by different local and international agencies for regulating the environment exposed to AMD. Legal battels regarding the negative impact of AMD have been recorded since the 1960s. In fact, there are many groups who do not have the means to pursue legal action (like Canadian geese) or cannot afford the costly battels in courts. While, in many cases there are no responsible party from old and long abandoned mining companies.

Since the cost is one of the major issues in AMD treatments, three different approaches for neutralizing AMD are suggested in which involve less investment while also resolving other environmental concerns. Dumping buildings debris in AMD sites not only neutralizes the acidity of AMD but also frees landfill space by clearing concrete waste. Landfills of buildings waste are another environmental concern in modern society. Filling up AMD sites with surrounding sulfuric rock is another proposed solution which can address the AMD issue as well as clear the invaded lands of waste rocks from mines. Combination of both solutions as the third method also reduces AMD negative impacts while enhancing the sustainability of landfills. Also, the more innovative role for governments are suggesting by proposing the grants for collaboration of different researchers with industrial sectors, as well as incentives for mining owners who are pioneers in protecting the surrounding environment.

Essentially, to extend the life on the Earth people with related professional roles and authorities need to collaborate peacefully for enhancing the sustainability. This is possible by exploring more harmonized resolution to return the balance to ecosystems of different regions. The ultimate goal of this study was to draw attention to the horrific environmental impact of abandon mines, especially AMD and suggesting some solutions for tackling the issue.

Chapter 5: Metallic 3D printing: Study of Opportunities for Sustainable Future with a Case Study

Austin Anderson, Selso Gallegos, Behnaz Rezaie, and Fardad Azarmi

Forthcoming in Environmental Impact Assessment Review

5.1 Abstract

Additive manufacturing (AM), also known as 3D printing is a relatively new concept and promising technology for industrial production. It is important to investigate the environmental impact of AM process in light of the critical situation of the Earth. The elimination of some costly prefabrication processes such as molding or post fabrication stages such as machining and welding required in traditional manufacturing methods favor the AM process and provide great economic advantages. Furthermore, reduction of manufacturing steps contributes to environmental protection through fewer operations, less material and energy consumption, and reduced transportation. This study is a preliminary work for analyses of environmental impact and life cycle of some well-known AM technologies for manufacturing metallic parts and components. As a case study, fabrication of a pump impeller is simulated through a well-known metal production AM technology and a conventional technology such as casting process for direct comparison. Life Cycle Analysis (LCA) is applied to measure the environmental impact in five different stages of pump impeller lifetime with the two different fabrication processes. AM compared to casting has an environmental impact reduction of 15%, 20%, 65%, 20%, and 10% respectively in Global Warming Potential (GWP), Acidifications Potential (AP), Water Aquatic Eco-toxicity Potential (FAETP), Human Toxicity Potential (HTP), and Stratospheric Ozone Depletion (ODP). In the pre-manufacturing stage, the AM process has higher impact on the environment in comparison with casting process due to intense electricity consumption. Using hydroelectricity and renewable energy electricity mitigate the environmental impact of the AM process in pre-manufacturing and manufacturing stages as temporary until the advancement of AM technology for consuming less energy. Finally, a plan for future research to enhance the environmental sustainability of AM process is proposed

5.2 Introduction

Innovative ideas demand a quick and inexpensive prototyping method to be competitive in the market. AM is a game changer and it started a revolution in the manufacturing industry [201]. Parts and components are fabricated layer by layer onto a build platform in AM technology. In metal printing, a heat source is used to melt feedstock powders for formation (deposition) of a layer which rapidly

solidifies before deposition of the next layer [202]. Components with very complex geometries are manufactured using AM which are otherwise impossible to produce with conventional manufacturing methods [202]. Assemblies requiring several parts separately built and assembled are produced as one component using AM [202]. As manufacturing is shifted from conventional to AM, supply chains are expected to shorten due to reduced tooling requirements and localized production replacing centralized manufacturing [203], [204]. Another important characteristic of AM is the reduced likelihood of human error during manufacturing due to AM machines using digital computer aided design (CAD) files to provide the manufacturing specifications [205]. AM alters the design landscape by using digital CAD files which facilitate communication between design engineers and manufacturers, known as Direct Digital Manufacturing (DDM) [206]. DDM, with its ability to locally manufacture parts on demand from stored CAD files, reduces suppliers' demands that result in less transportation and ultimately less energy consumption and lower emissions [206].

The use of highly optimized tools and components produced using AM technology boost the efficiency of other manufacturing processes and allow the development of new hybrid processes. These hybrid processes lead to further customization of complex tooling that require fewer parts and assemblies, thus reduce the environmental burden [207]. This characteristic of AM alters business models by shifting the focus towards building durable, high-quality parts with less complexity to re-manufacture, such as a modular design that is easily upgradeable [207]. Having dedicated AM machine shops that handle large orders at once present the most economical and environmentally friendly scenario due to the machines being able to operate the maximum amount of time possible. AM machines that spend a majority of time idling waste significant amounts of energy and increases environmental concerns [208]. Comparison of low machine usage to high machine usage showed a lowering of environmental impact per component built by a factor of ten [208].

In general, AM process consume less energy which consequently results in reduction of CO₂ emissions of products with complex geometry over their life cycle. This characteristic of AM process has provided more liberty for designers, particularly for high value, low volume industries such as aerospace and medical [203]. Furthermore, AM has the potential to reduce economic costs by 170–593 billion US \$ and the primary energy supply by 2.54–9.30 EJ and CO₂ emissions by 130.5–525.5 Mt by 2025 [203].

LCA are used to quantify the environmental effects of processes or products. Several LCA's regarding AM have been performed. Mami et al explored the environmental and economic aspects of AM in relation to the aeronautics sector [209]. They propose an approach based upon industries

environmental targets and provide a recommendation for the eco-efficient application of AM technology. In their methodology, they derive a weighting factor between multiple normalized impact scored and the industries target goal. Conventional manufacturing of an aerospace component was compared with a normal AM process as well as a topology optimized AM component. They found that weight reduction (342 grams to 274 grams) from an optimized AM manufactured component made it the superior environmental technology.

Faludi et al extended the knowledge of AM environmental impacts by using an LCA to determine whether the environmental contributions of the raw material, printer hardware, or the process energy consumption was more influencing [210]. Their test specimen was a complex turbine manufactured using selective laser melting (SLM) with a cradle to cradle scope. They determined that electrical demands encompassed around 80% of embodied energy and around 66%-75% of the other environmental impact metrics. The electric demand was also sensitive to utilization rates of the machine, with more idle time resulting in more electrical energy.

Walachowicz et al. compared laser beam melting with traditional manufacturing methods (CNC machining) by repairing a burner for an industrial scale gas turbine [211]. They also explore recycling options on the environmental impact. They recorded the electricity consumption for the repair process as well as all other material flows. AM was found to be much more environmentally friendly due to its higher material efficiency. The conventional repair process wasted three times the mass of the AM repair process.

Turbine blades manufactured using SLM, Investment Casting and Precision Machining were compared via LCA by Torres-Carillo et al. [212]. Their investigation showed a decrease of CO₂ emissions from 7.32 tons to 7.02 tons by switching to the AM process.

Bekker and Verlinden performed an LCA of wire arc AM was compared to CNC milling and green sandcasting using stainless steel as the material [213]. They performed a cradle-to-gate LCA using empirical measurements of a wire and arc additive manufacturing (WAAM) process. They concluded that AM is equal to both the processes from an environmental standpoint when it has a 75% material utilization efficiency.

Böckin and Tillman performed an LCA using powder bed fusion technology for the automotive industry by considering a complete product lifecycle in comparison with conventional manufacturing [214]. They showed weight reduction of an AM part played an important role during the use phase of

the products, suggesting that lower weight products that produced using AM resulted in significant environmental benefits.

AM offers many potential benefits, however, the environmental effects need a complete investigation. This study presents the fundamental methods of the AM processes and describe different types of available AM technology with focus on exploration of environmental and economic aspects of the technology. Then, using LCA methodology, a comparative evaluation of a conventional manufacturing process and a well-known AM technology is investigated by fabrication of a metallic component. Fabrication of the case study part is simulated for both processes using open source data for the Life Cycle Inventory (LCI). Comparison of the LCA outcomes for two process is discussed and validated with other studies and methods for improving each process are suggested. Finally, future research for advancing the AM process are suggested with respect to environmental sustainability. The present work is an introduction for environmental sustainability examination of the AM process in general and is a foundation for future studies. The comprehensive sustainability inspection of different types of AM processes with actual experiments will be conducted by LCA to have the numerical values of environmental impacts.

5.3 Metal Additive Manufacturing

A 3D model developed by a CAD software is exported to the printing machine. This model is sliced into many individual layers to be fabricated during printing [202]. Different technologies can be used to form the product layer by layer according to the CAD model. Each technology has its own characteristics, advantages, disadvantages, and applications. Metal AM generally is compiled into three main categories [215]:

- powder bed systems (PBS),
- powder feed systems (PFS)
- wire feed systems (WFS)

These category identifications are not standardized in research and industry; however, the metal AM technology is the same among all methods. Proper energy input is essential for the success of the powders feed methods, since reduced part density in the form of voids appear in materials when the energy input during manufacturing is too low [202]. Conversely, too much energy input reduces density by entrapping gas within the part during the melting process [202]. In addition, surface quality of manufactured parts is essential to the success of many components. Factors for powders based

systems that effect surface quality include the type of alloy, powders shape and size, energy source focal point size, and feed rates [216].

5.3.1 Powder Bed Systems

PBS construct components by raking a thin layer of metallic powder across a work surface and melting the powders in the specified geometry of the final solidified part [202]. Typical heat sources for melting powders are laser beams or electron beams. They require a support structure for heat dissipation as well as for the structure of the part [202]. The high levels of heat dissipation require pre-heating (200°C-500°C) of the bed in order to reduce warping [202]. In comparison to other metal AM processes, PBS build volume is less than $0.03 m^3$, that results in limitation of the size of components [215].

PBS lasers have wavelengths of infra-red range with spot sizes between 50-180 μm , and laser beam melting (LBM) layer thicknesses are around 20-100 μm [202]. The choice of laser has significant impact on the quality of the product and it depends to absorptivity of materials for melting the desired powders sufficiently at given feed rate [217]. Inert gases such as Nitrogen or Argon are used to aid in keeping oxygen levels low for preventing any harmful chemical reactions [202].

5.3.2 Powder Feed Systems

PFS's utilize a nozzle to spray powders onto a surface to create the desired geometry instead of raking the powders across the surface like PBS [215]. As the powders are sprayed, a heat source melts the powders similar to PBS [215]. The printing process is carried out by a raster motion of laser beam in a rectangular pattern across the stationary work piece [202]. Inert gasses in PFS are Helium and Argon to protect against oxidation [218].

PFS often have larger build volumes like the Optomec 850-R-unit of $1.2 m^3$ compared to PBS [215]. Build rates of $300 cm^3/h$ (higher than PBS) are achieved using a layer thickness between 40 μm to 1 mm [202]. In addition to building new components PFS allows for rebuilding or repairing of existing products [215]. The subsets of PFS include [202]:

- Laser metal deposition (LMD)
- Electron beam melting
- Plasma arc beam melting.

The major focus of this research is on LMD. However, some other AM technologies have also been discussed in this study. A high-power laser source provides required energy for melting metallic powders in LMD process. There are many different aliases and commercialized variations of this

technology such as direct metal deposition, laser direct casting, laser engineered net shaping, laser cladding, and laser deposition welding. These different names are adopted by various institutions and companies while they are essentially the same technology of using a laser to melt and deposit powders into a substrate [216].

5.3.3 *Wire Feed Systems*

WFS are extremely similar to PFS with a metallic wire instead of the metallic powders being the main difference [215]. Due to the large availability and low price of wire, WFS are less expensive than powder based systems [219]. WFS are capable of high build rates, associated with large molten pools, and large build volumes in comparison to PFS and PBS [219]. Because of rough surfaces, WFS often require post process machining to achieve the desired static and dynamic qualities [219]. WFS energy sources are divided into three subgroups like in PFS [220]:

- Electron beam based
- Laser beam based
- Electrical Arc based

The most common energy source for WFS technology is laser beam due to its high precision. However, it is an inefficient technology (2-5% efficiency) in terms of energy consumption. In comparison, the efficiency of electron beam sources are approximately 15-20% but it requires high vacuum working environments, which can limit its application [220]. Metal arc welding have considerably higher efficiencies than both laser beam and electron energy sources, sometimes reaching up to 90% [220]. However, higher accuracy of laser beam technology makes it more demanding instead of its lower efficiency.

5.4 **Economics Aspects of Additive Manufacturing**

Recent analysis of the market capabilities of AM predict that the AM industry will reach a market size of \$50 billion between 2029 and 2031 and \$100 billion by 2044 [221]. The majority of these markets are expected to be developed in the aerospace, automotive, and healthcare industries [222]. Additionally, it is expected that AM technology to highly implement in manufacturing of tools and molds with internal cooling by optimized channels that reduce thermal stress in loading dies which results in higher production rates [222]. As the technology further develops and penetrates the market, economies of scale have been found to be a reality, meaning that larger volume productions of materials using AM may be economically feasible [223]. AM is foreseen to rapidly alter the manufacturing market from manual engineer-to-order production, to a customer individual mass

production market [224]. The implementation of AM into the market will integrate customers more closely to the manufacturers supply chain by reducing lead times, low volume products that would often take significant amounts of time to manufacture [224].

5.5 Environmental Aspects of Additive Manufacturing

5.5.1 Consumption Reduction

Compared to traditional methods in which material is removed from a larger block, AM fabrication is considerably less wasteful since parts are built layer by layer [205]. AM technology is more environmental friendly than traditional machining processes because little metal debris or chips are produced during fabrication process [225]. The majority (approximately 90%) of environmental impact in AM technology is a result of the atomization process required for feedstock powders manufacturing. The atomization process in powder manufacturing consumes high energy but results in small amounts of waste since it is a semi closed loop processing cycle [225].

The major sustainable benefits of utilization of AM technology are [205]:

- More efficient designed products
- Shorter supply chains, localized production, and condensed transportation routes.

Furthermore, these environmental advantages of AM technology have great impact on strengthening the local economy and social value [205].

The Solid Freeform Fabrication (SFF) and Direct Metal Deposition (DMD) as a die and mold manufacturing processes have high potential to drastically reduce conventional supply chain operations such as casting, forging, and machining, which results in dropping product lead times as well as the fossil fuel consumption, pollution, and resource wastes [226]. In a study by Morrow et al., three case studies considered: a simple injection mold insert, a mirror fixture, and a stamping die used in the auto industry for comparison of DMD and Computer Numerical Control (CNC) methods. The biggest defining parameter for energy consumption was the solid-to-volume cavity ratio, with low ratios tending to favor DMD processes while high ratios were more appropriate for CNC machining. The outcomes suggested that part geometry played a critical role in the comparison of the technologies, with more complex parts DMD is environmentally more favorable. For production of parts with low solid-to-cavity volume ratios, AM has been shown to be more efficient in terms of materials, time, and energy compared to milling process. Solid-to-cavity volume ratio is the ratio of component mass to

the mass of the minimally bounding volume of the component assuming it is completely solid and composed of identical material as the component [226].

5.5.2 *Resource Protection*

Typical options for material disposal include recycling, re-using, repairing, or placing parts of the product in a landfill. Worldwide waste has been predicted to reach 2.2 billion tons by 2025, resulting in significant problems [227]. Unfortunately, despite expanded recycling networks, the human population has been increasing their resource consumption year over year [228]. One of the key advantages of AM is recycling capability of the product at the end of life (EOL). Recycling materials is crucial and has a huge impact on protecting resources as well as saving energy and water from reduced mining of new materials. Additionally, reducing waste allows the landfills to last longer. Practice for using recycled materials are as follows:

5.5.2.1 Recycled Powders

The material waste, emissions, and cost are reduced by using more recycled materials instead of unused original feedstock powders [229]. However, some studies have shown that the recycled powders can oftentimes contain incorrect particle sizes, which needed further refinement in order for the powders to be appropriate for re-use in fabrication [229]. In certain industries, particularly aerospace, the component demands high quality materials, which limits the use of re-used powders. Comparison between different manufacturing processes indicated that [229]:

- Approximately 87% of the materials in conventional manufacturing processes end up as waste while AM technologies such as LMD has almost no waste.
- A large amount (~70%) of waste powder from some manufacturing processes such as EBM cannot be re-used without proper treatment and recycling process.
- There is additional waste from the post processing due to material removal.

The average mass ratio of initial material to final product is reported to be in the range of 12:1 to 25:1 using traditional processes for manufacturing aerospace components made from titanium, while for AM processes this ratio is much lower, around 1.5:1 [229]. Furthermore, the use of topology optimization such as building honeycomb structures or internal cooling channels significantly cuts down on weight of components, which is particularly attractive for the aerospace industry [229]. However, the requirement of having a support structure to stabilize and fix objects during printing process may result in production of some waste materials during AM process. Currently, the possibility of proper recycling and reuse of support material is under investigation by industry [229].

5.5.2.2 Recycled Products

It is feasible to utilize both AM and traditional manufacturing technologies to take EOL parts and efficiently produce new parts in order to bypass the recycling stage. With this strategy, new products are fabricated from old products that possess similar mechanical properties of conventionally processed products [230]. Appropriate utilization of this approach can significantly reduce material and energy consumption during the manufacturing process [230]. Comparison between the primary energy usage of AM versus traditional manufacturing processes used in the refurbishing of EOL parts showed that the conventional repair process required significantly higher energy than the AM repair process, particularly in the amount of required materials.

5.6 Advantages and Disadvantages of Metal Additive Manufacturing

Application of AM technology to produce metallic parts and components exhibit many advantages over using traditional manufacturing techniques. Some of those advantages are small while others are considered game changers and have a significant effect on manufacturing of specific products. As with any revolutionary idea there are also some drawbacks that preclude AM from completely taking over and replacing traditional manufacturing processes. Many of these advantages and disadvantages are studied to either further their advancement or mitigate their weaknesses.

5.6.1 Advantages of metal Additive Manufacturing

- No significant tooling or molding process is required for the AM process [205].
- Digital designs easily are shared and edited using modern CAD software [205].
- The high rate of material recovery (approx. 97%) compared to traditional methods [218].
- Fabrication of highly complex geometries products that are not possible otherwise [218].
- When properly processed, static mechanical properties of metal AM materials are comparable to conventionally fabricated metallic components [215].
- Smaller and more localized supply chains leading to shorter lead times and less capital required [218].
- Opportunity for the refurbishing of parts that would otherwise be un-repairable, such as turbine blades, bearing seals, and shafts [217].
- Multiple materials are deposited in a continuous spray within a single component, allowing for new hybrid material compositions [217].
- AM processes require no cutting fluids [231].
- Wear-resistant alloys are easily deposited onto tool surfaces that lead to a significant extension of useful life for metal tooling [226].

- AM allows for further use of aging products by building retrofits and extending the operational life of equipment [232].

5.6.2 *Disadvantages of metal Additive Manufacturing*

- Low production volumes limit the technology only to be applicable for the production of highly customized products that are expensive and difficult to manufacture via traditional methods [205].
- Microstructural and mechanical anisotropy results in weakened properties within the direction normal to the plane of deposition [215].
- Rapid heating and melting that negatively affect fatigue characteristics [215].
- Post-processing may require depending upon the requirements of the component [217].
- Low volume production makes mass producing items via AM difficult to achieve economies of scale [215].
- Intellectual property and copyright issues have the potential to arise from the ability to easily distribute and share digital designs [224].
- High energy investment required to operate machinery [231].

5.7 **Additive Manufacturing Sustainability Advancement**

Although the field of metal processing via AM technology is relatively young, there is always effort to continually improve energy and materials efficiency for LMD technology. Various approaches are currently being researched with the goal of working towards enhancing AM technology, some are discussed below.

One of the drawbacks of LMD is the low energy efficiency. One method of increasing the efficiency is increasing the deposition speed by supplementing inductive assisted laser cladding [233]. Inductive heating is added to the laser process and compensates for rapid heat loss from the laser. The use of inductive heating during manufacturing increases deposition rates by a factor of approximately 2-2.5 while doubling the overall energy efficiency of the process [233]. Furthermore, adding the induction heat reduces spatial temperature gradients in the materials, which results in more durable structures.

The use of mechanical milling to produce feedstock powders for AM process makes it possible to develop a sustainable powders production route by making powders from a variety of materials chips with different sizes [234]. Due to the nature of mechanical milling, there is no requirement for high temperatures, which allows for significantly lower energy consumption in comparison to traditional atomization processes [234]. The powders are formed using a novel two-stage mechanical milling approach and have near-spherical morphology and particle diameters of 38–150 μm , making them comparable to conventionally produced powders [234].

The process chambers of the AM technology is improved with access to higher quality chamber seals, which reduces the consumed process gasses to generate the inert process atmosphere [235]. The accurate control of subsystems within the machine yields energy savings by turning off various parts of the machine in standby mode and downtime. A final design improvement is implemented a variable volume process chamber, where the height, width, and depth of the chamber adjusted to suit the requirement of the product for manufacturing and resulted in less energy consumption [235].

Efficient powders heating leads to less energy consumption. Improving laser technology results in efficiency increase of AM process, since lasers contribute to significant energy demand [236]. Consequently, using advanced lasers with high wall plug efficiency mitigates the significant energy consumption.

5.8 Life Cycle Assessment of Laser Metal Deposition

LCA as an essential tool for determining the environmental effects of a product or system and are commonly applied to evaluate sustainability. LCA's were deemed important enough for an international code, ISO 14040, to be created to enable the practice of LCA's within industry and research under a standardized method. LCAs is a tool for the analysis of effects of a process or product on the environment such as greenhouse gas emissions, ozone depletion, smog creation, eutrophication, acidification, depletion of resources, water use, land use, and many other aspects that are quantified and understood through impact assessments results from LCAs [237]. The four basic elements of LCA are the goal, scope, inventory analysis, and impact assessment. Interpretation of results follow the four basic elements and are defined for LMD machines in this study.

5.8.1 Case Study

The environmental aspects of manufacturing a stainless-steel pump impeller using LMD technology in comparison with casting method as a conventional process is the main goal of this section. The LCA is used as tool for this investigation with the functional unit being 1 produced pump impeller of a mass of 10.79 kg. The dimension and mass properties of the impeller are defined in Figure 1. While there are other aspects of both the AM and conventional process that are considered in this study. For simplicity several variables considered negligible for both process.

This LCA has a goal of demonstrating how the LCA process aids in identifying the environmental impacts of manufacturing the impeller via LMD processes in comparison to a conventional manufacturing process such as casting. The direct comparison of methods allows for the areas of greatest and smallest environmental impact to be identified for future improvement and understanding.

By understanding the weaknesses and strengths of using LMD to replace casting processes, manufacturers of pump impellers and other similar products determine what manufacturing process yields the minimum environmental impact while still producing a high-quality component.

There are several unrestricted and commercial LCA Software packages with databases available such as GaBi, SimaPro, and openLCA. In this study, openLCA is used since its associated databases cover the presented case study. Although, the data sets in openLCA are based mainly for Europe, most of the data points are a global reference from the selected data sets [238].

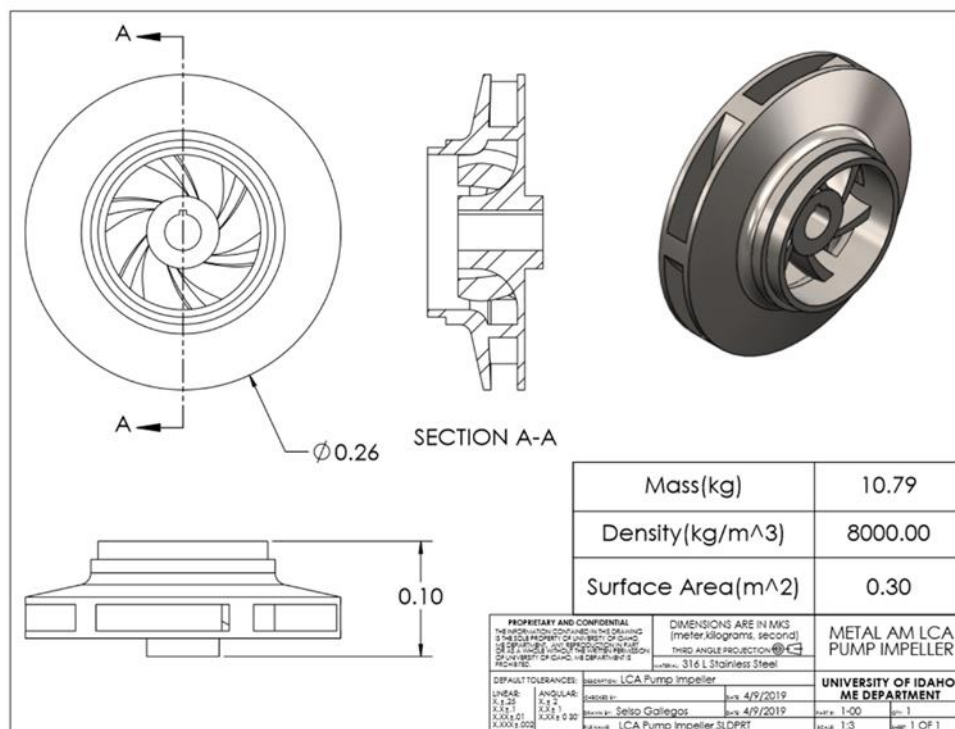


Figure 5.1: Drawing of pump impeller used for analysis

The aim of LCA is to quantify the consumed energy, released emissions, and environmental impacts of LMD manufactured impeller and casting manufactured impeller during 5 stages of pre-manufacturing, manufacturing, use, transportation, and EOL. The service stage of the impeller is not considered because the impeller rotation environmental impacts is negligible. Although, post processing sometimes is required in order to achieve a high-quality surface finish, it is not considered a requirement of the LMD process like it is for the casting process. GWP, AP, FAETP, HTP, and ODP are among the environmental impact indicators used to quantify the environmental impacts of the two processes.

5.8.2 *Life Cycle Inventory*

The LCI of the process is summarized in Figure 2 and Figure 3 for the LMD and Casting process for five different stages for the pump impeller.

5.8.2.1 Pre-Manufacturing

Generally, the pre-manufacturing stage of an LMD process includes mining and extraction of the raw materials in addition to the production of the metallic powders. a large variety of metals, including tool steel, stainless steel, titanium, titanium alloys, aluminum casting alloys, nickel-based superalloys, cobalt-chromium alloys, gold, and silver can be used as feedstock materials for LMD technology [239]. The mining and smelting of these materials has been fairly well documented and its environmental impacts are generally understood [240]. The environmental effects of mining are substantial and thus recycling materials should be strongly considered during the pre-manufacturing process due to economic and environmental considerations [241]. The powder formation process is generally referred to as the atomization process. The basic principle of the atomization process involves a stream of molten metal being rapidly disintegrated and cooled by a materials into individual particles [242]. Various techniques such as water, gas, centrifugal, vacuum, and ultrasonic atomization are used [242]. Water and gas atomization are the most common techniques used in industry [242]. Electrical energy is the major source utilized for heating materials in all pre-manufacturing techniques.

A couple of assumptions are required for better organization of the results:

First: the raw materials input for the powders atomization processes are sintered Iron (Fe) with a global reference value from the free Ecoinvent database on openLCA [243]. This data includes both material and energy requirements to obtain iron sinter. The materials efficiency for the atomization processes is assumed 90% efficient while the materials efficiency for the LMD manufacturing processes is also assumed 90% efficient. These values were estimated based upon values used in literature which were very high (95-98%), and so a more conservative 90% was thought to be more appropriate [211].

Second: the electricity and nitrogen gas required to produce 1 kg of steel powders is the same as required for titanium [244].

Table 1 summarizes the inputs used to model the Stainless-Steel atomization processes for the LMD case study. The casting process is estimated from Yilmaz et al. by scaling their inputs down in order

to achieve the required 10.79 kg of steel impeller [245]. Their casting process is assumed to be the best available technology.

Table 5.1: Pump impeller pre-manufacturing inputs/outputs for LMD

Pre-Manufacturing LMD				
Input	Unit	Amount/Unit	Total Amount	Reference
Electricity (Atomization)	kWh	6.60	71.15	[244]
Nitrogen Gas	kg	5.17	67.46	[244]
Sinter	kg	13.04	13.04	[246]
Output	Unit	Amount/Unit	Total Amount	
Metallic Powders	kg	11.86	11.86	

Similarly, the inputs for the casting process are outlined in Table 2 for the pump impeller.

Table 5.2: Pump impeller pre-manufacturing inputs/outputs for the casting process

Pre-Manufacturing Casting		
Input	Unit	Total Amount
Sinter	kg	40
Electricity (mold making)	kWh	6.85
Electricity (core preparation)	kWh	3.2
Electricity (Steel Production)	kWh	260.77
Sand (mold making)	kg	108.7
Bentonite	kg	6.3
Coal Dust	kg	6.3
Water	kg	4.85
Sand (core preparation)	kg	65.2
Phenol-formaldehyde resin	kg	2.6
Output	Unit	Total Amount
Ductile Steel	kg	21.73
Greensand Mold	kg	126.3
Core	kg	67.9

5.8.2.2 Manufacturing

Generally, the most complex part of LMD process occurs during the manufacturing stage. In this stage, the primary energy inputs are required in the following parts of the process [247]:

1. Laser system.
2. Stepper motors for machine.
3. Pre-heating of work surface.
4. Other miscellaneous parameters such as computer, fans, and lighting.
5. Post processing.

The amount of energy required for manufacturing a part is depending upon the required machining time during manufacturing process. Time required is a function of process control parameters such as laser power, laser speed, scanning pattern, hatch spacing, particle feed rate, and idle time [248]. Typical laser size is on the order of 100-5000 W with beam diameters approximately around 1 mm in size [248]. Laser speeds are typically on the order to 1 to 20 mm/s and particle feed rates are in the range of 1 to 10 g/min [248]. Idle time is dependent upon the scanning pattern as well as the geometry and materials of the part and range from 0 to 1000 seconds, which results in a highly variable amount of energy expenditure.

Preheating of the work surface is used to reduce laser power requirements, improve radiation absorptivity of the powders and wettability of the substrate [249]. Typically, infrared or resistive heaters are used to heat the process chamber to temperatures ranging from 80°C to 900°C, depending on the materials used and desired component properties [249]. Much like the atomization process, gasses such as Argon or Nitrogen are typically used.

Post-processing is often required for LMD constructed parts in order to achieve the desired hardness or fatigue properties [250]. Annealing is often used which requires heat treatment for up to an hour at high temperatures. One of the benefits associated with LMD is the ability to recycle unused powders during the application process. Some sprayed powders onto the work piece do not melt by the laser beam during printing process. A large portion of the un-melted powders can be collected and reused for AM process. The recovery rate is estimated to be in the range of 95-98% for 3D printing of metallic materials [205].

Regarding the case study, Table 3 provides a summary of assumed variables used for the construction of the pump impeller. The mass efficiency of the powder process is assumed to be 90% [205]. Laser power is highly dependent upon build size, speed, material, as well as other parameters such as idle time. For this reason. The average laser power used by Faludi et al. were adapted due to the similarity in part size [210]. The average power consumed is 1 kW. The assumed particle feed rate (0.3 kg/h) [248] and powder mass ($m = 11.86$ kg) are used to calculate the time ($t = 39.53$ hours) required to print the impeller.. The Nitrogen gas consumption is assumed the same as atomization process [244]. The electricity consumed by auxiliary heating requirements, stepper motors, lights etc. are neglected for the purpose and scope of this LCA.

Table 5.3: Pump impeller manufacturing inputs/outputs for LMD

Manufacturing				
Input	Unit	Amount/Unit	Total Amount	Reference
Electricity	kWh	1	39.53	[244]
Nitrogen Gas	kg	5.17	61.33	[244]
Metallic Powders	kg	11.86	11.86	[244]
Output	Unit	Amount/Unit	Total Amount	
Pump Impeller	kg	10.78	10.78	

Table 4 depicts the adapted inputs for the manufacturing phase of the casting process for pump impeller. The ductile steel produced from the pre-manufacturing stage is then melted and cast using electricity into the mold and core.

Table 5.4: Pump impeller manufacturing inputs/outputs for casting

Manufacturing		
Input	Unit	Total Amount
Ductile Steel	kg	21.73
Electricity (melting)	kWh	2.2
Electricity (casting)	kWh	4.1
Greensand Mold	kg	126.3
Core	kg	67.9
Output	Unit	Total Amount
Good Casting	kg	10.79
Slag	kg	1.3
Used Sand	kg	180.8

5.8.2.3 Use (Service condition)

The application or service of a product or process should include all the energy and materials input plus emissions related to scope of the LCA. The scope definition of the project determines intensity of the product use investigation. When comparing two different products or processes, it is possible the product resulting from one process performs inherently better than another during its useful lifetime. Those results are considered when substantial information is available to accurately quantify the effect of the improved performance.

In this study, an LMD process yields a pump impeller that resulted in a well-documented improved efficiency over the same pump impeller manufactured from traditional methods. The effect is included in the use section. However, there is likely to be a great deal of uncertainty in obtaining the quantities required for analysis. In most cases, an uncertainty factor is included in processes to specify that a parameter is not 100% correct. LMD is used to repair and extend the life of components [248]. By extending the life of a component, the environmental impact resulting from replacement of the impeller is reduced over time by avoiding the manufacturing of a new impeller. Essentially, it is assumed that there is no impact from the service stage based on the quality of the LMD and casting manufactured impellers are similar enough that there is no change in operating efficiency of the impeller during use. Assuming constant quality eliminates the need to estimate two type of wearing for 3D printed and casted impellers over the operation.

5.8.2.4 Transportation

The effect of transportation for any process varies widely depending upon the required distances between various stages in the product or process lifecycle. Typical transportation processes involve several stages.

1. Raw materials from location of extraction to pre-manufacturing facility.
2. Pre-manufacturing to manufacturing facility.
3. Manufacturing facility to distribution center for product.
4. Shipping to customer.
5. Disposal to landfill site, recycling center, and/or repair facility.

One of the potential benefits of metal AM is its ability to allow for smaller supply chains [218]. Through AM process the number of stages in the traditional supply chain is reduced by redesigning/designing products with fewer components and manufacturing products near the consumers [231]. Powders production is accomplished using locally sourced recycled materials, thus eliminating the need for shipping materials extended distances. The LMD manufacturing facilities are constructed near atomization facilities to further limit transportation environmental effects. Therefore, five stages of transportation reduce in LMD manufacturing.

In this study, transportation parameters for the pump impeller are summarized in Table 5. Both the LMD and casting process are assumed to experience similar transportation needs, and thus Table 5 is applicable for both processes. They are broken down into the type of shipping and life cycle. Due to the fact that majority of the data sets used in the LCA originate from Europe, the LCA and the parameters for transportation are based out of locations in Europe. Between pre-manufacturing and

manufacturing, the feedstock metallic powder travels approximately 400km via ship from Town Castle, United Kingdom to Bremerhaven, Germany. After the part is manufactured in Bremerhaven, it transports via train 504km to Frankfurt, Germany where it is implemented. Once the impeller reaches its EOL it ships via truck for 225 km from Frankfurt, Germany for recycling.

Table 5.5: Pump Impeller Transportation for LMD and casting processes

Transportation				
Transport				
Method	LCA Phase	Cargo(kg)	Distance(km)	Reference
	Pre-Manufacturing to			
Ship	Manufacturing	11.86	400.00	[251]
Train	Manufacturing to Use	13.04	504.00	[251]
Truck	Use to EOL	10.78	225.00	[251]

5.8.2.5 End of Life

Since LMD utilizes metal powders as the feedstock materials, there are typically many avenues available for recycling metal powders [252]. Due to economic incentives, the recycling of valuable metals [253] as well as electronic waste [246] are receiving many attention. The goal of recycling within AM is often to create a closed loop product life cycle, wherein the product materials at the EOL is completely recovered for use in other products.

The different metallic wastes and scraps are split into several categories, each representing a portion of the product lifecycle, although there is no scrap in LMD process. Home scrap represents the materials waste generated during manufacturing that is directly inserted back into the process [252]. For metal AM, this would be the powders waste from one build being reused into another process. New scrap refers to manufacturing waste of materials that have known properties and known value that is not recycled within the process but instead shipped to another facility [252]. Due to the majority of powders being recycled within the product production chain, the amount of new waste generated from metal AM is likely negligible. Old scrap is materials that has reached the product EOL, and generally requires more energy input to recover [252]. Functional recycling is used when old scrap is separated easily and combined with old scrap of similar composition to create new metal in the same family of materials [252].

In this study, when the pump impeller reaches its EOL, it is recycled back into powders that would be used to for another Stainless-Steel part made by LMD. The amount of energy required to recycle 1 kg of Stainless Steel is 7.96 kWh [254]. It is assumed that 90% of the impeller is recovered and turned back into stainless steel powder. The amount of nitrogen gas and electricity required for atomization of the recycled steel is assumed the same as what is used in the pre-manufacturing phase.

Table 5.6: Pump impeller EOL inputs/outputs for LMD

EOL				
Input	Unit	Amount/Unit	Total Amount	Reference
Steel Impeller	kg	1	10.78	
Electricity (Atomization)	kWh	6.60	64.03	[244]
Nitrogen Gas	kg	5.17	55.74	[244]
Output	Unit	Amount/Unit	Total Amount	
Metallic Powders	kg	9.70	9.70	

Table 6 outlines the inputs and outputs for the recycling process of the LMD while Table 7 indicates EOL process for the casting operation, which was estimated from [245]. The cast impeller is also recycled in a similar way, since both processes are composed of steel. The used sand is partially recovered since these can be re-used within the process. From literature, it is usually assumed that around 90% of sand can be recovered [255]. The values in table 7 are for a 90% recovery of steel and its sand. Further sensitivity analysis is provided to explore the effects of recycling rate on EOL impact.

Table 5.7: Pump impeller EOL inputs/outputs for casting

EOL		
Input	Unit	Total Amount
Electricity (Recycling)	kWh	85.8
Used Sand	kg	180.8
Steel Impeller	kg	10.79
Output	Unit	Total Amount
Recycled Sand	kg	162.7
Recycled Steel	kg	9.7

Figures 2 and 3 illustrate the LMD and casting processes in different stages of life, used for LCA. These figures show energy and materials flow in both LMD and casting processes for impeller fabrication.

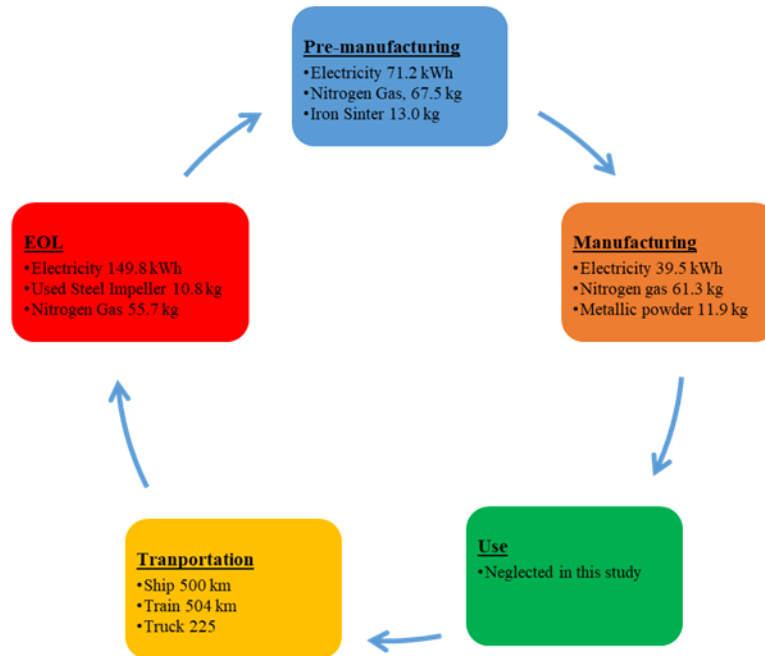


Figure 5.2: Summary of inputs for each stage of the LMD process

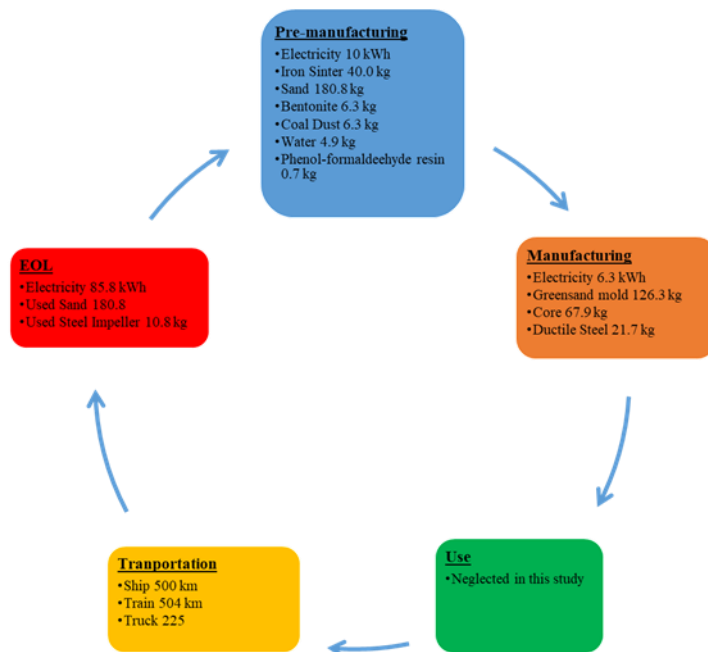


Figure 5.3: Summary of life cycle inputs for the casting process

5.8.3 *Impact Analysis*

The goal of Life Cycle Impact Assessment (LCIA) methods is to connect each LCI result to the selected environmental impacts [256]. Each LCI result will affect the impact category and feed the overall LCA result. LCIA should follow the definition and guidelines outlined in the ISO 14040 Standard. International standard ISO 14042 provides guidance for application of the LCIA [257].

The climate change potential is measured in kg of CO₂ emissions released directly or indirectly throughout the life stages of the product. It is commonly known as the Carbon Footprint or GWP of a process [258]. Analyzing the GWP is important because it is direct measure the climate change impact a process has on the environment [259]. The Acidification Potential (AP) is a measure of kg of SO₂ released into the environment by a process. AP is described as the soil and water destruction via acid rain caused by acidic air emissions released into the environment [260]. FWEP analyzes the environmental impact on fresh water ecosystems caused by toxic substance emissions to the soil water and air [261]. HTP is a measure of the potential harm a chemical emission has on the environment [261]. FWEP and HTP are measured in kg of one, 4-Dichlorobenzene (1,4DCB). One, 4DCB is an organic compound found in the atmosphere that has been classified by the EPA as a possible carcinogen that has detrimental impacts to the environment [262]. ODP is measured in kg of Chlorofluorocarbon (CFC), which is an organic compound produced as a by-product in different manufacturing processes [263]. It is composed of chlorine, carbon, and fluorine needs to evaluate because its' impacts are catastrophic to the environment [263]. CFC reacts with oxygen in the atmosphere and diminishes the ozone layer of the atmosphere in turn allowing more solar ultraviolet radiation to enter the atmosphere which impacts biological activity on the Earth's surface [263] like increasing skin cancer rates.

The Ecoinvent database developed by the Swiss Centre for LCI is used for impact analysis in this study [251]. CML 2001 is an operational guide for the ISO standards that provides impact categories and classification methods for an LCIA [243]. CML 2001 impact assessment method links the elementary flows of the Ecoinvent data to the characterization factors selected in the openLCA software project.

For this case study, CML 2001, Ecoinvent database, and openLCA are applied to quantify the impact categories. Table 8 provides an overview of the impact categories designated for the pump impeller case study impact assessment [243]. The impact categories are selected based on the most common environmental impact parameters.

Table 5.8: Pump Impeller Impact Categories

CML 2001 Impact Categories Implemented in Ecoinvent Database		
Impact Categories	Name	Unit
Climate Change	Upper Limit of Net GWP	kg CO ₂ -Eq
Acidification Potential	Generic	kg SO ₂ -Eq
Freshwater Aquatic Ecotoxicity	FAETP 100a	kg 1,4-DCB-Eq
Human Toxicity	HTP 100a	kg 1,4-DCB-Eq
Stratospheric Ozone Depletion	ODP 10a	kg CFC-1-Eq

5.8.4 Interpretation of Results

The overall GWP for the pump impeller of case study is 3.21 and 3.78 kg of CO₂ for the LMD process and the casting process respectively. This represents a 15% reduction of CO₂ by LMD process in comparison with casting process. Figure 4 shows the breakdown of the GWP of each life stage of the pump impeller.

Climate Change Upper Limit of Net GWP kg CO₂-Eq Acidification Potential Generic kg SO₂-Eq
 Freshwater Aquatic Ecotoxicity FAETP 100a kg 1,4-DCB-Eq Human Toxicity HTP 100a kg 1,4-

DCB-Eq Stratospheric Ozone Depletion ODP 10a kg CFC-1-Eq

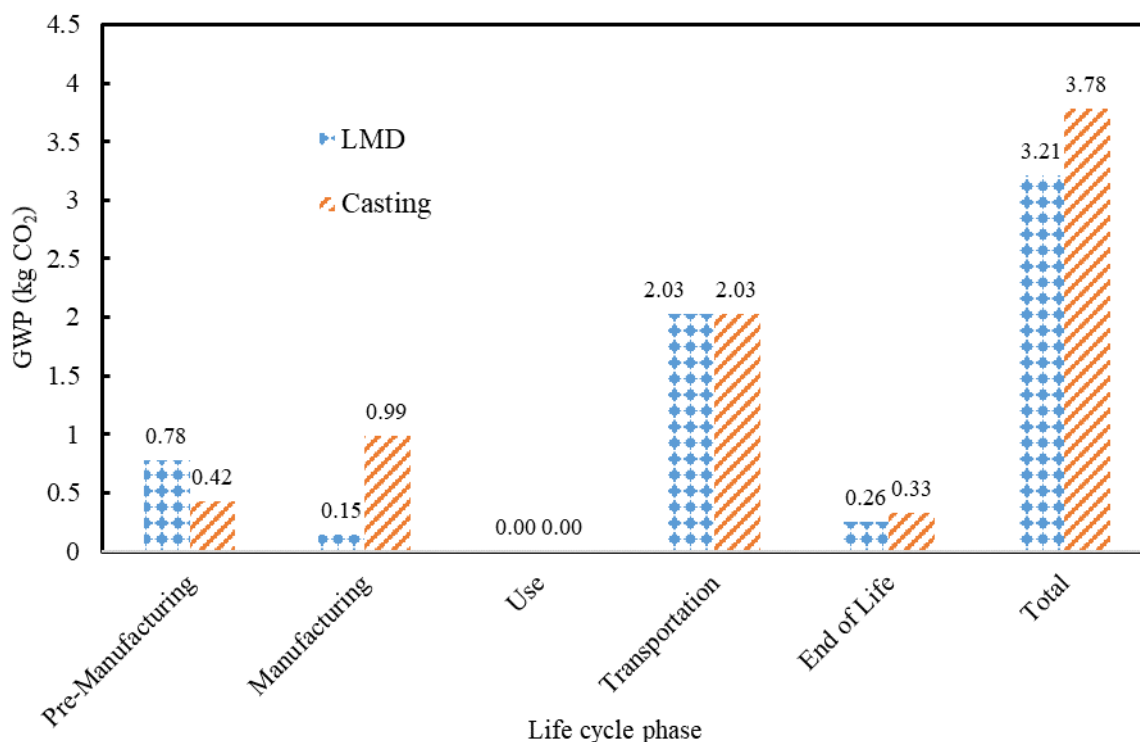


Figure 5.4: LMD and casting processes GWP comparison

For the LMD process, the transportation contributes the most CO₂ to the GWP, which is equal to casting. In pre-manufacturing stage, LMD consumes more electrical energy compared to casting. This is due to the high SEC required for powder production. LMD process performs better in the manufacturing stage, likely a result of the significant energy required for melting and casting as well as the significant amount of waste. In the last stage of EOL both processes show the benefits of recyclability, while the LMD process is superior.

The AP of LMD and casting are depicted in Figure 5. Similar to GWP, the pre-manufacturing process for LMD has significantly higher AP than the casting due to the high-energy requirement. The manufacturing stage for casting contains much higher acidification potential resulting from the output waste of the mold and cores. On contrary, LMD process is more sustainable than casting at EOL stage. In total, LMD process contributes 20% less to AP than casting.

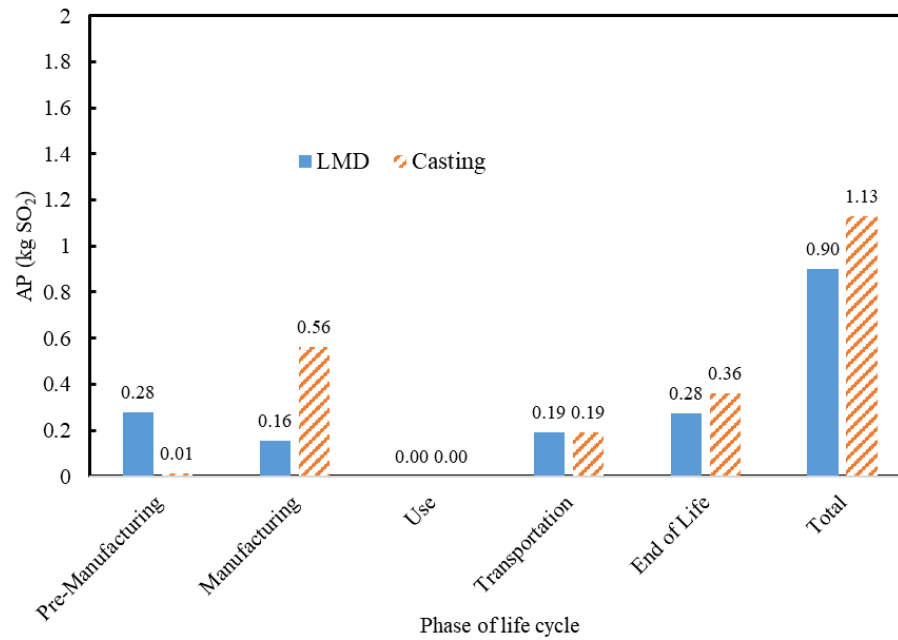


Figure 5.5: Acidification potential of LMD and casting processes

FAETP is illustrated for LMD and casting processes during each life stage in Figure 6. In the pre-manufacturing stage, casting has higher impact on FAETP because of sand molding process. Casting FAETP during the manufacturing phase is also much higher than LMD as a result of the significant amount of waste. Overall, LMD process has 65% less contribution on FAETP than casting.

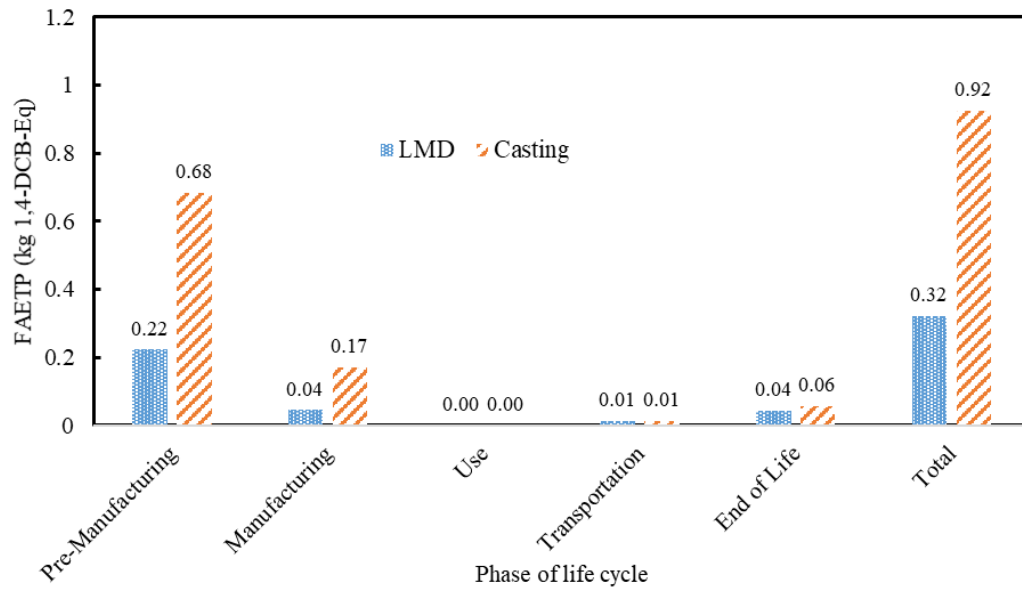


Figure 5.6: FAETP comparison between LMD and casting processes

HTP for LMD and casting processes in different life stages are shown in Figure 7. The LMD process shows the greatest quantity of HTP in the pre-manufacturing stage, followed by the EOL stage, because of high electricity consumption required for atomization. The casting process, with its required greensand molds, suffered in the manufacturing process. Transportation has the lowest effect on HTP. Generally, LMD process cause 20% less impact on HTP in comparison with the casting process.

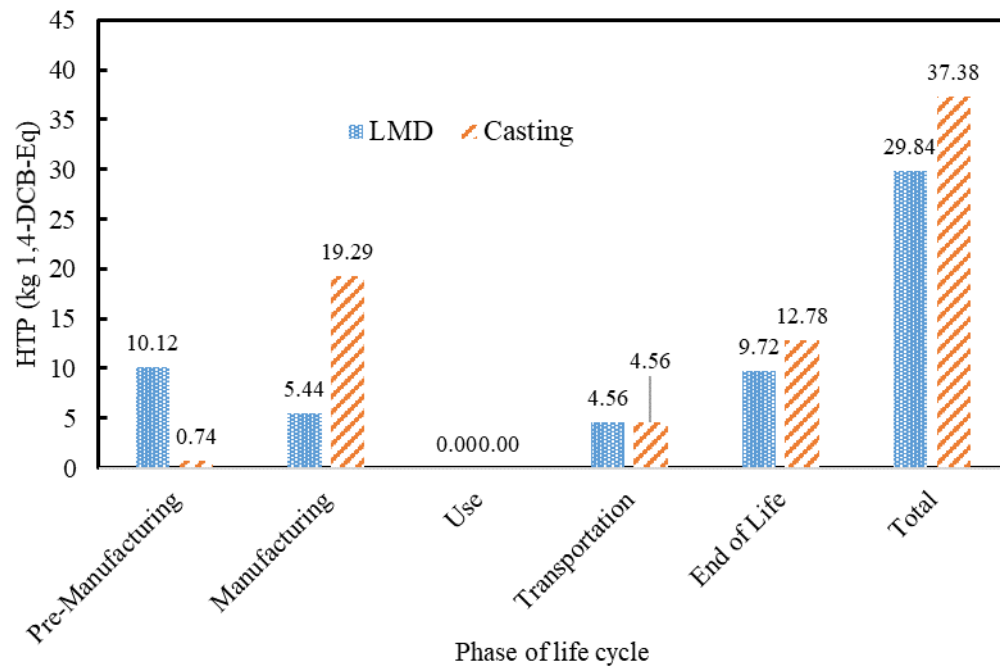


Figure 5.7: HTP for both LMD and casting processes

Figure 8 presents that ODP of LMD and casting processes in various stages. In pre-manufacturing stage, LMD has higher effect on ODP than the casting. While at the manufacturing stage, the LMD has much less impact on ODP than casting. It concludes that LMD has 10% less impact on ODP in comparison to casting.

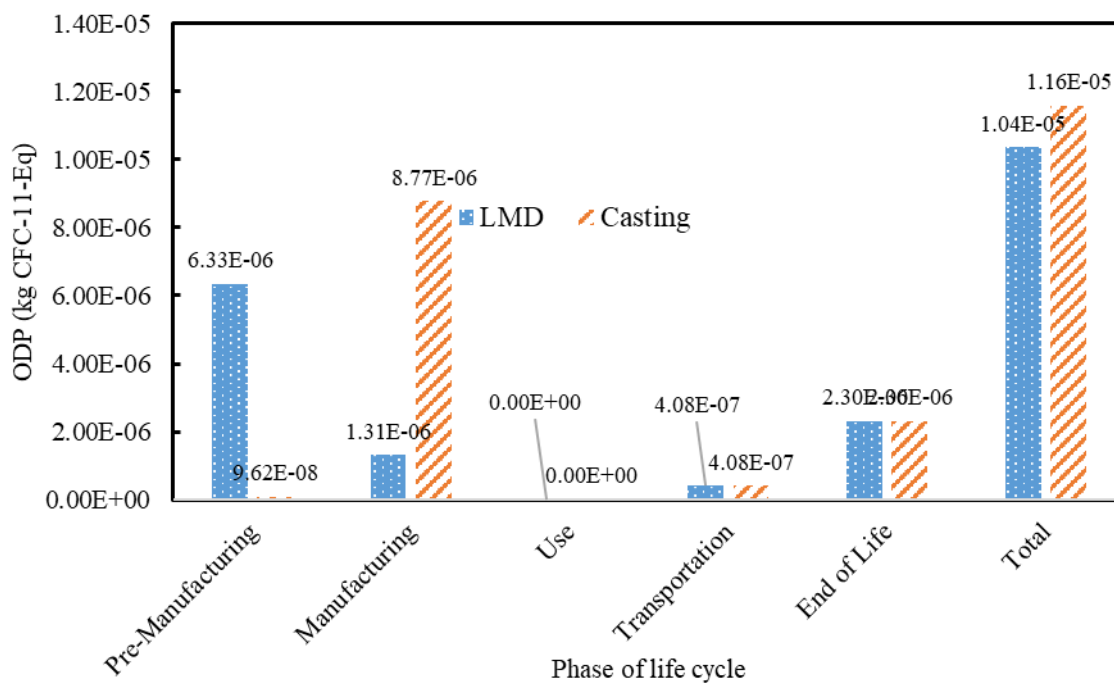


Figure 5.8: Ozone depletion potential for LMD and casting processes

5.9 Validation

Since online data was used for the case study, other similar case studies were investigated to validate the outcomes of the study. Peng et al. conducted an experiment for fabrication of an impeller applied in turbomachines with different production methods including AM and casting processes [264]. Their results showed that the environmental impact through indicators of GWP, AP, Chinese resource depletion potential (CADP), and respiratory inorganics (RI) were much lower in AM process in comparison with casting. Table 9 compares the findings from this study with the one reported by Peng et al. for AM processed case studies.

When taking into account the variability of many different parameters in the LMD process, such as build rate, powder size, SEC of powder consumption, and materials utilization efficiency, the authors believe the results of the case study presented in this study are in acceptable agreement with the similar studies.

Table 5.9: Results comparison

	Built Rate (kg/h)	Laser (kW)	SEC (kWh/kg)	Powder Efficiency (%)	Environmental Impact Indicators	Outcome
This study	0.3	1	6.6	90	GWP, AP, FAETP, HTP, ODP	AM Superior
Peng et al.	0.47	1	0.6	92.5	GWP, AP, CADP, RI	AM Superior

5.10 Discussion of Results

To depict picture complete portrait of the AM process, the advantages and disadvantages are compared to a conventional casting process. Manufacturing a pump impeller was considered as the case study while principles of LCA were used to quantify the environmental effects. Prior to discuss the numerical value of LCA in each process, it should be mentioned that the AM process and casting are closed cycle process from the point of material recyclability as depicted in Figures 2 and 3. The simulations concluded that LMD environmentally is more sustainable than casting process. Figure 9 illustrates the percentage reduction of LMD compared casting in GWP, AP, FAETP, HTP, and ODP.

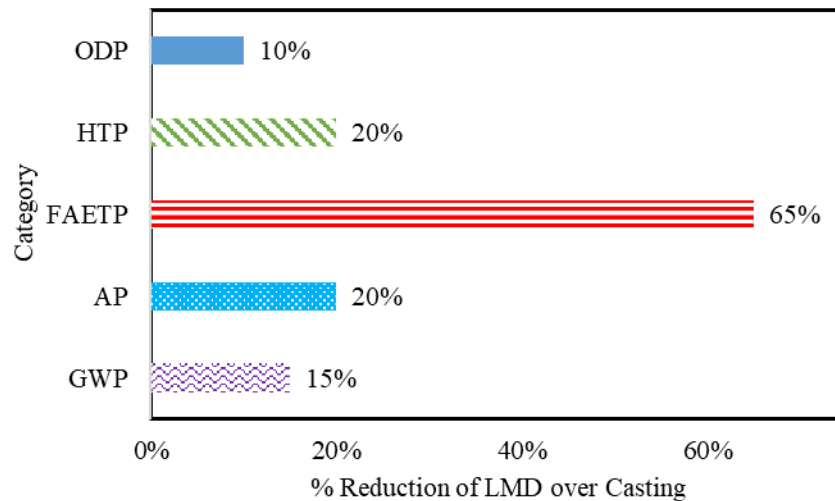


Figure 5.9: Summary of LMD environmental impact reduction over the casting process

The intense electricity consumption during the atomization process of powders in pre-manufacturing stage make LMD less attractive in comparison to casting process during this stage. In the other stages,

however there was a strong indication that LMD is more environmentally friendly. For further improvement, authors suggest using electricity generated from renewable energy resources and hydroelectricity to lessen the environmental impact of the LMD on the environment during pre-manufacturing, manufacturing and EOL. However, this is not the ultimate solution for improving the LMD process. Finding new methods to lower electricity demand as well as achieve higher build-up rates for the manufacturing stage are permanent solutions for enhancing the LMD.

The size of the laser and build-up rate of the machine depend on the manufacturer, and therefore, it accounts for a large change in total energy required for the manufacturing process. The large difference in SEC for the powder production is an interesting fact. The build-up rate, powder size, SEC of powder consumption, powder type, and powder utilization efficiency influence the LCA of the AM process. In particular, the SEC of the atomization process was found to be highly variable. 6.60 kWh/kg was used for this LCA, yet in literature it is reported as a range for steel from 4.2 kWh/kg to 7.2 kWh/kg [265].

Finding the impact of different recycling rates in the EOL stage for both casting and LMD were performed as part of a sensitivity analysis. Recycling rates of 50% and 70% are shown in Figure 10 for both processes. The values indicate the increased GWP resulting from additional virgin resources being required to make up for the decreased recycling rates. For example, a 70% recycling rate would result in an increase of GWP of 0.08 for the LMD process since the required material would have to be obtained from the pre-manufacturing process again.

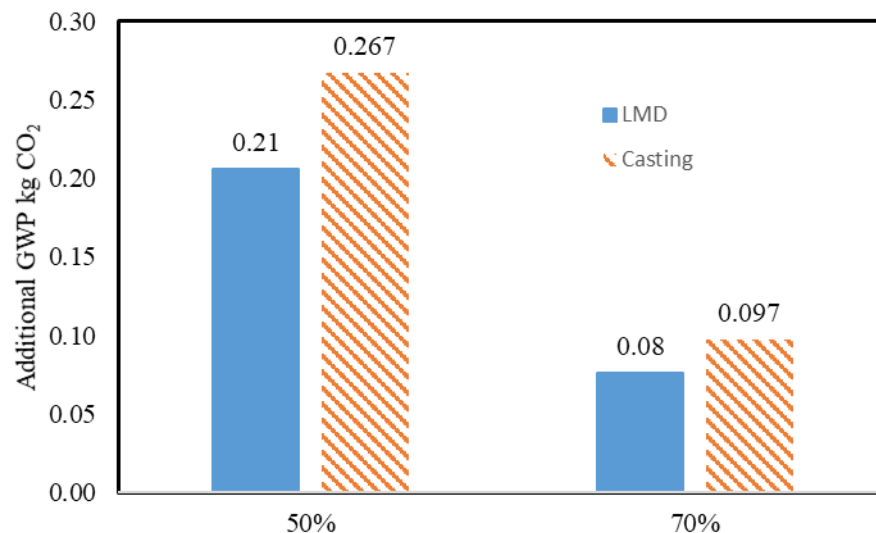


Figure 5.10: GWP increases resulting from decreased recycling rates.

A similar sensitivity analysis on the average laser power shows increased GWP if the average power is increased. Figure 11 shows the total GWP if the laser power is 1 kW, 1.5 kW, or 2 kW.

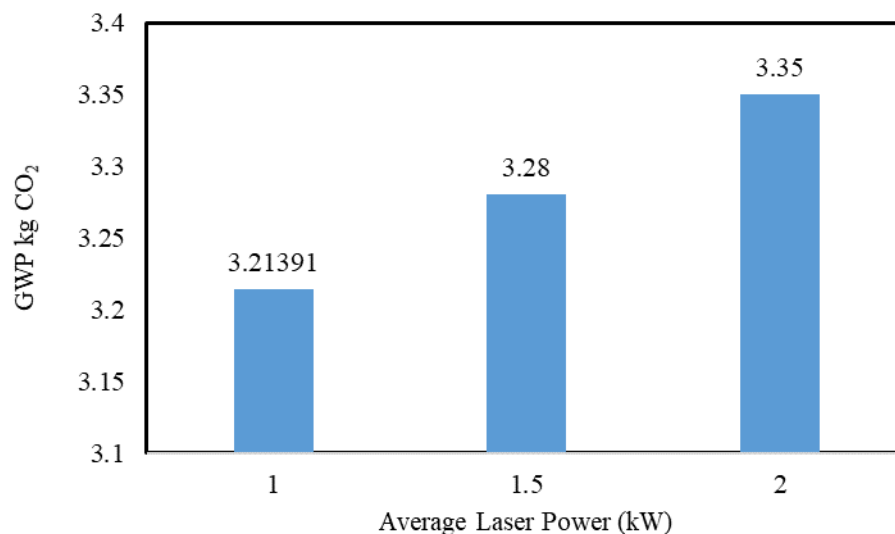


Figure 5.11: Average laser power and GWP

5.11 Conclusions

The field of AM is growing rapidly, and modern fabrication is trending towards a revolution. Due to the potential environmental impacts resulting from AM, the effects of the process need more investigation. This study presented an overview of fundamental technology used to fabricate AM metal parts, followed by environmental and economic advantages of AM. There is no need for expensive molding or different stages of machining in the AM process, which presents a great economical advantage while lowering harmful contribution to the environment through fewer operations, less materials and reduced transportation. The most desirable characteristics of AM process are its recyclability, possibility of reusing feedstock materials, and its high material efficiency. Recycling the waste powders during the AM process and at EOL make AM an attractive technology. The drawbacks of AM have also been presented to show a more realistic picture of the AM process. To compare the AM process with the conventional processes, the fabrication of a pump impeller was simulated in this study for LMD as a well-known AM process and casting process. To study the environment impact of these two processes, an LCA was applied to establish numerical values for environmental impact in five different life cycle stages of a pump impeller. The environmental impact indicators were GWP, AP, FAETP, HTP, and ODP. The outcomes indicated that in the pre-manufacturing stage, AM process has higher environmental impact compared to casting. This was attributed to the intense electricity consumption required for the atomization process. In the manufacturing stage, LMD was superior to

casting due to its low waste. Although it was favorable to casting, the low speed of the AM process increases the total energy used. Different laser power was explored and found to have little effect on the environmental effects. An increase of average power from 1 kW to 1.5 kW increased the GWP by only 2%. Ultimately, a pump impeller produced by LMD has anywhere from 10% to 65% less impact on the environment depending upon the impact category.

In conclusion the recyclability of the AM process has the greatest advantage from point of environmental protection. Although, there are weaknesses in the pre-manufacturing and manufacturing stages that cause greater strain on the environment, these weaknesses are mitigated by using electricity generated from hydro resources and renewable energy. Renewable energy sources will have lower GWP and AP compared to fossil fuels, and their use may help offset the intense energy demand of LMD.

This study is a preliminary work in this area and further research on enhancing the sustainability of AM technology is needed in future to focus on improving its sustainability in following areas:

- developing powders manufacturing technologies with lower energy consumption,
- investigating the impact of dominant parameters (SEC, built rate, powders efficiency, etc.) on the LCA of AM process,
- optimization of key parameters for the efficient outcome,
- increasing the production speed of AM process during the manufacturing. This will advance the economics of AM process as well by making it less expensive to construct the required parts.

Chapter 6: Conclusion

6.1 Conclusions

This thesis has presented several analyses of commonly used technologies and means of acquiring energy or materials with regard to developing a sustainable system. These include analysis of geothermal energy resources and how they can be levered more successfully, district cooling systems coupled with cold thermal energy storage, the acid mine drainage problem within the mining industry, and laser metal deposition.

Each analysis has discussed how factors such as policy, society, economy, design limitations, performance, and efficiency shape the implementation of each system. This analysis clearly shows that there are always advantages and disadvantages associated with every design. Each technology has potential for improvements ranging from simple process level improvements to complex technological advances that offer potential to dramatically increase performance. Common among all levels of improvements is the requirement of capital investment prior to implementation of any upgrades in performance. Economic decisions have been shown to be a significant driver for whether or not systems become implemented. This thesis has shown that economic conditions play an important role in sustainability. If money were no object, it would be relatively easy to implement sustainable practices and a sustainable future would be within reach. Many of the technologies discussed in this thesis have high investment costs, particularly in geothermal systems. These high investment costs can deter investors from implementing improvements and stand in the way of sustainability.

Additionally, in current scenarios, the return on investment can be not sufficiently high enough to warrant the installation of sustainable upgrades. For that reason, this author concludes that governmental policy should play a bigger role in the development of sustainable technologies. Policy such as tax incentives and small subsidies may help spur more innovation within these fields and remove some of the personal risk for investors. Policy can also be focused on education of the people regarding possible alternatives. Geothermal energy, for example, is a large unknown within society due to lack of public knowledge and awareness. Increasing public awareness allows for more potential investors as well as giving people more informed opinions with which they can use to affect policy.

Despite the significant cost that may be required for large scale sustainable design, this analysis has shown that both small and large improvements that advance the sustainability of systems can be accomplished using both state of the art technology as well as simple, inexpensive upgrades.

Geothermal energy is characterized by the difficulty in finding suitable locations for extraction. However, the emergence of hybrid geothermal-solar systems that boost efficiencies and production, offer an easy way to increase the economic and thermodynamic performance without dramatic change. With the current trend of solar power decreasing in price, this option is rapidly becoming a much more attainable option to retrofit existing power plants by superheating the working fluid or preheating the geothermal brine. Modern computing methods also present significant advances in the optimization of multivariable systems that can be used to create complex control algorithms that greatly enhance energy and exergy efficiency of geothermal systems while reducing cost of the produced electricity or energy. Perhaps more promising is the potential of enhanced geothermal systems. By being able to safely produce artificial geothermal systems wherever suitably hot rock is found, significant amounts of sustainable energy can be obtained for years to come.

In general, designing systems that are capable of matching generation and production to their intended load allows for the highest efficiencies to be achieved. This was shown by thermodynamically analyzing a district cooling system coupled with cold thermal energy storage. It was found that reductions of 592 MWh are possible simply by adjusting the production of chilled water to match the demand of the load. Not only did this save approximately 107,000 kg CO₂ per month, it also resulted in a cost savings of \$56,000. This approach indicates that many large systems have potential to enhance their sustainability through better load matching.

Acid mine drainage has decimated several ecosystems by increasing the acidity of local water supplies to the point that very few organisms can survive it. Different options were discussed as to remediating the problem. Passive approaches show promise as they require little to no maintenance after installation. Additionally, their ability to naturally filter out the acidity over time presents, in this authors view, the most long-term sustainable option for rehabilitation of damaged land. Among active approaches, membrane technology is the current trend of research due to its ability to remove over 95% of the AMD contaminates, provide clean drinking water, and reclaim rare earth metals at the same time.

Additive manufacturing of metals, discussed in chapter 5, offer a potential revolution of how products and components are designed and manufactured. Their ability to generate complex shapes just as easily as simple shapes allows for significant design flexibility that is not easily attainable when using traditional manufacturing methods such as milling and casting. New designs that have potential to increase component efficiency or reduce material consumption are possible with AM technology. Also, very promising in terms of sustainability is the ability to refurbish and repair worn components.

The result is longer lasting materials, which can reduce cost and reduce material usage, both being beneficial for sustainability. The comparison for manufacturing a pump impeller using laser metal deposition and traditional casting showed that, while AM has an intense energy requirement, AM is superior to casting from an environmental perspective. The conclusions from that study have also been validated by comparison of results to similar studies involving AM and traditional manufacturing comparisons. While there is certain to be lots of uncertainty in the exact emissions and environmental impacts resulting from AM, it is safe to say, that AM certainly is no worse for the environment than traditional manufacturing. Thus, factors that play into the decision to use AM or traditional methods of manufacturing should be focused on design intent and cost of production.

6.2 Future Study

While this thesis has touched upon many different technologies and presented opportunities for advancing the sustainability, there is significant amounts of additional research and development that will continue the march towards sustainability. Enhanced geothermal systems require more research into developing the proper fracture techniques for implementation in pilot programs. There is an abundance of research in the modeling and simulation of fracture growth, but very little experimental work.

Within the UI district cooling system, future study can focus on implementing more sophisticated optimization algorithms to minimize energy consumption and maximize efficiency based upon the dynamic cooling load. This is likely to require a great deal of cooling system data from previous years in order to develop the proper algorithm, but there is potential to have the system operate at its best all the time depending upon its cooling load required.

AMD is recognized as a serious problem and many sites are under remediation construction. However, there is much more work to be done in researching membrane technology systems in conjunction with passive and active treatment options. Research should focus on making the systems more cost effective for implementation within industry.

The advantages of LCA's in order to quantify the environmental effects are well established. However, their use should be further extended into more fields. By performing more LCA's, the environmental impact for many processes can be very well understood. This understanding can motivate more research into further improvement.

The above suggested future study is only a tiny fragment of the possible research areas that can be explored within these fields. With the implementation of modern computing and data analytics, there

has never been a better time to develop sustainable technology than now. No matter the future direction of research, it is hope that sustainable technology solutions become more prioritized.

References

- [1] Nasruddin *et al.*, “Potential of geothermal energy for electricity generation in Indonesia: A review,” *Renewable and Sustainable Energy Reviews*, vol. 53. 2016, doi: 10.1016/j.rser.2015.09.032.
- [2] I. B. Fridleifsson, “Geothermal energy for the benefit of the people,” *Renew. Sustain. Energy Rev.*, vol. 5, no. 3, pp. 299–312, Sep. 2001, doi: 10.1016/S1364-0321(01)00002-8.
- [3] R. Bertani, “Geothermal power generation in the world 2010–2014 update report,” *Geothermics*, vol. 60, pp. 31–43, Mar. 2016, doi: 10.1016/J.GEOTHERMICS.2015.11.003.
- [4] R. Shortall, B. Davidsdottir, and G. Axelsson, “Geothermal energy for sustainable development: A review of sustainability impacts and assessment frameworks,” *Renew. Sustain. Energy Rev.*, vol. 44, pp. 391–406, Apr. 2015, doi: 10.1016/J.RSER.2014.12.020.
- [5] P. Olasolo, M. C. Juárez, M. P. Morales, S. D’Amico, and I. A. Liarte, “Enhanced geothermal systems (EGS): A review,” *Renew. Sustain. Energy Rev.*, vol. 56, pp. 133–144, Apr. 2016, doi: 10.1016/J.RSER.2015.11.031.
- [6] E. E. (Stathis) Michaelides, “Future directions and cycles for electricity production from geothermal resources,” *Energy Convers. Manag.*, vol. 107, pp. 3–9, Jan. 2016, doi: 10.1016/J.ENCONMAN.2015.07.057.
- [7] G. Neupane, E. D. Mattson, T. L. McIning, C. D. Palmer, R. W. Smith, and T. R. Wood, “Deep Geothermal Reservoir Temperatures in the Eastern Snake River Plain, Idaho Using Multicomponent Geothermometry 38 th Workshop on Geothermal Reservoir Engineering,” 2014.
- [8] I. S. Moeck, “Catalog of geothermal play types based on geologic controls,” *Renew. Sustain. Energy Rev.*, vol. 37, pp. 867–882, Sep. 2014, doi: 10.1016/J.RSER.2014.05.032.
- [9] S. Mohammadzadeh Bina, S. Jalilinasrabady, H. Fujii, and N. A. Pambudi, “Classification of geothermal resources in Indonesia by applying exergy concept,” *Renew. Sustain. Energy Rev.*, vol. 93, pp. 499–506, Oct. 2018, doi: 10.1016/J.RSER.2018.05.018.
- [10] S. Jalilinasrabady and R. Itoi, “Classification of Geothermal Energy Resources in Japan Applying Exergy Concept,” 2012, doi: 10.1002/er.3002.

- [11] A. Barbacki, “Classification of geothermal resources in Poland by exergy analysis—Comparative study,” *Renew. Sustain. Energy Rev.*, vol. 16, no. 1, pp. 123–128, Jan. 2012, doi: 10.1016/J.RSER.2011.07.141.
- [12] S. Vargas Payera, “Understanding social acceptance of geothermal energy: Case study for Araucanía region, Chile,” *Geothermics*, vol. 72, pp. 138–144, Mar. 2018, doi: 10.1016/J.GEOTHERMICS.2017.10.014.
- [13] L. Romanach, S. Carr-Cornish, and G. Muriuki, “Societal acceptance of an emerging energy technology: How is geothermal energy portrayed in Australian media?,” *Renew. Sustain. Energy Rev.*, vol. 42, pp. 1143–1150, Feb. 2015, doi: 10.1016/J.RSER.2014.10.088.
- [14] J. W. Lund and T. L. Boyd, “Direct utilization of geothermal energy 2015 worldwide review,” *Geothermics*, vol. 60, pp. 66–93, Mar. 2016, doi: 10.1016/J.GEOTHERMICS.2015.11.004.
- [15] J. Limberger *et al.*, “Geothermal energy in deep aquifers: A global assessment of the resource base for direct heat utilization,” *Renew. Sustain. Energy Rev.*, vol. 82, pp. 961–975, Feb. 2018, doi: 10.1016/J.RSER.2017.09.084.
- [16] S. Haehnlein, P. Bayer, and P. Blum, “International legal status of the use of shallow geothermal energy,” *Renew. Sustain. Energy Rev.*, vol. 14, no. 9, pp. 2611–2625, Dec. 2010, doi: 10.1016/J.RSER.2010.07.069.
- [17] R. DiPippo, *Geothermal power plants: principles, applications, case studies, and environmental impact*. Butterworth-Heinemann, 2012.
- [18] S. J. Zarrouk and H. Moon, “Efficiency of geothermal power plants: A worldwide review,” *Geothermics*, vol. 51, pp. 142–153, Jul. 2014, doi: 10.1016/J.GEOTHERMICS.2013.11.001.
- [19] B. F. Tchanche, G. Lambrinos, A. Frangoudakis, and G. Papadakis, “Low-grade heat conversion into power using organic Rankine cycles – A review of various applications,” *Renew. Sustain. Energy Rev.*, vol. 15, no. 8, pp. 3963–3979, Oct. 2011, doi: 10.1016/J.RSER.2011.07.024.
- [20] S. Quoilin, M. Van Den Broek, S. Declaye, P. Dewallef, and V. Lemort, “Techno-economic survey of Organic Rankine Cycle (ORC) systems,” *Renew. Sustain. Energy Rev.*, vol. 22, pp. 168–186, Jun. 2013, doi: 10.1016/J.RSER.2013.01.028.
- [21] L. A. Prananto, F. B. Juangsa, R. M. Iqbal, M. Aziz, and T. A. F. Soelaiman, “Dry steam cycle application for excess steam utilization: Kamojang geothermal power plant case study,” *Renew. Energy*, vol. 117, pp. 157–165, Mar. 2018, doi: 10.1016/J.RENENE.2017.10.029.

- [22] S. Jalilinasrabady, R. Itoi, P. Valdimarsson, G. Saevarsdottir, and H. Fujii, "Flash cycle optimization of Sabalan geothermal power plant employing exergy concept," *Geothermics*, vol. 43, pp. 75–82, Jul. 2012, doi: 10.1016/J.GEOTHERMICS.2012.02.003.
- [23] S. Mohammadzadeh Bina, S. Jalilinasrabady, and H. Fujii, "Exergoeconomic analysis and optimization of single and double flash cycles for Sabalan geothermal power plant," *Geothermics*, vol. 72, pp. 74–82, Mar. 2018, doi: 10.1016/J.GEOTHERMICS.2017.10.013.
- [24] L. Cao, J. Wang, P. Zhao, and Y. Dai, "Thermodynamic comparison among double-flash flash-Kalina and flash-ORC geothermal power plants," *Int. J. Thermodyn.*, vol. 19, no. 1, p. 53, Mar. 2016, doi: 10.5541/ijot.5000156088.
- [25] A. H. Mosaffa and A. Zareei, "Proposal and thermoeconomic analysis of geothermal flash binary power plants utilizing different types of organic flash cycle," *Geothermics*, vol. 72, pp. 47–63, Mar. 2018, doi: 10.1016/J.GEOTHERMICS.2017.10.011.
- [26] A. D. Atrens, H. Gurgenci, and V. Rudolph, "CO₂ Thermosiphon for Competitive Geothermal Power Generation," *Energy and Fuels*, vol. 23, pp. 553–557, 2009, doi: 10.1021/ef800601z.
- [27] N. A. Pambudi, R. Itoi, S. Jalilinasrabady, and M. Gürtürk, "Sustainability of geothermal power plant combined with thermodynamic and silica scaling model," *Geothermics*, vol. 71, pp. 108–117, Jan. 2018, doi: 10.1016/J.GEOTHERMICS.2017.09.003.
- [28] M. Kanoglu and A. Bolatturk, "Performance and parametric investigation of a binary geothermal power plant by exergy," *Renew. Energy*, vol. 33, no. 11, pp. 2366–2374, Nov. 2008, doi: 10.1016/J.RENENE.2008.01.017.
- [29] H. D. Madhawa Hettiarachchi, M. Golubovic, W. M. Worek, and Y. Ikegami, "Optimum design criteria for an Organic Rankine cycle using low-temperature geothermal heat sources," *Energy*, vol. 32, no. 9, pp. 1698–1706, Sep. 2007, doi: 10.1016/J.ENERGY.2007.01.005.
- [30] F. Heberle and D. Brüggemann, "Exergy based fluid selection for a geothermal Organic Rankine Cycle for combined heat and power generation," *Appl. Therm. Eng.*, vol. 30, no. 11–12, pp. 1326–1332, Aug. 2010, doi: 10.1016/J.APPLTHERMALENG.2010.02.012.
- [31] Z. Shengjun, W. Huaixin, and G. Tao, "Performance comparison and parametric optimization of subcritical Organic Rankine Cycle (ORC) and transcritical power cycle system for low-temperature geothermal power generation," *Appl. Energy*, vol. 88, no. 8, pp. 2740–2754, Aug. 2011, doi: 10.1016/J.APENERGY.2011.02.034.

- [32] F. Heberle, M. Preißinger, and D. Brüggemann, “Zeotropic mixtures as working fluids in Organic Rankine Cycles for low-enthalpy geothermal resources,” *Renew. Energy*, vol. 37, no. 1, pp. 364–370, Jan. 2012, doi: 10.1016/J.RENENE.2011.06.044.
- [33] V. Zare, “A comparative exergoeconomic analysis of different ORC configurations for binary geothermal power plants,” *Energy Convers. Manag.*, vol. 105, pp. 127–138, Nov. 2015, doi: 10.1016/J.ENCONMAN.2015.07.073.
- [34] S. Mohammadzadeh Bina, S. Jalilinasrabady, and H. Fujii, “Thermo-economic evaluation of various bottoming ORCs for geothermal power plant, determination of optimum cycle for Sabalan power plant exhaust,” *Geothermics*, vol. 70, pp. 181–191, Nov. 2017, doi: 10.1016/J.GEOTHERMICS.2017.06.007.
- [35] A. H. Mosaffa, N. H. Mokarram, and L. G. Farshi, “Thermo-economic analysis of combined different ORCs geothermal power plants and LNG cold energy,” *Geothermics*, vol. 65, pp. 113–125, Jan. 2017, doi: 10.1016/J.GEOTHERMICS.2016.09.004.
- [36] N. Shokati, F. Ranjbar, and M. Yari, “Exergoeconomic analysis and optimization of basic, dual-pressure and dual-fluid ORCs and Kalina geothermal power plants: A comparative study,” *Renew. Energy*, vol. 83, pp. 527–542, Nov. 2015, doi: 10.1016/J.RENENE.2015.04.069.
- [37] C. Rubio-Maya, V. M. Ambríz Díaz, E. Pastor Martínez, and J. M. Belman-Flores, “Cascade utilization of low and medium enthalpy geothermal resources – A review,” *Renew. Sustain. Energy Rev.*, vol. 52, pp. 689–716, Dec. 2015, doi: 10.1016/J.RSER.2015.07.162.
- [38] K. M. Powell, K. Rashid, K. Ellingwood, J. Tuttle, and B. D. Iverson, “Hybrid concentrated solar thermal power systems: A review,” *Renew. Sustain. Energy Rev.*, vol. 80, pp. 215–237, Dec. 2017, doi: 10.1016/J.RSER.2017.05.067.
- [39] J. M. Cardemil, F. Cortés, A. Díaz, and R. Escobar, “Thermodynamic evaluation of solar-geothermal hybrid power plants in northern Chile,” *Energy Convers. Manag.*, vol. 123, pp. 348–361, Sep. 2016, doi: 10.1016/J.ENCONMAN.2016.06.032.
- [40] C. Zhou, E. Doroodchi, and B. Moghtaderi, “An in-depth assessment of hybrid solar-geothermal power generation,” *Energy Convers. Manag.*, vol. 74, pp. 88–101, Oct. 2013, doi: 10.1016/J.ENCONMAN.2013.05.014.

- [41] F. Ruzzenenti, M. Bravi, D. Tempesti, E. Salvatici, G. Manfrida, and R. Basosi, "Evaluation of the environmental sustainability of a micro CHP system fueled by low-temperature geothermal and solar energy," *Energy Convers. Manag.*, vol. 78, 2014, doi: 10.1016/j.enconman.2013.11.025.
- [42] M. Ayub, A. Mitsos, and H. Ghasemi, "Thermo-economic analysis of a hybrid solar-binary geothermal power plant," *Energy*, vol. 87, pp. 326–335, Jul. 2015, doi: 10.1016/J.ENERGY.2015.04.106.
- [43] N. Bonyadi, E. Johnson, and D. Baker, "Technoeconomic and exergy analysis of a solar geothermal hybrid electric power plant using a novel combined cycle," *Energy Convers. Manag.*, vol. 156, pp. 542–554, Jan. 2018, doi: 10.1016/J.ENCONMAN.2017.11.052.
- [44] F. A. Boyaghchi, M. Chavoshi, and V. Sabeti, "Optimization of a novel combined cooling, heating and power cycle driven by geothermal and solar energies using the water/CuO (copper oxide) nanofluid," *Energy*, vol. 91, pp. 685–699, Nov. 2015, doi: 10.1016/J.ENERGY.2015.08.082.
- [45] M. Al-Ali and I. Dincer, "Energetic and exergetic studies of a multigenerational solar–geothermal system," *Appl. Therm. Eng.*, vol. 71, no. 1, pp. 16–23, Oct. 2014, doi: 10.1016/J.APPLTHERMALENG.2014.06.033.
- [46] G. Dimarzio, L. Angelini, W. Price, C. Chin, and S. Harris, "The Stillwater Triple Hybrid Power Plant: Integrating Geothermal, Solar Photovoltaic and Solar Thermal Power Generation," in *World Geothermal Congress 2015*, 2015.
- [47] M. Ciani Bassetti, D. Consoli, G. Manente, and A. Lazzaretto, "Design and off-design models of a hybrid geothermal-solar power plant enhanced by a thermal storage," *Renew. Energy*, vol. 128, pp. 460–472, May 2017, doi: 10.1016/J.RENENE.2017.05.078.
- [48] I. Thain and R. Dipippo, "Hybrid Geothermal-Biomass Power Plants: Applications, Designs and Performance Analysis," *World Geotherm. Congr.*, pp. 19–25, 2015.
- [49] K. Beckers, M. Lukawski, G. Aguirre, and Hillson, "Hybrid Low-Grade Geothermal-Biomass Systems for Direct-Use and Co-Generation: from Campus Demonstration to Nationwide Energy Player," in *Fortieth Workshop on Geothermal Reservoir Engineering Stanford University*, 2015, pp. 26–28.

- [50] X. Zhang *et al.*, “Thermodynamic and economic assessment of a novel CCHP integrated system taking biomass, natural gas and geothermal energy as co-feeds,” *Energy Convers. Manag.*, vol. 172, pp. 105–118, Sep. 2018, doi: 10.1016/J.ENCONMAN.2018.07.002.
- [51] S. Moret, E. Peduzzi, L. Gerber, and F. Maréchal, “Integration of deep geothermal energy and woody biomass conversion pathways in urban systems,” *Energy Convers. Manag.*, vol. 129, pp. 305–318, Dec. 2016, doi: 10.1016/j.enconman.2016.09.079.
- [52] C. Yilmaz, M. Kanoglu, and A. Abusoglu, “Thermoeconomic cost evaluation of hydrogen production driven by binary geothermal power plant,” *Geothermics*, vol. 57, pp. 18–25, Sep. 2015, doi: 10.1016/J.GEOTHERMICS.2015.05.005.
- [53] C. Yilmaz, M. Kanoglu, A. Bolatturk, and M. Gadalla, “Economics of hydrogen production and liquefaction by geothermal energy,” *Int. J. Hydrogen Energy*, vol. 37, no. 2, pp. 2058–2069, Jan. 2012, doi: 10.1016/J.IJHYDENE.2011.06.037.
- [54] E. G. Brown, “California Energy Commission California Air Resources Board Joint Agency Staff Report on Assembly Bill 8: Assessment of Time and Cost Needed to Attain 100 Hydrogen Refueling Stations in California.”
- [55] E. Gholamian, A. Habibollahzade, and V. Zare, “Development and multi-objective optimization of geothermal-based organic Rankine cycle integrated with thermoelectric generator and proton exchange membrane electrolyzer for power and hydrogen production,” *Energy Convers. Manag.*, vol. 174, pp. 112–125, Oct. 2018, doi: 10.1016/J.ENCONMAN.2018.08.027.
- [56] V. Zare and V. Palideh, “Employing thermoelectric generator for power generation enhancement in a Kalina cycle driven by low-grade geothermal energy,” *Appl. Therm. Eng.*, vol. 130, pp. 418–428, Feb. 2018, doi: 10.1016/J.APPLTHERMALENG.2017.10.160.
- [57] A. Habibollahzade, E. Houshfar, M. Ashjaee, E. Gholamian, and A. Behzadi, “Energy Equipment and Systems Enhanced performance and reduced payback period of a low grade geothermal-based ORC through employing two TEGs,” 2019.
- [58] D. W. Brown and D. V. Duchane, “Scientific progress on the Fenton Hill HDR project since 1983,” *Geothermics*, vol. 28, no. 4–5, pp. 591–601, Aug. 1999, doi: 10.1016/S0375-6505(99)00030-9.
- [59] S.-M. Lu, “A global review of enhanced geothermal system (EGS),” *Renew. Sustain. Energy Rev.*, vol. 81, pp. 2902–2921, Jan. 2018, doi: 10.1016/J.RSER.2017.06.097.

- [60] C. Jain, C. Vogt, and C. Clauser, “Maximum potential for geothermal power in Germany based on engineered geothermal systems,” *Geotherm. Energy*, vol. 3, no. 1, p. 15, Dec. 2015, doi: 10.1186/s40517-015-0033-5.
- [61] C. R. Chamorro, J. L. García-Cuesta, M. E. Mondéjar, and A. Pérez-Madrado, “Enhanced geothermal systems in Europe: An estimation and comparison of the technical and sustainable potentials,” *Energy*, vol. 65, pp. 250–263, Feb. 2014, doi: 10.1016/J.ENERGY.2013.11.078.
- [62] K. V. Wong and N. Tan, “Feasibility of Using More Geothermal Energy to Generate Electricity,” *J. Energy Resour. Technol.*, vol. 137, no. 4, p. 041201, Jul. 2015, doi: 10.1115/1.4028138.
- [63] H. Hofmann, G. Blöcher, N. Börsing, N. Maronde, N. Pastrik, and G. Zimmermann, “Potential for enhanced geothermal systems in low permeability limestones – stimulation strategies for the Western Malm karst (Bavaria),” *Geothermics*, vol. 51, pp. 351–367, Jul. 2014, doi: 10.1016/J.GEOTHERMICS.2014.03.003.
- [64] S. Held, A. Genter, T. Kohl, T. Kölbl, J. Sausse, and M. Schoenball, “Economic evaluation of geothermal reservoir performance through modeling the complexity of the operating EGS in Soultz-sous-Forêts,” *Geothermics*, vol. 51, pp. 270–280, Jul. 2014, doi: 10.1016/J.GEOTHERMICS.2014.01.016.
- [65] Z. Hou *et al.*, “Preliminary geological, geochemical and numerical study on the first EGS project in Turkey,” *Environ. Earth Sci.*, vol. 73, no. 11, pp. 6747–6767, Jun. 2015, doi: 10.1007/s12665-015-4407-6.
- [66] G. Liu, B. Zhou, and S. Liao, “Inverting methods for thermal reservoir evaluation of enhanced geothermal system,” *Renew. Sustain. Energy Rev.*, vol. 82, pp. 471–476, Feb. 2018, doi: 10.1016/J.RSER.2017.09.065.
- [67] A. Troiano, M. G. Di Giuseppe, A. Monetti, D. Patella, C. Troise, and G. De Natale, “Fluid injection in Enhanced Geothermal Systems: a study on the detectability of self-potential effects and on their correlation with induced seismicity,” *Geothermics*, vol. 65, pp. 280–294, Jan. 2017, doi: 10.1016/J.GEOTHERMICS.2016.05.003.
- [68] B. Fritz, E. Jacquot, B. Jacquemont, A. Baleyrou-Bailly, M. Rosener, and O. Vidal, “Geochemical modelling of fluid–rock interactions in the context of the Soultz-sous-Forêts geothermal system,” *Geosci.*, no. 342, pp. 653–667, 2010.

- [69] K. Yost, A. Valentin, and H. H. Einstein, “Estimating cost and time of wellbore drilling for Engineered Geothermal Systems (EGS) – Considering uncertainties,” *Geothermics*, vol. 53, pp. 85–99, Jan. 2015, doi: 10.1016/J.GEOTHERMICS.2014.04.005.
- [70] C.-L. Wang, W.-L. Cheng, Y.-L. Nian, L. Yang, B.-B. Han, and M.-H. Liu, “Simulation of heat extraction from CO₂-based enhanced geothermal systems considering CO₂ sequestration,” *Energy*, vol. 142, pp. 157–167, Jan. 2018, doi: 10.1016/J.ENERGY.2017.09.139.
- [71] K. Pruess, “Enhanced geothermal systems (EGS) using CO₂ as working fluid—A novel approach for generating renewable energy with simultaneous sequestration of carbon,” *Geothermics*, vol. 35, no. 4, pp. 351–367, Aug. 2006, doi: 10.1016/J.GEOTHERMICS.2006.08.002.
- [72] G. Cui, L. Zhang, B. Ren, C. Enechukwu, Y. Liu, and S. Ren, “Geothermal exploitation from depleted high temperature gas reservoirs via recycling supercritical CO₂: Heat mining rate and salt precipitation effects,” *Appl. Energy*, vol. 183, pp. 837–852, Dec. 2016, doi: 10.1016/J.APENERGY.2016.09.029.
- [73] M. D. Aminu, S. A. Nabavi, C. A. Rochelle, and V. Manovic, “A review of developments in carbon dioxide storage,” *Appl. Energy*, vol. 208, pp. 1389–1419, Dec. 2017, doi: 10.1016/J.APENERGY.2017.09.015.
- [74] Y. Kim, H. Jang, J. Kim, and J. Lee, “Prediction of storage efficiency on CO₂ sequestration in deep saline aquifers using artificial neural network,” *Appl. Energy*, vol. 185, pp. 916–928, Jan. 2017, doi: 10.1016/J.APENERGY.2016.10.012.
- [75] M. Martín-Gamboa, D. Iribarren, and J. Dufour, “On the environmental suitability of high- and low-enthalpy geothermal systems,” *Geothermics*, vol. 53, pp. 27–37, Jan. 2015, doi: 10.1016/J.GEOTHERMICS.2014.03.012.
- [76] C. Tomasini-Montenegro, E. Santoyo-Castelazo, H. Gujba, R. J. Romero, and E. Santoyo, “Life cycle assessment of geothermal power generation technologies: An updated review,” *Appl. Therm. Eng.*, vol. 114, pp. 1119–1136, Mar. 2017, doi: 10.1016/J.APPLTHERMALENG.2016.10.074.
- [77] P. Bayer, L. Rybach, P. Blum, and R. Brauchler, “Review on life cycle environmental effects of geothermal power generation,” *Renew. Sustain. Energy Rev.*, vol. 26, pp. 446–463, 2013, doi: 10.1016/j.rser.2013.05.039.

- [78] M. Bravi and R. Basosi, “Environmental impact of electricity from selected geothermal power plants in Italy,” *J. Clean. Prod.*, vol. 66, pp. 301–308, Mar. 2014, doi: 10.1016/J.JCLEPRO.2013.11.015.
- [79] E. Buonocore, L. Vanoli, A. Carotenuto, and S. Ulgiati, “Integrating life cycle assessment and energy synthesis for the evaluation of a dry steam geothermal power plant in Italy,” *Energy*, vol. 86, pp. 476–487, Jun. 2015, doi: 10.1016/J.ENERGY.2015.04.048.
- [80] S. Frick, M. Kaltschmitt, and G. Schröder, “Life cycle assessment of geothermal binary power plants using enhanced low-temperature reservoirs,” *Energy*, vol. 35, no. 5, pp. 2281–2294, May 2010, doi: 10.1016/J.ENERGY.2010.02.016.
- [81] L. Bruscoli, D. Fiaschi, G. Manfrida, and D. Tempesti, “Improving the Environmental Sustainability of Flash Geothermal Power Plants—A Case Study,” *Sustainability*, vol. 7, no. 12, pp. 15262–15283, Nov. 2015, doi: 10.3390/su71115262.
- [82] O. Hanbury and V. R. Vasquez, “Life cycle analysis of geothermal energy for power and transportation: A stochastic approach,” *Renew. Energy*, vol. 115, pp. 371–381, Jan. 2018, doi: 10.1016/J.RENENE.2017.08.053.
- [83] S. Hähnlein, P. Bayer, G. Ferguson, and P. Blum, “Sustainability and policy for the thermal use of shallow geothermal energy,” *Energy Policy*, vol. 59, pp. 914–925, Aug. 2013, doi: 10.1016/J.ENPOL.2013.04.040.
- [84] H. Hondo, “Life cycle GHG emission analysis of power generation systems: Japanese case,” *Energy*, vol. 30, pp. 2042–2056, 2005, doi: 10.1016/j.energy.2004.07.020.
- [85] A. Pratiwi, G. Ravier, and A. Genter, “Life-cycle climate-change impact assessment of enhanced geothermal system plants in the Upper Rhine Valley,” *Geothermics*, vol. 75, pp. 26–39, Sep. 2018, doi: 10.1016/J.GEOTHERMICS.2018.03.012.
- [86] S.-Y. Pan, M. Gao, K. J. Shah, J. Zheng, S.-L. Pei, and P.-C. Chiang, “Establishment of enhanced geothermal energy utilization plans: Barriers and strategies,” *Renew. Energy*, vol. 132, pp. 19–32, Mar. 2019, doi: 10.1016/J.RENENE.2018.07.126.
- [87] V. Stefánsson, “Investment cost for geothermal power plants,” *Geothermics*, vol. 31, no. 2, pp. 263–272, Apr. 2002, doi: 10.1016/S0375-6505(01)00018-9.
- [88] M. Kanoğlu and Y. A. Çengel, “Economic evaluation of geothermal power generation, heating, and cooling,” *Energy*, vol. 24, no. 6, pp. 501–509, Jun. 1999, doi: 10.1016/S0360-5442(99)00016-X.

- [89] M. Z. Lukawski *et al.*, “Cost analysis of oil, gas, and geothermal well drilling,” *J. Pet. Sci. Eng.*, vol. 118, pp. 1–14, Jun. 2014, doi: 10.1016/J.PETROL.2014.03.012.
- [90] P. Heidinger, “Integral modeling and financial impact of the geothermal situation and power plant at Soultz-sous-Forêts,” *C. R. Geosci.*, vol. 342, pp. 626–635, 2010, doi: 10.1016/j.crte.2009.10.010.
- [91] S. Van Erdeweghe, J. Van Bael, B. Laenen, and W. D ’haeseleer, “Feasibility study of a low-temperature geothermal power plant for multiple economic scenarios,” *Energy*, vol. 155, pp. 1004–1012, 2018.
- [92] S. Karimi and S. Mansouri, “A comparative profitability study of geothermal electricity production in developed and developing countries: Exergoeconomic analysis and optimization of different ORC configurations,” *Renew. Energy*, vol. 115, pp. 600–619, Jan. 2018, doi: 10.1016/J.RENENE.2017.08.098.
- [93] C. Clauser and M. Ewert, “The renewables cost challenge: Levelized cost of geothermal electric energy compared to other sources of primary energy – Review and case study,” *Renew. Sustain. Energy Rev.*, vol. 82, pp. 3683–3693, Feb. 2018, doi: 10.1016/J.RSER.2017.10.095.
- [94] A. C. Sener, J. R. van Dorp, and J. D. Keith, “Perspectives on the Economics of Geothermal Power,” *Geotherm. Resour. Counc. Trans.*, vol. 33, pp. 29–36, 2009.
- [95] T. Reber, K. Beckers, and J. Tester, “The transformative potential of geothermal heating in the U.S. energy market: A regional study of New York and Pennsylvania,” *Energy Policy*, no. 70, pp. 30–44, 2014.
- [96] A. Franco and M. Vaccaro, “A combined energetic and economic approach for the sustainable design of geothermal plants,” *Energy Convers. Manag.*, vol. 87, pp. 735–745, Nov. 2014, doi: 10.1016/J.ENCONMAN.2014.07.073.
- [97] Q. Zhang, S. Chen, Z. Tan, T. Zhang, and B. Mclellan, “Investment strategy of hydrothermal geothermal heating in China under policy, technology and geology uncertainties,” *J. Clean. Prod.*, vol. 207, pp. 17–29, Jan. 2019, doi: 10.1016/J.JCLEPRO.2018.09.240.
- [98] C. J. Vörösmarty, P. Green, J. Salisbury, and R. B. Lammers, “Global water resources: vulnerability from climate change and population growth.,” *Science*, vol. 289, no. 5477, pp. 284–8, Jul. 2000, doi: 10.1126/SCIENCE.289.5477.284.

- [99] S. Hienuki, Y. Kudoh, and H. Hondo, "Life cycle employment effect of geothermal power generation using an extended input–output model: the case of Japan," *J. Clean. Prod.*, vol. 93, pp. 203–212, Apr. 2015, doi: 10.1016/J.JCLEPRO.2015.01.008.
- [100] R. DiPippo, "Geothermal power plants: Evolution and performance assessments," *Geothermics*, vol. 53, pp. 291–307, Jan. 2015, doi: 10.1016/J.GEOTHERMICS.2014.07.005.
- [101] K. Li, H. Bian, C. Liu, D. Zhang, and Y. Yang, "Comparison of geothermal with solar and wind power generation systems," *Renew. Sustain. Energy Rev.*, vol. 42, pp. 1464–1474, Feb. 2015, doi: 10.1016/J.RSER.2014.10.049.
- [102] S. Thorhallsson, "Common problems faced in geothermal generation and how to deal with them," 2012.
- [103] M. Karadas, H. M. Celik, U. Serpen, and M. Toksoy, "Multiple regression analysis of performance parameters of a binary cycle geothermal power plant," *Geothermics*, vol. 54, pp. 68–75, Mar. 2015, doi: 10.1016/J.GEOTHERMICS.2014.11.003.
- [104] E. Gaucher *et al.*, "Induced seismicity in geothermal reservoirs: A review of forecasting approaches," *Renew. Sustain. Energy Rev.*, vol. 52, pp. 1473–1490, 2015, doi: 10.1016/j.rser.2015.08.026.
- [105] V. Oye, P. Jousset, N. Deichmann, R. Gritto, and A. McGarr, "Analysis of induced seismicity in geothermal reservoirs – An overview," *Geothermics*, vol. 52, pp. 6–21, Oct. 2014, doi: 10.1016/J.GEOTHERMICS.2014.06.005.
- [106] S. Bilgen, "Structure and environmental impact of global energy consumption," *Renew. Sustain. Energy Rev.*, vol. 38, pp. 890–902, 2014, doi: 10.1016/J.RSER.2014.07.004.
- [107] B. Bhandari, K.-T. Lee, G.-Y. Lee, Y.-M. Cho, and S.-H. Ahn, "Optimization of Hybrid Renewable Energy Power Systems: A Review," *Int. J. Precis. Eng. Manuf. Technol.*, vol. 2, no. 1, pp. 99–112, 2015, doi: 10.1007/s40684-015-0013-z.
- [108] "U.S. Energy Information Administration (EIA) - Total Energy Monthly Data," 2019. [Online]. Available: <https://www.eia.gov/totalenergy/data/monthly/#summary>. [Accessed: 19-Apr-2019].
- [109] N. Abas, A. Kalair, and N. Khan, "Review of fossil fuels and future energy technologies," *Futures*, vol. 69, pp. 31–49, 2015, doi: 10.1016/J.FUTURES.2015.03.003.

- [110] A. Lake, B. Rezaie, and S. Beyerlein, "Review of district heating and cooling systems for a sustainable future," *Renew. Sustain. Energy Rev.*, vol. 67, pp. 417–425, Jan. 2017, doi: 10.1016/J.RSER.2016.09.061.
- [111] B. Rezaie and M. A. Rosen, "District heating and cooling: Review of technology and potential enhancements," *Appl. Energy*, vol. 93, pp. 2–10, May 2012, doi: 10.1016/J.APENERGY.2011.04.020.
- [112] "Washington state (Initiative 1631)." [Online]. Available: <https://www.carbontax.org/washington-state-initiative-1631/>. [Accessed: 19-Apr-2019].
- [113] B. Rezaie, B. V. Reddy, and M. A. Rosen, "An enviro-economic function for assessing energy resources for district energy systems," *Energy*, vol. 70, pp. 159–164, Jun. 2014, doi: 10.1016/J.ENERGY.2014.03.101.
- [114] M. Müller *et al.*, "Evaluation of grid-level adaptability for stationary battery energy storage system applications in Europe," *J. Energy Storage*, vol. 9, pp. 1–11, Feb. 2017, doi: 10.1016/J.EST.2016.11.005.
- [115] G. Alva, L. Liu, X. Huang, and G. Fang, "Thermal energy storage materials and systems for solar energy applications," *Renew. Sustain. Energy Rev.*, vol. 68, pp. 693–706, Feb. 2017, doi: 10.1016/J.RSER.2016.10.021.
- [116] B. Rismanchi, R. Saidur, G. BoroumandJazi, and S. Ahmed, "Energy, exergy and environmental analysis of cold thermal energy storage (CTES) systems," *Renew. Sustain. Energy Rev.*, vol. 16, no. 8, pp. 5741–5746, Oct. 2012, doi: 10.1016/J.RSER.2012.06.002.
- [117] I. Dincer, "On thermal energy storage systems and applications in buildings," *Energy Build.*, vol. 34, no. 4, pp. 377–388, May 2002, doi: 10.1016/S0378-7788(01)00126-8.
- [118] E. D. Kerme, A. Chafidz, O. P. Agboola, J. Orfi, A. H. Fakeeha, and A. S. Al-Fatesh, "Energetic and exergetic analysis of solar-powered lithium bromide-water absorption cooling system," *J. Clean. Prod.*, vol. 151, pp. 60–73, May 2017, doi: 10.1016/j.jclepro.2017.03.060.
- [119] A. Jafari and A. Haghighi Poshtiri, "Passive solar cooling of single-storey buildings by an adsorption chiller system combined with a solar chimney," *J. Clean. Prod.*, vol. 141, pp. 662–682, Jan. 2017, doi: 10.1016/J.JCLEPRO.2016.09.099.
- [120] S.-F. Lee and S. A. Sherif, "Thermodynamic analysis of a lithium bromide/water absorption system for cooling and heating applications," *Int. J. Energy Res.*, vol. 25, no. 11, pp. 1019–1031, Sep. 2001, doi: 10.1002/er.738.

- [121] A. Razmi, M. Soltani, F. M. Kashkooli, and L. Garousi Farshi, "Energy and exergy analysis of an environmentally-friendly hybrid absorption/recompression refrigeration system," *Energy Convers. Manag.*, vol. 164, pp. 59–69, May 2018, doi: 10.1016/J.ENCONMAN.2018.02.084.
- [122] Klein, Sanford and G. Nellis, *Thermodynamics*. Cambridge University Press, New York, 2012.
- [123] R. U. Ayres, L. W. Ayres, and K. Martinas, "Eco-Thermodynamics: Exergy and Life Cycle Analysis," Fontainebleau, 1996.
- [124] J. Szargut, D. R. Morris, and F. R. Steward, "Exergy analysis of thermal, chemical, and metallurgical processes." Hemisphere Publishing, New York, NY, 01-Jan-1987.
- [125] I. Dincer and M. A. Rosen, "Thermodynamic aspects of renewables and sustainable development," *Renew. Sustain. Energy Rev.*, vol. 9, no. 2, pp. 169–189, Apr. 2005, doi: 10.1016/J.RSER.2004.02.002.
- [126] I. Dincer, "The role of exergy in energy policy making," *Energy Policy*, vol. 30, no. 2, pp. 137–149, Jan. 2002, doi: 10.1016/S0301-4215(01)00079-9.
- [127] M. A. Rosen and I. Dincer, "Exergy as the confluence of energy, environment and sustainable development," *Exergy, An Int. J.*, vol. 1, no. 1, pp. 3–13, Jan. 2001, doi: 10.1016/S1164-0235(01)00004-8.
- [128] A. Bejan, "Fundamentals of exergy analysis, entropy generation minimization, and the generation of flow architecture," *Int. J. Energy Res.*, vol. 26, no. 7, pp. 545–565, Jun. 2002, doi: 10.1002/er.804.
- [129] A. Şencan, K. A. Yakut, and S. A. Kalogirou, "Exergy analysis of lithium bromide/water absorption systems," *Renew. Energy*, vol. 30, no. 5, pp. 645–657, Apr. 2005, doi: 10.1016/J.RENENE.2004.07.006.
- [130] M. Kilic and O. Kaynakli, "Second law-based thermodynamic analysis of water-lithium bromide absorption refrigeration system," *Energy*, vol. 32, no. 8, pp. 1505–1512, Aug. 2007, doi: 10.1016/J.ENERGY.2006.09.003.
- [131] M. M. Talbi and B. Agnew, "Exergy analysis: an absorption refrigerator using lithium bromide and water as the working fluids," *Appl. Therm. Eng.*, vol. 20, no. 7, pp. 619–630, May 2000, doi: 10.1016/S1359-4311(99)00052-6.

- [132] T. Avanesian and M. Ameri, "Energy, exergy, and economic analysis of single and double effect LiBr–H₂O absorption chillers," *Energy Build.*, vol. 73, pp. 26–36, Apr. 2014, doi: 10.1016/J.ENBUILD.2014.01.013.
- [133] T. K. Gogoi and D. Konwar, "Exergy analysis of a H₂O–LiCl absorption refrigeration system with operating temperatures estimated through inverse analysis," *Energy Convers. Manag.*, vol. 110, pp. 436–447, Feb. 2016, doi: 10.1016/J.ENCONMAN.2015.12.037.
- [134] S. C. Kaushik and A. Arora, "Energy and exergy analysis of single effect and series flow double effect water–lithium bromide absorption refrigeration systems," *Int. J. Refrig.*, vol. 32, no. 6, pp. 1247–1258, Sep. 2009, doi: 10.1016/J.IJREFRIG.2009.01.017.
- [135] M. A. Rosen and I. Dincer, "Exergy methods for assessing and comparing thermal storage systems," *Int. J. Energy Res.*, vol. 27, no. 4, pp. 415–430, Mar. 2003, doi: 10.1002/er.885.
- [136] M. A. Rosen and I. Dincer, "Efficiency Assessment of Glycol Cold Thermal Energy Storage and Effect of Varying Environment Temperature," *Trans. Can. Soc. Mech. Eng.*, vol. 33, no. 1, pp. 119–130, 2009.
- [137] M. A. Rosen, N. Pedinelli, and I. Dincer, "Energy and exergy analyses of cold thermal storage systems," *Int. J. Energy Res.*, vol. 23, no. 12, pp. 1029–1038, Oct. 1999, doi: 10.1002/(SICI)1099-114X(19991010)23:12<1029::AID-ER538>3.0.CO;2-C.
- [138] Y. H. Zurigat, K. J. Maloney, and A. J. Ghajar, "A Comparison Study of One-Dimensional Models for Stratified Thermal Storage Tanks," *J. Sol. Energy Eng.*, vol. 111, no. 3, pp. 204–210, Aug. 1989, doi: 10.1115/1.3268308.
- [139] E. M. Kleinbach, W. A. Beckman, and S. A. Klein, "Performance study of one-dimensional models for stratified thermal storage tanks," *Sol. Energy*, vol. 50, no. 2, pp. 155–166, Feb. 1993, doi: 10.1016/0038-092X(93)90087-5.
- [140] A. Lake and B. Rezaie, "Energy and exergy efficiencies assessment for a stratified cold thermal energy storage," *Appl. Energy*, vol. 220, pp. 605–615, Jun. 2018, doi: 10.1016/J.APENERGY.2018.03.145.
- [141] W. P. Bahnfleth and A. Musser, "Thermal Performance of a Full-Scale Stratified Chilled-Water Thermal Storage Tank," *Am. Soc. Heating, Refrig. Air-Conditioning Eng. Trans.*, vol. 104, no. 2, pp. 377–388, 1998.
- [142] S. Penoncello, *Thermal energy systems : design and analysis*, 1st ed. CRC Press, 2015.

- [143] S. Klein, "TRNSYS 17.2," 2014.
- [144] M. Compton and B. Rezaie, "Enviro-exergy sustainability analysis of boiler evolution in district energy system," *Energy*, vol. 119, pp. 257–265, Jan. 2017, doi: 10.1016/J.ENERGY.2016.11.139.
- [145] M. Compton, B. Rezaie, and M. A. Rosen, "Exergy approach for advancing sustainability of a biomass boiler," *Int. J. Exergy*, vol. 27, no. 1, pp. 62–80, 2018, doi: 10.1504/IJEX.2018.093900.
- [146] "Weather Data by Location | EnergyPlus." [Online]. Available: https://energyplus.net/weather-location/north_and_central_america_wmo_region_4/USA/WA/USA_WA_Pullman-Moscow.Rgnl.AP.727857_TMY3. [Accessed: 19-Apr-2019].
- [147] "How much carbon dioxide is produced when different fuels are burned? - FAQ - U.S. Energy Information Administration (EIA)." [Online]. Available: <https://www.eia.gov/tools/faqs/faq.php?id=73&t=11>. [Accessed: 22-Apr-2019].
- [148] Z. Malolepszy, "Low Temperature, Man-made Geothermal Reservoirs In Abandoned Workings Of Underground Mines," in *PROCEEDINGS: Twenty-Eighth Workshop on Geothermal Reservoir Engineering*, 2003, p. 7.
- [149] G. S. Simate and S. Ndlovu, "Acid mine drainage: Challenges and opportunities," *J. Environ. Chem. Eng.*, vol. 2, no. 3, pp. 1785–1803, Sep. 2014, doi: 10.1016/J.JECE.2014.07.021.
- [150] H. Wang *et al.*, "Bacterial, archaeal, and fungal community responses to acid mine drainage-laden pollution in a rice paddy soil ecosystem," *Sci. Total Environ.*, vol. 616–617, pp. 107–116, Mar. 2018, doi: 10.1016/j.scitotenv.2017.10.224.
- [151] J. Raymond and R. Therrien, "Low-temperature geothermal potential of the flooded Gaspé Mines, Québec, Canada," *Geothermics*, vol. 37, no. 2, pp. 189–210, Apr. 2008, doi: 10.1016/J.GEOTHERMICS.2007.10.001.
- [152] D. B. Johnson and K. B. Hallberg, "Acid mine drainage remediation options: a review," *Sci. Total Environ.*, vol. 338, no. 1–2, pp. 3–14, 2005, doi: 10.1016/j.scitotenv.2004.09.002.
- [153] N. F. Gray, "Environmental impact and remediation of acid mine drainage: a management problem," *Environ. Geol.*, vol. 30, no. 7, 1997.
- [154] P. L. Young, "The longevity of minewater pollution: a basis for decision-making," *Sci. Total Environ.*, vol. 194–195, pp. 457–466, Feb. 1997, doi: 10.1016/S0048-9697(96)05383-1.

- [155] H. Cheng, Y. Hu, J. Luo, B. Xu, and J. Zhao, "Geochemical processes controlling fate and transport of arsenic in acid mine drainage (AMD) and natural systems," *J. Hazard. Mater.*, vol. 165, no. 1–3, pp. 13–26, Jun. 2009, doi: 10.1016/J.JHAZMAT.2008.10.070.
- [156] A. Akcil and S. Koldas, "Acid Mine Drainage (AMD): causes, treatment and case studies," *J. Clean. Prod.*, 2006.
- [157] A. Herlihy, P. Kaufmann, M. Mitch, and D. Brown, "Regional estimates of acid mine drainage impact on streams in the mid-atlantic and Southeastern United States," *Water. Air. Soil Pollut.*, vol. 50, no. 1–2, pp. 91–107, Mar. 1990, doi: 10.1007/BF00284786.
- [158] D. W. Blowes, C. J. Ptacek, J. L. Jambor, and C. G. Weisener, "The Geochemistry of Acid Mine Drainage," in *Treatise on Geochemistry*, vol. 9, Elsevier, 2003, pp. 149–204.
- [159] J. A. Grout and C. D. Levings, "Effects of acid mine drainage from an abandoned copper mine, Britannia Mines, Howe Sound, British Columbia, Canada, on transplanted blue mussels (*Mytilus edulis*)," *Mar. Environ. Res.*, vol. 51, no. 3, pp. 265–288, Apr. 2001, doi: 10.1016/S0141-1136(00)00104-5.
- [160] P. A. Raymond and N.-H. Oh, "Long term changes of chemical weathering products in rivers heavily impacted from acid mine drainage: Insights on the impact of coal mining on regional and global carbon and sulfur budgets," *Earth Planet. Sci. Lett.*, vol. 284, no. 1–2, pp. 50–56, Jun. 2009, doi: 10.1016/J.EPSL.2009.04.006.
- [161] N. J. Smucker and M. L. Vis, "Acid mine drainage affects the development and function of epilithic biofilms in streams," *J. North Am. Benthol. Soc.*, vol. 30, no. 3, pp. 728–738, Sep. 2011, doi: 10.1899/10-139.1.
- [162] J. M. Castro and J. N. Moore, "Pit lakes: their characteristics and the potential for their remediation," *Environ. Geol.*, vol. 39, no. 11, pp. 1254–1260, Oct. 2000, doi: 10.1007/s002549900100.
- [163] K. Elsbeth Watson, "CU Scholar Impacts of Acid Mine Drainage on Breeding Birds and Benthic Invertebrates in the Snake River Watershed, Summit County, Colorado Recommended Citation," 2018.
- [164] J. Robbins, "Hordes of Geese Die on a Toxic Lake in Montana - The New York Times," pp. 6–6, 2016.
- [165] C. M. Custer, C. Yang, J. G. Crock, V. Shearn-Bochsler, K. S. Smith, and P. L. Hageman, "Exposure of insects and insectivorous birds to metals and other elements from abandoned

- mine tailings in three Summit County drainages, Colorado,” *Environ. Monit. Assess.*, vol. 153, no. 1–4, pp. 161–177, 2009, doi: 10.1007/s10661-008-0346-y.
- [166] B. Gazea, K. Adam, and A. Kontopoulos, “A review of passive systems for the treatment of acid mine drainage,” *Miner. Eng.*, vol. 9, no. 1, pp. 23–42, Jan. 1996, doi: 10.1016/0892-6875(95)00129-8.
- [167] N. J. Tucci and C. H. Gammons, “Influence of Copper Recovery on the Water Quality of the Acidic Berkeley Pit Lake, Montana, U.S.A.,” *Environ. Sci. Technol.*, vol. 49, no. 7, pp. 4081–4088, Apr. 2015, doi: 10.1021/es504916n.
- [168] R. K. Wieder, “A survey of constructed wetlands for acid coal mine drainage treatment in the Eastern United States,” *Wetlands*, vol. 9, no. 2, pp. 299–315, Dec. 1989, doi: 10.1007/BF03160750.
- [169] M. A. Palmer *et al.*, “Science and regulation. Mountaintop mining consequences,” *Science*, vol. 327, no. 5962, pp. 148–9, Jan. 2010, doi: 10.1126/science.1180543.
- [170] I. S. Chang, P. K. Shin, and B. H. Kim, “Biological treatment of acid mine drainage under sulphate-reducing conditions with solid waste materials as substrate,” *Water Res.*, vol. 34, no. 4, pp. 1269–1277, Mar. 2000, doi: 10.1016/S0043-1354(99)00268-7.
- [171] C. Ayora *et al.*, “Recovery of Rare Earth Elements and Yttrium from Passive-Remediation Systems of Acid Mine Drainage,” *Environ. Sci. Technol.*, vol. 50, no. 15, pp. 8255–8262, 2016.
- [172] J. Skousen *et al.*, “Review of Passive Systems for Acid Mine Drainage Treatment,” *Mine Water Environ.*, vol. 36, no. 1, pp. 133–153, Mar. 2017, doi: 10.1007/s10230-016-0417-1.
- [173] F. Macías, R. Pérez-López, M. A. Caraballo, C. R. Cánovas, and J. M. Nieto, “Management strategies and valorization for waste sludge from active treatment of extremely metal-polluted acid mine drainage: A contribution for sustainable mining,” *J. Clean. Prod.*, vol. 141, pp. 1057–1066, Jan. 2017, doi: 10.1016/j.jclepro.2016.09.181.
- [174] M. Rodríguez-Galán, F. M. Baena-Moreno, S. Vázquez, F. Arroyo-Torralvo, L. F. Vilches, and Z. Zhang, “Remediation of acid mine drainage,” *Environ. Chem. Lett.*, vol. 17, no. 4, pp. 1529–1538, Dec. 2019, doi: 10.1007/s10311-019-00894-w.
- [175] S. Ryu, G. Naidu, M. A. Hasan Johir, Y. Choi, S. Jeong, and S. Vigneswaran, “Acid mine drainage treatment by integrated submerged membrane distillation–sorption system,” *Chemosphere*, vol. 218, pp. 955–965, Mar. 2019, doi: 10.1016/j.chemosphere.2018.11.153.

- [176] A. O. Aguiar, L. H. Andrade, B. C. Ricci, W. L. Pires, G. A. Miranda, and M. C. S. Amaral, "Gold acid mine drainage treatment by membrane separation processes: An evaluation of the main operational conditions," *Sep. Purif. Technol.*, vol. 170, pp. 360–369, Oct. 2016, doi: 10.1016/j.seppur.2016.07.003.
- [177] K. Ambiado, C. Bustos, A. Schwarz, and R. Bórquez, "Membrane technology applied to acid mine drainage from copper mining," *Water Sci. Technol.*, vol. 75, no. 3, pp. 705–715, Feb. 2017, doi: 10.2166/wst.2016.556.
- [178] V. Masindi, M. S. Osman, and R. Shingwenyana, "Valorization of acid mine drainage (AMD): A simplified approach to reclaim drinking water and synthesize valuable minerals-Pilot study," *J. Environ. Chem. Eng.*, vol. 7, no. 3, Jun. 2019, doi: 10.1016/j.jece.2019.103082.
- [179] B. K. Pramanik, L. Shu, J. Jegatheesan, K. Shah, N. Haque, and M. A. Bhuiyan, "Rejection of rare earth elements from a simulated acid mine drainage using forward osmosis: The role of membrane orientation, solution pH, and temperature variation," *Process Saf. Environ. Prot.*, vol. 126, pp. 53–59, Jun. 2019, doi: 10.1016/j.psep.2019.04.004.
- [180] P. K. Das, "Phytoremediation and Nanoremediation : Emerging Techniques for Treatment of Acid Mine Drainage Water," *Sci. J.*, vol. 3, no. 2, pp. 190–196, 2018, doi: 10.14429/dlsj.3.11346.
- [181] L. Canopoli, S. Wagland, and F. Coulon, "Landfill mining report 2016," Apr. 2017, doi: 10.17862/CRANFIELD.RD.4898183.V1.
- [182] C. M. Everling, "Chasing Results from the Chasing Arrows: Strategies for the United States to Stop Wasting Time and Resources When It Comes to Recycling," *UIC John Marshall Law Rev.*, vol. 52, 2018.
- [183] R. Jin and Q. Chen, "Overview of Concrete Recycling Legislation and Practice in the United States," *J. Constr. Eng. Manag.*, vol. 145, no. 4, p. 05019004, Apr. 2019, doi: 10.1061/(ASCE)CO.1943-7862.0001630.
- [184] "Water Archives - National Mining Association," 2019. [Online]. Available: <https://nma.org/category/water/>. [Accessed: 24-Nov-2019].
- [185] 30 U.S.C. 25 - *Surface Mining Control and Reclamation - USCODE-2011-title30-chap25*. 2011.

- [186] S. Naidoo, “An assessment of the impacts of acid mine drainage on socio-economic development in the Witwatersrand: South Africa,” *Environ. Dev. Sustain.*, vol. 17, no. 5, pp. 1045–1063, Oct. 2015, doi: 10.1007/s10668-014-9589-7.
- [187] O. US EPA, “Superfund: National Priorities List (NPL),” 2019. .
- [188] “The Minerals and Metals Policy of the Government of Canada ,” 1996.
- [189] *Canadian Environmental Protection Act, 1999*. 1999.
- [190] *Canadian Metal and Diamond Mining Effluent Regulations*. 2002.
- [191] “Mine Environmental Neutral Drainage (MEND),” 1989. [Online]. Available: <http://mend-nedem.org/default/>. [Accessed: 06-Jan-2020].
- [192] “European Commission DG Environment Establishment of guidelines for the inspection of mining waste facilities, inventory and rehabilitation of abandoned facilities and review of the BREF document Annex 3 Supporting document on closure methodologies for closed and abandoned mining waste facilities,” 2012.
- [193] C. Wolkersdorfer, P. L. Younger, and R. Bowell, “PADRE-Partnership for Acid Drainage Remediation in Europe,” 2006, pp. 675–676.
- [194] J. Craynon, “Future Directions of the Coal Mining Sector of the Acid Drainage Technology Initiative and the Needs For Acid Drainage Research,” in *Proceedings America Society of Mining and Reclamation*, 2004, pp. 412–419, doi: 10.21000/JASMR04010366.
- [195] “Australian Centre for Sustainable Mining Practices,” 2009. [Online]. Available: <http://www.acsmp.unsw.edu.au/about-acsmp-1>. [Accessed: 25-Nov-2019].
- [196] *Committee to Save Mokelumne River v. East Bay Util.* 1993.
- [197] *US v. Iron Mountain Mines*, 724 F. Supp. 2d 1086 - Dist. Court, ED California. 2010.
- [198] *Bellaire Corp. v. American Empire Surplus*, 115 NE 3d 805 -. 2018.
- [199] *West Virginia Highlands Conservancy, Inc. v. Huffman*, 625 F. 3d 159 - Court of Appeals, 4th Circuit. 2010.
- [200] *Sunnyside Gold Corporation v. Environmental Protection Agency*, Court of Appeals, Dist. of Columbia Circuit. 2017.
- [201] B. Berman, “3-D printing: The new industrial revolution,” *Bus. Horiz.*, vol. 55, no. 2, pp. 155–162, Mar. 2012, doi: 10.1016/J.BUSHOR.2011.11.003.

- [202] D. Herzog, V. Seyda, E. Wycisk, and C. Emmelmann, “Additive manufacturing of metals,” *Acta Mater.*, vol. 117, pp. 371–392, Sep. 2016, doi: 10.1016/J.ACTAMAT.2016.07.019.
- [203] M. Gebler, A. J. M. Schoot Uiterkamp, and C. Visser, “A global sustainability perspective on 3D printing technologies,” *Energy Policy*, vol. 74, pp. 158–167, Nov. 2014, doi: 10.1016/J.ENPOL.2014.08.033.
- [204] V. Petrovic, J. Vicente Haro Gonzalez, O. Jordá Ferrando, J. Delgado Gordillo, J. Ramón Blasco Puchades, and L. Portolés Griñan, “Additive layered manufacturing: sectors of industrial application shown through case studies,” *Int. J. Prod. Res.*, vol. 49, no. 4, pp. 1061–1079, Feb. 2011, doi: 10.1080/00207540903479786.
- [205] M. Ford, Simon; Despeisse, “Additive manufacturing and sustainability: an exploratory study of the advantages and challenges,” *J. Clean. Prod.*, vol. 137, pp. 1573–1587, Nov. 2016, doi: 10.1016/J.JCLEPRO.2016.04.150.
- [206] D. Chen, S. Heyer, S. Ibbotson, K. Salonitis, J. G. Steingrímsson, and S. Thiede, “Direct digital manufacturing: definition, evolution, and sustainability implications,” *J. Clean. Prod.*, vol. 107, pp. 615–625, Nov. 2015, doi: 10.1016/J.JCLEPRO.2015.05.009.
- [207] M. Despeisse, M. Yang, S. Evans, S. Ford, and T. Minshall, “Sustainable Value Roadmapping Framework for Additive Manufacturing,” *Procedia CIRP*, vol. 61, pp. 594–599, 2017, doi: 10.1016/j.procir.2016.11.186.
- [208] J. Faludi, C. Bayley, S. Bhogal, and M. Iribarne, “Comparing environmental impacts of additive manufacturing vs traditional machining via life-cycle assessment,” *Rapid Prototyp. J.*, vol. 21, no. 1, pp. 14–33, Jan. 2015, doi: 10.1108/RPJ-07-2013-0067.
- [209] F. Mami, J. P. Revéret, S. Fallaha, and M. Margni, “Evaluating Eco-Efficiency of 3D Printing in the Aeronautic Industry,” *J. Ind. Ecol.*, vol. 21, no. S1, pp. S37–S48, Nov. 2017, doi: 10.1111/jiec.12693.
- [210] J. Faludi, M. Baumers, I. Maskery, and R. Hague, “Environmental Impacts of Selective Laser Melting: Do Printer, Powder, Or Power Dominate?,” *J. Ind. Ecol.*, vol. 21, no. S1, pp. S144–S156, Nov. 2017, doi: 10.1111/jiec.12528.
- [211] F. Walachowicz *et al.*, “Comparative Energy, Resource and Recycling Lifecycle Analysis of the Industrial Repair Process of Gas Turbine Burners Using Conventional Machining and Additive Manufacturing,” *J. Ind. Ecol.*, vol. 21, pp. 205–215, 2017, doi: 10.1111/jiec.12637.

- [212] S. Torres-Carrillo, H. R. Siller, C. Vila, C. López, and C. A. Rodríguez, “Environmental analysis of selective laser melting in the manufacturing of aeronautical turbine blades,” *J. Clean. Prod.*, vol. 246, p. 119068, Feb. 2020, doi: 10.1016/j.jclepro.2019.119068.
- [213] A. C. M. Bekker and J. C. Verlinden, “Life cycle assessment of wire + arc additive manufacturing compared to green sand casting and CNC milling in stainless steel,” *J. Clean. Prod.*, vol. 177, pp. 438–447, Mar. 2018, doi: 10.1016/j.jclepro.2017.12.148.
- [214] D. Böckin and A. M. Tillman, “Environmental assessment of additive manufacturing in the automotive industry,” *J. Clean. Prod.*, vol. 226, pp. 977–987, Jul. 2019, doi: 10.1016/j.jclepro.2019.04.086.
- [215] W. E. Frazier, “Metal Additive Manufacturing: A Review,” *J. Mater. Eng. Perform.*, vol. 23, no. 6, pp. 1917–1928, Jun. 2014, doi: 10.1007/s11665-014-0958-z.
- [216] N. Shamsaei, A. Yadollahi, L. Bian, and S. M. Thompson, “An overview of Direct Laser Deposition for additive manufacturing; Part II: Mechanical behavior, process parameter optimization and control,” *Addit. Manuf.*, vol. 8, pp. 12–35, Oct. 2015, doi: 10.1016/J.ADDMA.2015.07.002.
- [217] D. D. Gu, W. Meiners, K. Wissenbach, and R. Poprawe, “Laser additive manufacturing of metallic components: materials, processes and mechanisms,” *Int. Mater. Rev.*, vol. 57, no. 3, pp. 133–164, 2012, doi: 10.1179/1743280411Y.0000000014.
- [218] T. Peng, K. Kellens, R. Tang, C. Chen, and G. Chen, “Sustainability of additive manufacturing: An overview on its energy demand and environmental impact,” *Addit. Manuf.*, vol. 21, pp. 694–704, May 2018, doi: 10.1016/J.ADDMA.2018.04.022.
- [219] T. DebRoy *et al.*, “Additive manufacturing of metallic components – Process, structure and properties,” *Prog. Mater. Sci.*, vol. 92, pp. 112–224, Mar. 2018, doi: 10.1016/J.PMATSCI.2017.10.001.
- [220] D. Ding, Z. Pan, D. Cuiuri, and H. Li, “Wire-feed additive manufacturing of metal components: technologies, developments and future interests,” *Int. J. Adv. Manuf. Technol.*, vol. 81, no. 1–4, pp. 465–481, Oct. 2015, doi: 10.1007/s00170-015-7077-3.
- [221] S. A. M. Tofail, E. P. Koumoulos, A. Bandyopadhyay, S. Bose, L. O’Donoghue, and C. Charitidis, “Additive manufacturing: scientific and technological challenges, market uptake and opportunities,” *Mater. Today*, vol. 21, no. 1, pp. 22–37, Jan. 2018, doi: 10.1016/J.MATTOD.2017.07.001.

- [222] M. Yakout, M. A. Elbestawi, and S. C. Veldhuis, "A Review of Metal Additive Manufacturing Technologies," *Solid State Phenom.*, vol. 278, pp. 1–14, Jul. 2018, doi: 10.4028/www.scientific.net/SSP.278.1.
- [223] M. Baumer, P. Dickens, C. Tuck, and R. Hague, "The cost of additive manufacturing: machine productivity, economies of scale and technology-push," *Technol. Forecast. Soc. Change*, vol. 102, pp. 193–201, Jan. 2016, doi: 10.1016/J.TECHFORE.2015.02.015.
- [224] K. Oettmeier and E. Hofmann, "Impact of additive manufacturing technology adoption on supply chain management processes and components," *J. Manuf. Technol. Manag.*, vol. 27, no. 7, pp. 944–968, Sep. 2016, doi: 10.1108/JMTM-12-2015-0113.
- [225] N. Serres, D. Tidu, S. Sankare, and F. Hlawka, "Environmental comparison of MESO-CLAD® process and conventional machining implementing life cycle assessment," *J. Clean. Prod.*, vol. 19, no. 9–10, pp. 1117–1124, Jun. 2011, doi: 10.1016/J.JCLEPRO.2010.12.010.
- [226] W. R. Morrow, H. Qi, I. Kim, J. Mazumder, and S. J. Skerlos, "Environmental aspects of laser-based and conventional tool and die manufacturing," *J. Clean. Prod.*, vol. 15, no. 10, pp. 932–943, Jan. 2007, doi: 10.1016/J.JCLEPRO.2005.11.030.
- [227] J. K. H. Chan, "The ethics of working with wicked urban waste problems: The case of Singapore's Semakau Landfill," *Landsc. Urban Plan.*, vol. 154, pp. 123–131, Oct. 2016, doi: 10.1016/J.LANDURBPLAN.2016.03.017.
- [228] J. R. Catlin and Y. Wang, "Recycling gone bad: When the option to recycle increases resource consumption," *J. Consum. Psychol.*, vol. 23, no. 1, pp. 122–127, Jan. 2013, doi: 10.1016/J.JCPS.2012.04.001.
- [229] C. Villamil, J. Nylander, S. I. Hallstedt, J. Schulte, and M. Watz, "Additive Manufacturing from a Strategic Sustainability Perspective," in *International Design Conference Design 2018*, 2018, doi: 10.21278/idc.2018.0353.
- [230] V. T. Le, H. Paris, and G. Mandil, "Process planning for combined additive and subtractive manufacturing technologies in a remanufacturing context," *J. Manuf. Syst.*, vol. 44, pp. 243–254, Jul. 2017, doi: 10.1016/J.JMSY.2017.06.003.
- [231] S. H. Huang, P. Liu, A. Mokasdar, and L. Hou, "Additive manufacturing and its societal impact: a literature review," doi: 10.1007/s00170-012-4558-5.
- [232] T. Stock and G. Seliger, "Opportunities of Sustainable Manufacturing in Industry 4.0," *Procedia CIRP*, vol. 40, pp. 536–541, Jan. 2016, doi: 10.1016/J.PROCIR.2016.01.129.

- [233] C. Leyens and E. Beyer, “Innovations in laser cladding and direct laser metal deposition,” in *Laser Surface Engineering: Processes and Applications*, Elsevier Inc., 2014, pp. 181–192.
- [234] B. Fullenwider, P. Kiani, J. M. Schoenung, and K. Ma, “Two-stage ball milling of recycled machining chips to create an alternative feedstock powder for metal additive manufacturing,” *Powder Technol.*, vol. 342, pp. 562–571, Jan. 2019, doi: 10.1016/J.POWTEC.2018.10.023.
- [235] K. Kellens, R. Renaldi, W. Dewulf, J. Kruth, and J. R. Duflou, “Environmental impact modeling of selective laser sintering processes,” *Rapid Prototyp. J.*, vol. 20, no. 6, pp. 459–470, Oct. 2014, doi: 10.1108/RPJ-02-2013-0018.
- [236] A. J. Pinkerton, “Lasers in additive manufacturing,” *Opt. Laser Technol.*, vol. 78, pp. 25–32, Apr. 2016, doi: 10.1016/J.OPTLASTEC.2015.09.025.
- [237] G. Rebitzer *et al.*, “Life cycle assessment: Part 1: Framework, goal and scope definition, inventory analysis, and applications,” *Environ. Int.*, vol. 30, no. 5, pp. 701–720, Jul. 2004, doi: 10.1016/J.ENVINT.2003.11.005.
- [238] “LCA data | openLCA.org.” GreenDelta.
- [239] M. Seifi, A. Salem, J. Beuth, O. Harrysson, and J. J. Lewandowski, “Overview of Materials Qualification Needs for Metal Additive Manufacturing,” *JOM*, vol. 68, no. 3, pp. 747–764, Mar. 2016, doi: 10.1007/s11837-015-1810-0.
- [240] S. Kosai and E. Yamasue, “Global warming potential and total material requirement in metal production: Identification of changes in environmental impact through metal substitution,” *Sci. Total Environ.*, vol. 651, pp. 1764–1775, Feb. 2019, doi: 10.1016/J.SCITOTENV.2018.10.085.
- [241] H. U. Sverdrup, K. V. Ragnarsdottir, and D. Koca, “An assessment of metal supply sustainability as an input to policy: security of supply extraction rates, stocks-in-use, recycling, and risk of scarcity,” *J. Clean. Prod.*, vol. 140, pp. 359–372, Jan. 2017, doi: 10.1016/J.JCLEPRO.2015.06.085.
- [242] A. J. Pinkerton and L. Li, “Rapid prototyping using direct laser deposition—the effect of powder atomization type and flowrate,” *Proc. Inst. Mech. Eng. Part B J. Eng. Manuf.*, vol. 217, no. 6, pp. 741–752, Jun. 2003, doi: 10.1243/09544050360673134.
- [243] R. Frischknecht *et al.*, “Swiss Centre for Life Cycle Inventories A joint initiative of the ETH domain and Swiss Federal Offices Implementation of Life Cycle Impact Assessment Methods Data v2.0 (2007),” 2007.

- [244] H. Paris, H. Mokhtarian, E. Coatanéa, M. Museau, and I. F. Ituarte, “Comparative environmental impacts of additive and subtractive manufacturing technologies,” *CIRP Ann.*, vol. 65, no. 1, pp. 29–32, Jan. 2016, doi: 10.1016/J.CIRP.2016.04.036.
- [245] O. Yilmaz, A. Anctil, and T. Karanfil, “LCA as a decision support tool for evaluation of best available techniques (BATs) for cleaner production of iron casting,” *J. Clean. Prod.*, vol. 105, pp. 337–347, Oct. 2015, doi: 10.1016/J.JCLEPRO.2014.02.022.
- [246] Z. Sun, Y. Xiao, H. Agterhuis, J. Sietsma, and Y. Yang, “Recycling of metals from urban mines – a strategic evaluation,” *J. Clean. Prod.*, vol. 112, pp. 2977–2987, Jan. 2016, doi: 10.1016/J.JCLEPRO.2015.10.116.
- [247] R. Sreenivasan, A. Goel, and D. L. Bourell, “Sustainability issues in laser-based additive manufacturing,” *Phys. Procedia*, vol. 5, pp. 81–90, Jan. 2010, doi: 10.1016/J.PHPRO.2010.08.124.
- [248] S. M. Thompson, L. Bian, N. Shamsaei, and A. Yadollahi, “An overview of Direct Laser Deposition for additive manufacturing; Part I: Transport phenomena, modeling and diagnostics,” *Addit. Manuf.*, vol. 8, pp. 36–62, Oct. 2015, doi: 10.1016/J.ADDMA.2015.07.001.
- [249] I. Yadroitsev, P. Krakhmalev, I. Yadroitsava, S. Johansson, and I. Smurov, “Energy input effect on morphology and microstructure of selective laser melting single track from metallic powder,” *J. Mater. Process. Technol.*, vol. 213, no. 4, pp. 606–613, Apr. 2013, doi: 10.1016/J.JMATPROTEC.2012.11.014.
- [250] C. Selcuk, “Laser metal deposition for powder metallurgy parts,” *Powder Metall.*, vol. 54, no. 2, pp. 94–99, 2011, doi: 10.1179/174329011X12977874589924.
- [251] R. Frischknecht *et al.*, “Overview and methodology. Data v2.0 (2007). Ecoinvent report No. 1 (Technical Report) | ETDEWEB,” 2007.
- [252] T. E. Graedel *et al.*, “What Do We Know About Metal Recycling Rates?,” *J. Ind. Ecol.*, vol. 15, no. 3, pp. 355–366, Jun. 2011, doi: 10.1111/j.1530-9290.2011.00342.x.
- [253] P. Fröhlich, T. Lorenz, G. Martin, B. Brett, and M. Bertau, “Valuable Metals-Recovery Processes, Current Trends, and Recycling Strategies,” *Angew. Chemie Int. Ed.*, vol. 56, no. 10, pp. 2544–2580, Mar. 2017, doi: 10.1002/anie.201605417.

- [254] J. Johnson, B. K. Reck, T. Wang, and T. E. Graedel, “The energy benefit of stainless steel recycling,” *Energy Policy*, vol. 36, no. 1, pp. 181–192, Jan. 2008, doi: 10.1016/J.ENPOL.2007.08.028.
- [255] K. Salonitis, M. R. Jolly, B. Zeng, and H. Mehrabi, “Improvements in energy consumption and environmental impact by novel single shot melting process for casting,” *J. Clean. Prod.*, vol. 137, pp. 1532–1542, Nov. 2016, doi: 10.1016/j.jclepro.2016.06.165.
- [256] O. Jolliet *et al.*, “IMPACT 2002+: A new life cycle impact assessment methodology,” *Int. J. Life Cycle Assess.*, vol. 8, no. 6, pp. 324–330, Nov. 2003, doi: 10.1007/BF02978505.
- [257] S.-O. Ryding, “ISO 14042 Environmental management, Life cycle assessment, Life cycle impact assessment,” *Int. J. Life Cycle Assess.*, vol. 4, no. 6, pp. 307–307, Nov. 1999, doi: 10.1007/BF02978514.
- [258] C. C. Pertsova, *Ecological economics research trends*. Nova Science Publishers, 2007.
- [259] US EPA, “Understanding Global Warming Potentials,” *epa.gov*. [Online]. Available: <https://www.epa.gov/ghgemissions/understanding-global-warming-potentials>. [Accessed: 19-Aug-2019].
- [260] S. Renou, J. S. Thomas, E. Aoustin, and M. N. Pons, “Influence of impact assessment methods in wastewater treatment LCA,” *J. Clean. Prod.*, vol. 16, no. 10, pp. 1098–1105, Jul. 2008, doi: 10.1016/J.JCLEPRO.2007.06.003.
- [261] R. K. Rosenbaum *et al.*, “USEtox—the UNEP-SETAC toxicity model: recommended characterisation factors for human toxicity and freshwater ecotoxicity in life cycle impact assessment,” *Int. J. Life Cycle Assess.*, vol. 13, no. 7, pp. 532–546, Nov. 2008, doi: 10.1007/s11367-008-0038-4.
- [262] epa.gov, “1,4-Dichlorobenzene (para-Dichlorobenzene),” 1992.
- [263] F. S. Rowland, “Stratospheric Ozone Depletion,” in *Twenty Years of Ozone Decline*, Dordrecht: Springer Netherlands, 2009, pp. 23–66.
- [264] S. Peng *et al.*, “Toward a Sustainable Impeller Production: Environmental Impact Comparison of Different Impeller Manufacturing Methods,” *J. Ind. Ecol.*, vol. 21, no. S1, pp. S216–S229, Nov. 2017, doi: 10.1111/jiec.12628.

- [265] K. Kellens, M. Baumers, T. G. Gutowski, W. Flanagan, R. Lifset, and J. R. Duflou, “Environmental Dimensions of Additive Manufacturing: Mapping Application Domains and Their Environmental Implications,” *J. Ind. Ecol.*, vol. 21, no. S1, pp. S49–S68, Nov. 2017, doi: 10.1111/jiec.12629.

Appendix 1

Chapter 2: Supplemental Information on TRNSYS Model

A1.1 Introduction

In this appendix, a component description for all components used in chapter 2's study. Each component has a brief description of how it is used as well as the design parameters and system operating points that were used within the model. The intent of this appendix is to provide additional information and description for the user to gain some familiarity with TRNSYS.

A1.2 TRNSYS Component Description and Model Layout

The component description is shown in table A1.1 while the model layout is shown in figure A1.1.

Table A1: Description of additional system components in the TRNSYS model.

Single Absorber:	Effect	Type 616 model of a single effect steam-fired absorption chiller using manufacturer performance data files. The component attempts to deliver the user-specified set point temperature for the chilled water stream based on the current cooling capacity.	
		Design capacity (kW)	2170
		Design COP	0.8
		Auxiliary electrical power (kW)	5
		Chilled water inlet temperature (°C)	12.2
		Chilled water flowrate (kg/s)	93.4
		Chilled water set point (°C)	6.67
		Cooling water inlet temperature (°C)	29.4
		Cooling water flowrate (kg/s)	163.5
SCCP Chiller (2X):	Electric	Type666 model of a vapor compression water-cooled chiller. It relies on catalog data provided as external text files to determine chiller performance. These two chillers are located in the SCCP.	
		Rated capacity (kW)	1758
		Rated COP	7.2
		Chilled water flowrate at capacity (kg/s)	53.7
		Cooling water flowrate (kg/s)	100
		Cooling water temperature (°C)	23
		Chilled water set point (°C)	7

NCCP Chiller:	Electric	Similar to the two chillers at the SCCP, this chiller is an electric vapor compression chiller that determines operating performance based on external text files. This chiller is located in the NCCP.	
		Rated capacity (kW)	4220
		Rated COP	6.2
		Chilled water flowrate at capacity (kg/s)	151.4
		Cooling water flowrate (kg/s)	200
		Cooling water temperature (°C)	23
		Chilled water set point (°C)	7
<hr/>			
Cold TES Tank		Type 534 model of a cylindrical tank with a vertical configuration. The fluid in the storage tank interacts with the environment (through thermal losses from the top, bottom and sides) and with the entering and returning flows from the chillers and campus load. The tank is divided into isothermal temperature nodes (to model stratification observed in storage tanks) where the user controls the degree of stratification through the specification of the number of "nodes". Each constant-volume node is assumed to be isothermal and interacts thermally with the nodes above and below through several mechanisms: fluid conduction between nodes and through fluid movement.	
		Number of tank nodes	100
		Number of ports	1
		Tank volume (m ³)	8750
		Tank height (m)	24
<hr/>			
Chiller Pumps:	Supply	Type741 model of a variable speed pump that is able to produce any mass flowrate between zero and its rated flowrate. The pump's power draw is calculated from pressure rise, overall pump efficiency, motor efficiency and fluid characteristics. Type 741 sets the downstream flowrate based on its rated flowrate parameter and the current value	

of its control signal input. These pumps set the flowrate for each chiller.

Overall pump efficiency (%)	60
Pump motor efficiency (%)	90
Pressure drop (kPa)	85

Campus Pumps:	Supply	Type742 model of a pump sets its fluid outlet mass flowrate equal to the user specified inlet mass flowrate. Type742 sets the downstream flow but does not take either a maximum allowable flowrate or a control signal. The pump's power draw is calculated based upon the pressure drop across campus.
		Overall pump efficiency (%) 60
		Pump motor efficiency (%) 90
		Pressure Drop (kPa) 85

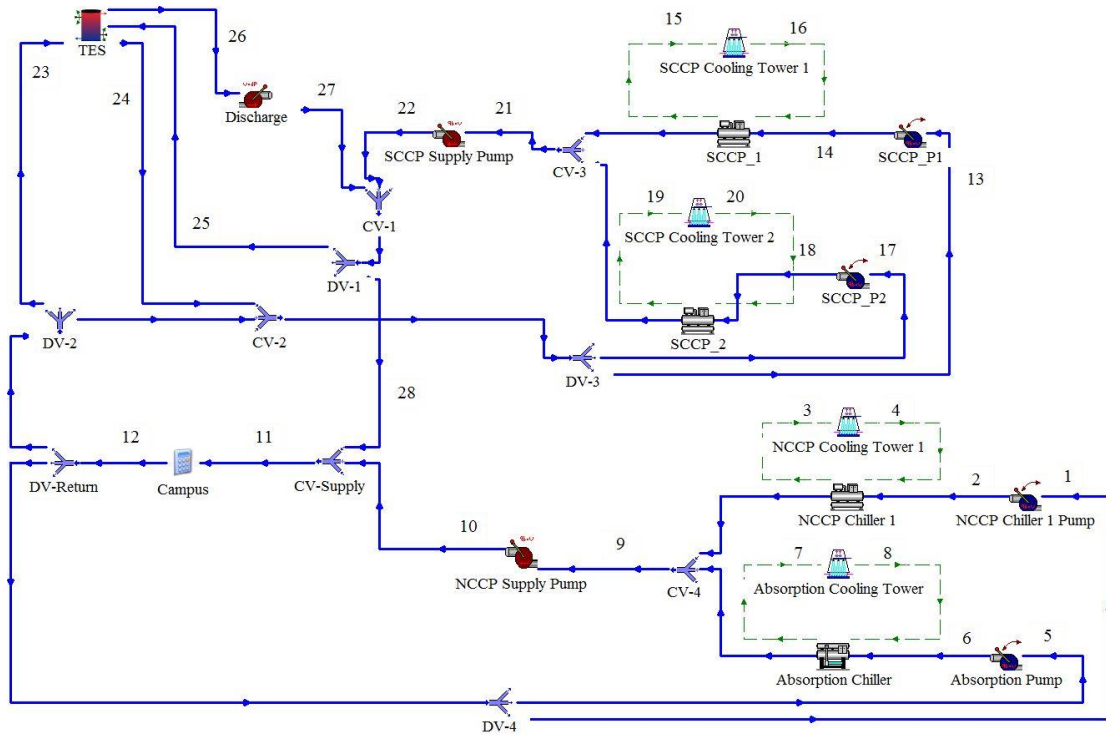
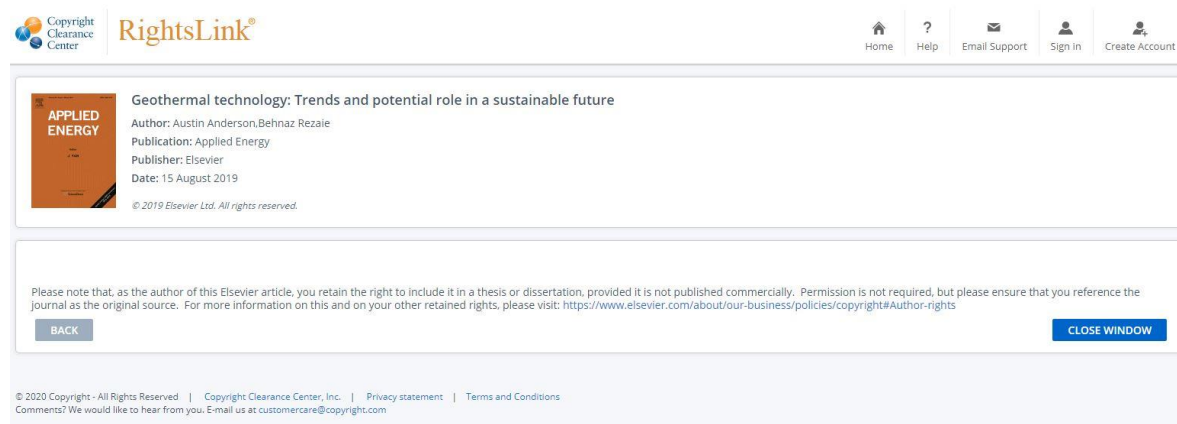


Figure A1: Complete model view of all components.

Appendix 2

Chapter 3: Copyright Approval from the Journal Applied Energy

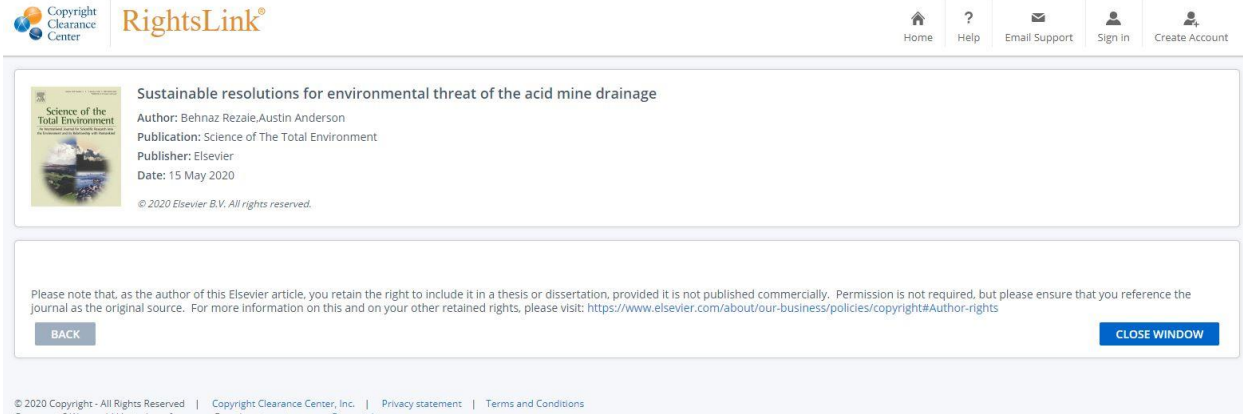


The screenshot displays the Copyright Clearance Center RightsLink interface. At the top left, the Copyright Clearance Center logo and the RightsLink logo are visible. On the top right, there are navigation links: Home, Help, Email Support, Sign in, and Create Account. The main content area features a publication card for "APPLIED ENERGY" with the title "Geothermal technology: Trends and potential role in a sustainable future". The author is listed as Austin Anderson, Behnaz Rezaie. The publication is from Applied Energy, published by Elsevier, on 15 August 2019. A copyright notice states "© 2019 Elsevier Ltd. All rights reserved." Below the publication card, a disclaimer states: "Please note that, as the author of this Elsevier article, you retain the right to include it in a thesis or dissertation, provided it is not published commercially. Permission is not required, but please ensure that you reference the journal as the original source. For more information on this and on your other retained rights, please visit: <https://www.elsevier.com/about/our-business/policies/copyright#Author-rights>". At the bottom of the disclaimer, there are "BACK" and "CLOSE WINDOW" buttons. The footer contains copyright information: "© 2020 Copyright - All Rights Reserved | Copyright Clearance Center, Inc. | Privacy statement | Terms and Conditions" and a comment: "Comments? We would like to hear from you. E-mail us at customer-care@copyright.com".

Figure A2: Copyright approval for publication from Applied Energy.

Appendix 3


Chapter 4: Copyright Approval from the Journal Science of the Total Environment



The screenshot displays the Copyright Clearance Center RightsLink interface. At the top left, the Copyright Clearance Center logo and RightsLink® are visible. On the top right, there are navigation links: Home, Help, Email Support, Sign In, and Create Account. The main content area shows a copyright approval for the article "Sustainable resolutions for environmental threat of the acid mine drainage" by Behnaz Rezale Austin Anderson, published in Science of The Total Environment by Elsevier on May 15, 2020. A disclaimer states that the author retains the right to include the article in a thesis or dissertation, provided it is not published commercially. A "BACK" button is on the left and a "CLOSE WINDOW" button is on the right. The footer contains copyright information and contact details for the Copyright Clearance Center, Inc.

Copyright Clearance Center RightsLink®

Home Help Email Support Sign In Create Account

 Sustainable resolutions for environmental threat of the acid mine drainage
Author: Behnaz Rezale Austin Anderson
Publication: Science of The Total Environment
Publisher: Elsevier
Date: 15 May 2020
© 2020 Elsevier B.V. All rights reserved.

Please note that, as the author of this Elsevier article, you retain the right to include it in a thesis or dissertation, provided it is not published commercially. Permission is not required, but please ensure that you reference the journal as the original source. For more information on this and on your other retained rights, please visit: <https://www.elsevier.com/about/our-business/policies/copyright#Author-rights>

BACK CLOSE WINDOW

© 2020 Copyright - All Rights Reserved | Copyright Clearance Center, Inc. | Privacy statement | Terms and Conditions
Comments? We would like to hear from you. E-mail us at customer-care@copyright.com

Figure A3: Copyright approval for publication from Science of the Total Environment.